Analysis of *Ptp10D* and *Ptp4E* during ageing and in Parkinson Disease models in *Drosophila melanogaster*

By

Tahereh Zadabedini Masouleh, B.Sc.

A thesis submitted to the

School of Graduate Studies

In partial fulfillment of the requirement for the degree of

Master of Science

Department of Biology

Memorial University of Newfoundland

2019

St. John's Newfoundland and Labrador

Abstract

Parkinson Disease (PD) is an age-dependent neurological disease that diminishes locomotory abilities. PD is the second most common neurodegenerative disease, after Alzheimer Disease (AD), with a lifetime risk of approximately one in 40 in human. The symptoms of PD include resting tremors, rigidity, and bradykinesia and are caused by a loss of dopaminergic neurons in the *substantia nigra* of the midbrain. Based upon a recent study, a group of novel candidate genes was discovered with the potential to influence PD etiology. Protein tyrosine phosphatase receptor type H (*PTPRH*) is one of the candidate genes with an established role in controlling mitochondrial morphology, which is a very important organelle in the development of PD. Importantly, PTPRH protein has roles in many cellular processes, including cell growth, the mitotic cycle, and differentiation.

In the current study, *Ptp10D* and *Ptp4E* were identified as potential *D. melanogaster* homologues of *PTPRH* that are apparently the products of a gene duplication event. I show that *PTPRH* homologues in *D. melanogaster* have been conserved throughout evolution in vertebrates and invertebrates possessing a number of distinct conserved functional domains. Biometric, longevity, and climbing assays were performed to determine if altered expression of these genes could influence neurodevelopment, longevity and quality of life and/or produce novel models of PD. The individual inhibition of either *Ptp10D* or *Ptp4E* decreases the lifespan and locomotor ability over time. As well, directed loss of function has deleterious effects on neurodevelopment when inhibited in the compound eye. Interestingly, similar results

were observed with regards to longevity, climbing over time, and eye biometric analyses when *Ptp4E* was overexpressed. In conclusion, altered expression of homologues of *PTPRH* in *D. melanogaster*, either ectopic overexpression or inhibition via RNAi, influences overall health and ageing to result in new potential models of PD.

Acknowledgements

Foremost, I would like to express my sincere gratitude to my supervisor, Dr. Brian E. Staveley for the continuous support during my program, for his patience, guidance, and kindness. Besides my supervisor, I would also like to thank the rest of my thesis supervisory committee Dr. Andrew Lang and Dr. Youlian Tzenov for their encouragement, positive criticism, and insightful comments. My special thanks also goes to previous and present Staveley lab members, especially Azra, Tarana, and Kiana who I could always count on during hard and overwhelmed times. They have made this journey a million times better which I never forget.

I thank my friends Helia, Shokoufeh, Nima, Nahid, Mohammad, and Mahshid who always tried their best to help me overcome my stress and fears. Their kind heart and unconditional supports will never be forgotten. As well, I don't know how to express my gratefulness to my one and only, Sahand who has always believed in me. He was the one who I always lean on when I feel hopeless, exhausted, and homesick. I would also like to express my deepest gratitude to my parents, my wonderful sisters, and my baby niece, Maysa, who had learnt to tell "don't be scared" to me as her first words via video calls. I have to say, you don't know how much you have lifted my mood Maysa, thank you. I am so blessed to have you as my family in my life. Thanks for everything you have done for me.

Research for this thesis has been supported by Memorial University of Newfoundland, School of Graduate Studies Baseline Funding Scholarship, and Graduate Assistantship, Department of Biology. Funding of Dr. Brian Staveley's

research group is supported by grants from the Natural Sciences and Engineering Research Council of Canada (*"Signalling mechanisms integrating cell survival, organismal growth and stress-resistance in Drosophila"*), Parkinson Society of Newfoundland and Labrador (*"Novel aspects of intracellular trafficking in Drosophila models of Parkinson Disease"*), and Memorial University of Newfoundland Seed, Bridge and Multidisciplinary Fund ("*Novel aspects of intracellular trafficking in Drosophila models of Parkinson Disease"*).

Table of Contents

List of Figures

List of Tables

List of Abbreviations

°C – Degree Celsius

ATP – Adenosine Triphosphate

BLAST – Basic Local Alignment Search Tool

C. elegans – *Caenorhabditis elegans*

cm – Centimeter

CNS – Central Nervous System

CRC – Colorectal cancer

D. melanogaster – *Drosophila melanogaster*

DA – Dopaminergic

DDC – Dopa decarboxylase

FN3 – Fibronectin type 3

FPD – Familial Parkinson Disease

g/L – grams per liter

g/ml – grams per milliliter

GMR – Glass multiple reporter

GOF – Gain-Of-Function

GTP – guanosine triphosphate

GWAS – Genome Wide Association

HPA – Human Protein Atlas

LOF – Loss-Of-Function

LRRK2 – Leucine-rich repeat kinase 2

ml - milliliters

ml/L – milliliters per liter

MPTP – 1-methyl-4-phenyl-1,2,3,6-tetrahydropyridine

N/A – Not Applicable

NADH – Nicotinamide adenine dinucleotide phosphate

NCBI – National Center for Biotechnology Information

PD – Parkinson Disease

PTK – Protein tyrosine kinases

PTP – Protein tyrosine phosphatase

Ptp10D – Protein tyrosine phosphatase 10D

Ptp4E – Protein tyrosine phosphatase 4E

PTPRH – Protein tyrosine phosphatase receptor type H

RISC – RNA-induced silencing complex

RNA – Ribonucleic acid

RNAi – RNA interference

ROS – Reactive Oxygen Species

RPTP – Receptor protein tyrosine phosphatase

SAP-1 – Stomach cancer-associated protein-tyrosine phosphatase-1

SE – Standard error

SEM – Standard Error of the Mean

tBLASTn – Translated Nucleotide Basic Local Alignment Search Tool

TH – Tyrosine Hydroxylase

UAS – Upstream Activation Sequence

Uchl-1 – Ubiquitin c-terminal hydrolase 1

VSP35 – Vascular sorting protein 35

WES – Whole Exome Sequencing

Introduction

Purpose

Parkinson Disease (PD) is the most common neurodegenerative movement disease. As such, it is vital to understand the underlying mechanisms and pathways responsible for PD in order to treat and/or prevent it. The aim of this research is to characterize the potential relationship of the *Ptp10D* and/or *Ptp4E* genes and Parkinson disease through the examination of the consequences of inhibition and overexpression in the model organism *Drosophila melanogaster*.

Parkinson Disease

Parkinson Disease (PD) is a neurological disease in which age-dependent loss of locomotion abilities is the best-known feature. PD was first medically defined by Dr. James Parkinson in 1817 as a neurological disorder (Parkinson, 1817). In 1872, observations of patients with resting tremor led to classifying PD as a distinct neurological disorder which had been formerly categorized with other tremorous disorders such as multiple sclerosis based on early symptoms (Charcot, 1872). PD is characterized by degeneration of dopaminergic neurons in the *zona compacta* of the *substantia nigra* in the midbrain (Fearnley & Lees, 1991). Often the loss of dopaminergic neurons is accompanied by the presence of α-synuclein-enriched aggregation, which is a key component of Lewy bodies, abnormal aggregates of protein inside nerve cells (Goedert, 2001). These eosinophilic inclusions are believed to be a

neuropathological marker of PD (Savitt, Dawson, & Dawson, 2006). Although a great deal of effort has been devoted to discover the cause(s) of the disease, there is much left to discover.

There are motor and non-motor symptoms associated with this progressive neurodegenerative movement disease. Slowness of movement, rigidity, resting tremor, and postural disability are the conspicuous locomotion and motor control-related characteristics (Shahed & Jankovic, 2007). The presence of at least two of the principal symptoms is a requirement for diagnosis of the disease (Nussbaum & Polymeropoulos, 1997). In spite of the emphasis on motor symptoms, non-motor symptoms are important when it comes to the quality of life and life expectancy (Chaudhuri, Healy, & Schapira, 2006). Non-motor symptoms, including depression, anxiety, sleeping disorders, pain, and sexual dysfunction are common and occur across all stages of PD (Chaudhuri & Schapira, 2009). There is no curative treatment for this chronic disease, but some treatments are available to control some of the symptoms.

PD is the second most common neurodegenerative disease, after Alzheimer Disease (AD), with the lifetime risk of one in 40 (Schapira, 1995). The incidence rates of PD is from eight to 18 per 100,000 person-years (De Lau & Breteler, 2006). There is a sharp increase in the incidence after age 60 years, whereas the onset of the disease before age 50 years is rare (Erkkinen, Kim, & Geschwind, 2018). The average standardized incidence rate of PD in the US and other developed countries have been approximated 14 per 100,000 person-year. When studies were confined to cases over the age of 65, the average incidence rate was increased to 160 per 100,000 person-year,

to strongly suggest that PD is an age-dependent disease (Hirtz et al., 2007). An epidemiologic study was conducted of cases diagnosed with idiopathic PD Parkinson's disease from northern California has shown that the age-adjusted incidence rate for men was 19 per 100,000 and 9.9 per 100,000 person-years for women (male: female ratio= 1.9) (Van Den Eeden et al., 2003). Based on epidemiological research, age, race, and gender are the most important risk factors.

Based on several studies, the rate of incidence of PD in men is higher than women with the range of male to female ratios of 0.9 to 2.6 (De Lau & Breteler, 2006). A remarkably higher incidence rate of PD amongst men can be explained by neuroprotective effects of estrogens and recessive susceptibility of PD genes on the X chromosome (Wooten, Currie, Bovbjerg, Lee, & Patrie, 2004). The incidence of PD, regardless of age and gender, is the highest among the Hispanics in Northern California population. Non-Hispanic Caucasian Asians, and African Americans had lower rates, respectively (Van Den Eeden et al., 2003). This research suggests that the incidence of PD differs by ethnicity, which supports the role of hereditary in this disease.

For many years, no correlation between PD and inheritance was recognized and, therefore, environmental factors were considered as the only cause of the disease. However, in the past number of decades, the identification of genes for monogenic forms of the disease has led to a growing understanding of the molecular mechanisms of PD (Gasser, 2009). Approximately 10 to 15% of patients have a positive family history of PD in accordance with a Mendelian (autosomal dominant or autosomal recessive) inheritance (De Lau & Breteler, 2006). There is no specific clinical symptom which

distinguishes the familial form of the disease from sporadic except age: many patients with the familial form are younger at disease onset (Gasser, 2007). Although the familial form of PD comprises a small portion of cases the identification of associated genes and their functions has led to a deeper understanding of the pathogenesis of PD.

Genetics aspects of PD

William Gowers, a British neurologist, was the first who suggested that there might be hereditary factors by observing a suffering case in the relatives of a patient with PD (summarized in Schapira, 1995). To date, at least 24 chromosomal regions or loci (Table 1) have been linked to PD (Del Rey et al., 2018). However, only 19 distinct genes of 24 loci have been identified by performing linkage analysis and genome sequencing (Deng, Wang, & Jankovic, 2018). In addition, a genome-wide association study (GWAS) has shown over 20 common variants with small effect size on PD cases (Hernandez, Reed, & Singleton, 2016). Nine of the established PD genes are autosomal recessive and the rest are autosomal dominant genes.

In the late 20th century, the first PD gene (*SNCA*) was identified by linkage study in the familial form of PD (FPD) with autosomal dominant inheritance (Polymeropoulos et al., 1997). The *SNCA* gene encodes the α-synuclein protein in which missense mutations cause the accumulation of protein inclusions within the inner membrane of mitochondria and subsequent cell death (Liu et al., 2009). Afterward, mutations in *parkin/PARK2* were recognized in Japanese families with the young-onset of symptoms

(Kitada et al., 1998). In addition, a mutation in ubiquitin c-terminal hydrolase 1 (*Uchl-1)/PARK5* (Leroy et al., 1998) and Leucine-rich repeat kinase 2 *(LRRK2)/Park8* (Paisán-Ruíz et al., 2004) lead to the autosomal dominant form of PD. Furthermore, mutations in five more genes with a small sample size in FPD, including *HTRA2*, vascular sorting protein 35 (*vsp35*), *EIF4GI*, *DNAJC13*, and *CHCHD2*, have an autosomal dominant inheritance (Karimi-Moghadam, Charsouei, Bell, & Jabalameli, 2018). Many of PD-linked genes encode proteins which directly or indirectly have a role in mitochondrial homeostasis or mitophagy (Ryan, Hoek, Fon, & Wade-Martins, 2015). Mutation in three main genes including *PARK6 (PINK1), PARK2 (parkin),* and *PARK7 (DJ-1)* which play an important part in mitochondrial homeostasis leads to autosomal recessive or loss of function forms of PD (Bekris, Mata, & Zabetian, 2010). The list of PD-related genes is getting longer by the day (Table 1; based on (Del Rey et al., 2018; Zhang, Chen, Zhang, Wang, & Fernandez-Funez, 2018)), which highlights the role of genetics in this disease.

Table 1: PD-related genes and risk factors loci

Locus	Gene name	Location	Inheritance [a]	Onset [b]	Function
PARK1/4	*SNCA*	4q21.3-q22	AD	EO	Synaptic protein vesicles dynamics
PARK2	*PARKIN*	6q25.2-q27	AR	EO	Mitophagy
PARK3	Unknown	2p13	AD	LO	Unknown
PARK5	*UCHL1*	4p13	AD	LO	Proteasome
PARK6	*PINK1*	1p36.12	AR	EO	Mitophagy
PARK7	*DJ-1*	1p36.23	AR	EO	Mitophagy
PARK8	*LRRK2*	12q12	AD	LO	Autophagy
PARK9	*ATP13A2*	1p36	AR	EO	Lysosome
PARK10	Unknown	1p32	Risk factor	LO	Unknown
PARK11	*GIGYF2*	2q36-7	AD	LO	IGFs signalling
PARK12	*Unknown*	Xq21-q22	X-linked	LO	Unknown
PARK13	*HTRA2*	2p13.1	AD	LO/EO	Mitophagy
PARK14	*PLA2G6*	22q13.1	AR	EO	Lipid metabolism
PARK15	*FBXO7*	22q12.3	AR	EO	Mitophagy
PARK16	Unknown	1q32	Unknown	LO	Unknown
PARK17	*VPS35*	16q12	AD	LO	Endosomes
PARK18	*EIF4G1*	3q27.1	AD	LO	Protein translation
PARK19	*DNAJC6*	1p31.3	AR	EO	Endosomes
PARK20	*SYNJ1*	21q22.11	AR	EO	Endosomes
PARK21	*DNAJC13*	3q22.1	AD	LO	Endosomes
PARK22	*CHCHD2*	7p11.2	AD	LO/EO	Apoptosis
PARK23	*VPS13C*	15q22.2	AR	EO	Mitophagy
--	*GBA*	1q22	AD	LO	Lysosomes
--	*MAPT*	17q21.31	Sporadic risk factor	Unknown	Microtubules

[a] AD is autosomal dominant, AR is autosomal recessive

[b] EO is early-onset, LO is late-onset

Role of mitochondria in PD

Mitochondria, with their double-membrane structure, are crucial organelles that generate energy in cells in the form of Adenosine Triphosphate (ATP). For neuron-rich tissues like brain, mitochondria are of great importance due to the inability of these tissues to derive sufficient energy by glycolysis (Karbowski & Neutzner, 2012). There are various cellular mechanisms that help to maintain mitochondrial function through which either impaired harmful organelles are broken down or biogenesis of new mitochondria occurs. Balanced fission and fusion in mitochondria is a key aspect of their functionality in terms of protection of mitochondrial DNA, mitochondrial turnover, and bioenergetics function (Bose & Beal, 2016). Complex I, located in the inner membrane of mitochondria, plays a vital role in the oxidative phosphorylation system. Thus, damage to this complex leads to the dysfunction of mitochondria and subsequent dopaminergic (DA) neuron death (Schapira, 2007). Intact function of mitochondria is crucial to prevent the death of DA neurons and subsequent higher risk of PD.

Neurotoxin exposure, including 1-methyl-4-phenyl-1,2,3,6-tetrahydropyridine (MPTP) and rotenone, can lead to mitochondrial damage by affecting complex I activity and therefore they are considered as environmental factors related to PD (Philippens, 2018). Moreover, the rate of mitochondrial DNA mutation is higher in PD patients compared to the non-PD population with the same age (Wang, Abraham, Gao, & Yang, 2016). As a result of mitochondrial dysfunction, reactive oxygen species (ROS) are generated which leads to oxidative stress in the cell (Trushina & McMurray, 2007). Activation of cell death signalling pathways via the increase of ROS and oxidative stress

has been reported (Moon & Paek, 2015). Degeneration of DA neurons is catalyzed by oxidative stress and as such mitochondria are crucial in PD.

Most of the PD-linked genes encode proteins which directly or indirectly have a role in mitochondrial homeostasis. In fact, mutant forms of PD genes increase mitochondrial damage and impair clearance of dysfunctional mitochondria that cause cellular stress (Aryal & Lee, 2019). The α-synuclein protein, encoded by *SNCA*, is situated in association with the inner membrane of mitochondria by its mitochondrial specific signal in the N-terminal 32 amino acids. The process of α-synuclein aggregation in the mitochondrial membrane in dopaminergic neurons leads to complex I dysfunction and subsequent higher rate of ROS production (Devi, Raghavendran, Prabhu, Avadhani, & Anandatheerthavarada, 2008). As a result, mitochondrial membrane potential may become disrupted and this may eventually lead to cell death (Devoto & Falzone, 2017). PINK1 and Parkin are proteins with distinct roles in mitochondrial maintenance (Wang et al., 2016). PINK1 is localized in mitochondria and mutations in the gene that encodes this protein result in a rare form of autosomal recessive PD by deactivating NADH and disrupting the electron transport chain in mitochondria (Scialò et al., 2016). Moreover, the loss of *Parkin* causes mitochondrial degradation and increases cellular susceptibility to oxidative stress (Aryal & Lee, 2019). Mutations in *Parkin* have been shown to result in early onset juvenile autosomal recessive PD which is associated with accumulation of its substrates (Rakovic et al., 2011). The PINK1/Parkin pathway is essential for mitochondrial function. Null mutants of both protein encoding genes in *Drosophila* demonstrate impaired mitochondrial turnover and mitophagy (Vincow et al., 2013). Due

to the importance of mitochondria in PD etiology, many PD studies evaluate parameters which are related to mitochondrial morphology.

Given the role of Fbxo7 protein in inducing mitophagy via direct interactions with Parkin, it is marked as a PD gene involved in mitochondrial maintenance (Wang et al., 2016). Mutation in this gene leads to autosomal recessive PD at the early onset which highlights the effect of mitochondrial dysfunction and oxidative stress in PD pathogenesis.

Genes of interest

Protein tyrosine phosphatase receptor type H, *PTPRH* is a protein-coding gene. PTPRH, also called stomach cancer-associated protein-tyrosine phosphatase-1 (SAP-1) was first identified in human stomach cells (Matozaki, T. et al., 1994). This protein is a member of the protein tyrosine phosphatase (PTP) family. The presence of structurally conserved domain, which is called PTP, determines the membership (Andersen et al., 2001). PTPs remove phosphate groups from tyrosine residues in proteins and therefore are considered as part of a signal transduction pathway set of enzymes. The level of tyrosine phosphorylation in cellular proteins is controlled by PTPs and protein tyrosine kinases (PTKs), as PTKs phosphorylate proteins on tyrosine residues (Hunter, 1998). These signalling molecules have a role in plenty of cellular processes, including cell growth, the mitotic cycle, and differentiation (Moura & Conde, 2019). Each PTP contains one or two catalytic sites with a conserved amino acid sequence

(I/V)HCXAGXXR(S/T) G (X: any amino acid). In this sequence, cysteine has a crucial role in catalyzing dephosphorylation (Baig, Ahmad, Rabbani, & Choi, 2018). PTPs and PTKs together regulate the phosphorylation level of many signalling proteins and therefore have important roles in signalling pathways.

PTPs are categorized into three distinct groups: the classical PTPs, dual-specificity PTPs, and the low molecular weight PTPs. The classical PTPs are then divided into two subgroups named transmembrane receptor and non-receptor PTPs. Most transmembrane receptor-like PTPs (RPTPs) are made up of one to two cytoplasmic PTP catalytic domains, a membrane proximal and distal domain (D1and D2), and single transmembrane segment as well as an extracellular domain (Du & Grandis, 2015). PTPRH, the focus of this study, has one PTP conserved domain in the cytoplasm, a single transmembrane region, as well as an extracellular region in which there are eight fibronectin type III-like (FN3) structure repeats and multiple N-glycosylation sites (Hendriks, Elson, Harroch, & Stoker, 2008). The FN III repeats in PTPRH unlike other RPTP induce protein dimerization and thereby control the enzyme's activity (Wälchli, Espanel, & Van Huijsduijnen, 2005). Despite all of the studies that have been done on RPTPs with two catalytic domains, RPTPs with a single domain remained relatively known.

In humans, the *PTPRH* gene is located on the long arm of chromosome 19 in the q13.42 region. In studies on normal tissue, it was shown that *PTPRH* is widely expressed in brain, liver, and then at a lower level in heart and stomach (Matozaki, Takashi & Kasuga, 1996). Moreover, high expression of *PTPRH* was detected in pancreatic and

colorectal cancer cell lines (CRC). Therefore, it was considered as an oncogenic factor (Seo et al., 1997). However, it has been shown that there is a lower expression of *PTPRH* in an advanced stage of colorectal cancer and human hepatocellular cancer (Nagano et al., 2003). In one study, the mRNA expression in colorectal adenomas, normal mucosa, and CRC cells was compared by microarrays and the analysis showed that the *PTPRH* expression was reduced the most in CRC cells, which supports the possible tumor suppressor role of PTPRH (Skrzypczak et al., 2010). Later, another study measured the mRNA and protein level in healthy adenoma and mucosa, as well as CRC samples. Immunohistochemical staining of the tumor and normal mucosa samples was conducted to confirm the first set of results through which it has been proven that the protein expression was decreased in CRC samples. These results demonstrate that *PTPRH* is downregulated in the colorectal tumor (Bujko et al., 2017). Although there are unknown aspects concerning the role of PTPRH, it is likely that this protein has a tumor suppressor function.

To understand the distinct function of PTPRH, recognition of its physiological substrates is essential. The identification of substrates for this enzyme has been difficult due to the transient nature of the binding between PTPRH and its substrates (Matozaki, Takashi et al., 2010). In 2001, Noguchi et al. identified p130cas as a potential physiological substrate for PTPRH by the substrate-trapping method. This protein is a focal adhesion-associated phosphotyrosyl protein which is involved in various cellular processes including migration, apoptosis, and cell adhesion. It has been observed that besides p130cas, PTPRH induces dephosphorylation of focal adhesion kinase and

p62^{dok}, which are two other proteins of the integrin-signalling pathway (Noguchi et al., 2001). P130cas is involved in different cerebellum development stages (Hourani, Mendes, Berretta, & Moscato, 2007). Cerebellum is identified as a potential source of some of the PD symptoms which explains its possible role in the pathophysiology of PD (Wu & Hallett, 2013). Due to the different expression level of p130cas in PD, abnormal expression level of p130Cas may associated with PD (Sun, Ye, Zheng, & Yang, 2018). Based on the evidence for the potential roles of p30Cas in PD, PTPRH may be acting through focal adhesion substrates to influence PD.

Abundance of PTPRH in brain tissue (Matozaki, T. et al., 1994) and the presence of fibronectin type III-like domain in many neural cells suggest that PTPRH has a role in the signalling pathway of neural cell-cell adhesion (Noguchi et al., 2001). Furthermore, the overexpression of *PTPRH* in a fibroblast cell line leads to apoptotic cell death by at least two cellular mechanisms: inhibiting the survival signalling induced by both Akt (protein kinase B) and integrin-linked kinase (ILK) and activating the cellular pro-apoptotic pathway (Takada et al., 2002). These findings suggest that PTPRH affects signalling pathways regarding cell proliferation, survival, apoptosis, and cell motility.

Whole exome sequencing (WES) is one of the valuable tools when it comes to the identification of new genes that cause the familial form of PD. A large-scale whole exome sequencing was performed in 1148 unrelated PD cases in 2017 with the purpose of identifying and prioritizing novel PD candidate genes. The analysis focus was on genes with homozygous or compound heterozygous loss-of-function (LOF) variants.

Therefore, they selected cases with the younger age of PD onset which is related to recessive inheritance. The 27 candidate genes, including *PTPRH*, were found during their primary analysis with the confirmation of Sanger sequencing. Based on WES results, *PTPRH* is a compound heterozygote with the functional validation for assessment in both approved PD mechanisms: mitochondrial morphology and α-synuclein-induced neurodegeneration. Then, they examined each candidate gene on the expression networks derived from the human *substantia nigra* to produce a co-expression pattern with established PD genes. It was found that *PTPRH* is co-expressed with the gene *FBXO7* (Jansen et al., 2017). Mutant forms of *FBXO7* can lead to protein aggregation and subsequent impaired mitochondrial function due to FBXO7 interaction with PINK1 and parkin (Burchell et al., 2013). By use of enrichment analysis, it has been observed that *PTPRH* is expressed in an oligodendrocyte markers-enriched network (Jansen et al., 2017). Higher expression of *PTPRH* in this network suggests that this protein has a potential function in the *substantia nigra* of the midbrain which is associated with PD.

As it was noted before, mitochondrial dysfunction plays an important role in PD-causative mechanisms. After the identification of a group of novel candidate PD genes, Jansen and colleagues ran the second phase of their experiment to prioritize the genes based on their possible related function in PD. Due to this, they chose 13 candidate genes to see if the knockdown of each gene shows a substantial impact on at least one of the three parameters for quantification of mitochondrial morphology: mitochondrial number, axial length ratio, and roundness. Knockdown of *PTPRH* in neuroblastoma cell

lines leads to an increase in axial length ratio which demonstrates its role in mitochondrial morphology (Jansen et al., 2017). It is interesting to observe that based on the Human Protein Atlas (HPA) program, which tries to map all human proteins in different cells, tissues, and organs, the subcellular location of PTPRH is mitochondria (*https://www.proteinatlas.org/*). This information helps to prove the role of PTPRH in mitochondria and its subsequent role in PD formation.

***Drosophila melanogaster* as a model organism**

The fruit fly *Drosophila melanogaster* has been chosen for over a century as a model organism for genetic studies and it is one of the first organisms with a fully sequenced genome. For the first time, *D. melanogaster* was sequenced in March 2000 in order to verify the shot-gun sequencing approach (Jennings, 2011). Approximately 15000 genes have been identified in *D. melanogaster* which are all carried on only four chromosomes and they can be easily observed in the polytene chromosomes of the larval salivary gland (St. Johnston, 2002). Thus, a higher density of genes per chromosome can be observed compared to humans.

To enumerate the essential characteristics of *D. melanogaster* that make this fly as an effective model system, the close relationship between the fruit fly and human genome should first be considered. To be precise, 75% of human disease genes have a homologue in fruit flies, which are easy to manipulate (Pandey & Nichols, 2011). The other benefit of *D. melanogaster* that allows scientists to carry out research easily is its

12-day life cycle with a lot of offspring that is easy to keep and grow (Jennings, 2011). Short lifespan is another advantage of this organism which is especially beneficial for researching on neurodegenerative diseases (Prüßing, et al., 2013). Moreover, the presence of external components, including interommatidial bristles, compound eyes, and wing veins facilitates the observation of the impacts of various mutations on phenotype (St. Johnston, 2002). All these aspects make this organism a convenient model to work with in the laboratory condition.

Modeling human neurodegenerative diseases requires an organism with a complex central nervous system (CNS). Although fruit flies possess relatively small brains, their nervous system is more complex than that of in *C. elegans* (Nass & Przedborski, 2011). The *D. melanogaster* CNS consists of a three-lobed brain and a ventral nerve cord with bilateral symmetry (Nass & Przedborski, 2011). The larval *D. melanogaster* CNS contains approximately 125,000 neurons which increases up to 250,000 neurons in the complex adult CNS with millions of connections (Lambrechts, Faber, & Sibon, 2018). The ventral nerve cord is made up of ganglia containing motor neurons and interneurons, a necessity to manage the body segments that they innervate. However, the brain in *D. melanogaster* contains neurons playing role in memory, learning, and sensory processing (Keene & Waddell, 2007). As well, dopaminergic neurons which are of great importance in PD studies can be widely seen in the *D. melanogaster* CNS and they have important roles in memory, learning, mating, and locomotion control (Nass & Przedborski, 2011). This range of similarities between the

D. melanogaster and human nervous systems, in both components and functions, make this organism an ideal model for studying neurodegenerative disease, especially PD.

Drosophila melanogaster has been extensively used to address underlying mechanisms in a wide range of neurodegenerative diseases including polyglutamine disorder, Alzheimer Disease and Parkinson Disease (Lambrechts et al., 2018). Besides the advantages mentioned above, having compound eyes makes this model organism a unique tool for the study of human disease associated with the nervous system. The eye of *D. melanogaster* is a highly effective model system to analyze molecular interactions and developmental mechanisms of the nervous system (Şahin & Çelik, 2001). This anatomical feature provides an easy determination of any phenotypic change (Iyer et al., 2016). The *D. melanogaster* eye differentiates from the eye imaginal disc as a first part of the adult nervous system (Cagan, 2009). Each eye is made up of 700 to 800 eye units known as ommatidia. Ommatidia have a hexagonal shape with the same size and even spacing (Figure 1) (Tsachaki & Sprecher, 2012). Eight photoreceptor neurons, four non-neuronal cone cells and two pigment cells are present in each unit (Baker, Li, Quiquand, Ruggiero, & Wang, 2014). The presence of more than 6000 neurons in each eye leads to the visibility of any defects in eye development. Likewise, since the eye is a repetitive structure, gain or loss of function conditions which disturb eye development can be easily recognized in the adult eye as a "rough eye" (Lambrechts et al., 2018). Interommatidial bristle, ommatidia number, eye surface area, and size of ommatidia can be quantified in the rough eye (Iyer et al., 2016). This feature is beneficial to the study of gene functions or the effect of expressing mutant genes.

Despite all the advantages that flies offer to researchers, there are some drawbacks that should be taken into consideration while choosing this organism as a model of the study. One of the main drawbacks of working with flies is that they should be maintained in living stocks during the experiment since there is no practical way to freeze the stocks (Gonzalez, 2013). Sometimes, the homologue of the desired gene in invertebrates such as flies is not functionally and/or structurally relevant to the corresponding human protein or the proteins might not be well conserved (Nass & Przedborski, 2011). As an example, the LRRK2 protein in humans has an N-terminal domain which does not exist in its homologue in invertebrates, which can lead to a potential limitation (Marín, 2006). Therefore, taking advantage of *D. melanogaster* as an effective model organism is based on the research question.

***Drosophila melanogaster* genetic tools**

With the growing role of *D. melanogaster* in research, greater number of genetic tools have been developed. Forward genetic screens and reverse genetics are two ways of experimental manipulation employed in order to create *D. melanogaster* models of human disease. With the aid of forward genetic screens, phenotype producing genes can be selected in an unbiased manner to be analyzed based on the behavioral or cellular phenotypes produced (Jeibmann & Paulus, 2009). This tool allows researchers to identify unknown genes in a particular pathway, in which selected mutant genes are isolated to be mapped. Furthermore, protein-coding genes that are able to modify the

gene expression (suppressors/enhancer) can be detected through modifier screen in forward genetic screens.

Compared to forward genetics, reverse genetics is conducted to identify the potential function of a known human disease gene. One of the most instrumental manipulation tools which have been applied in reverse genetic is the *Gal4/UAS* system (see Figure 2). For the ectopic expression of a specific gene in tissue and the time-specific manner in *D. melanogaster*, the *Gal4/UAS* system is widely used (Brand & Perrimon, 1993). This binary system comprises two distinct transgenic lines: (1) the directing or driver line carrying the yeast transcription factor encoding *Gal4* transgene, derived from *Saccharomyces cerevisiae*, under any number of tissue-specific promoters, that encourages gene expression and (2) the responsive line have "upstream activating sequences" (UAS) which are the DNA-binding sites of the Gal4 protein positioned next to a gene of interest. Through a number of approaches, a selected gene is located close, usually immediately "downstream", to the UAS sequences, along with a selectable marker to monitor the presence or absence of the transgene. In the absence of the Gal4 protein the responsive transgene is inactive. Thus, after crossing the parental, the directing and the responding, lines, the critical class progeny contains the *Gal4* transgene and *UAS* target gene which can be now activated by the activity of the Gal4 protein (Phelps & Brand, 1998). This system induces the overexpression or inhibition of the gene of interest in the transgenic organism in our desired tissue (Sosa, De Gasperi, & Elder, 2012). For instance, by using *GMR* (glass multiple receptor) transgene in the *Gal4/UAS* system, a specific gene can be expressed in the developing *D. melanogaster*

eye and the resultant organ can be analyzed (Jeibmann & Paulus, 2009). Studying gain of function and loss of function phenotypes of the gene of interest in *D. melanogaster* can provide profound insight about underlying mechanisms in a particular disease.

Another extremely valuable method that has been used in combination with the *Gal4/UAS* system is directed double-stranded RNA interference (RNAi) in which the expression of a gene is inhibited by RNA interference and the phenotypic effect analyzed (Armstrong, Texada, Munjaal, Baker, & Beckingham, 2006). In an RNA-degrading mechanism, a ribonuclease III enzyme, also known as Dicer, was identified in *D. melanogaster* which can produce fragments of 22 nucleotides (Bernstein, Caudy, Hammond, & Hannon, 2001). It is interesting to know that these nucleases are conserved in worms, flies, fungi, and mammals (Agrawal et al., 2003). The single-stranded short interfering fragments, siRNAs, then are integrated into the RNA-induced silencing complex (RISC). RISC will degrade its complementary mRNA throughout the cytoplasm (Armstrong et al., 2006). By preventing the translation of particular mRNA, the expression of the corresponding gene is silenced so that the loss-of-function phenotype can be created which is of great importance in the study of different cellular pathways.

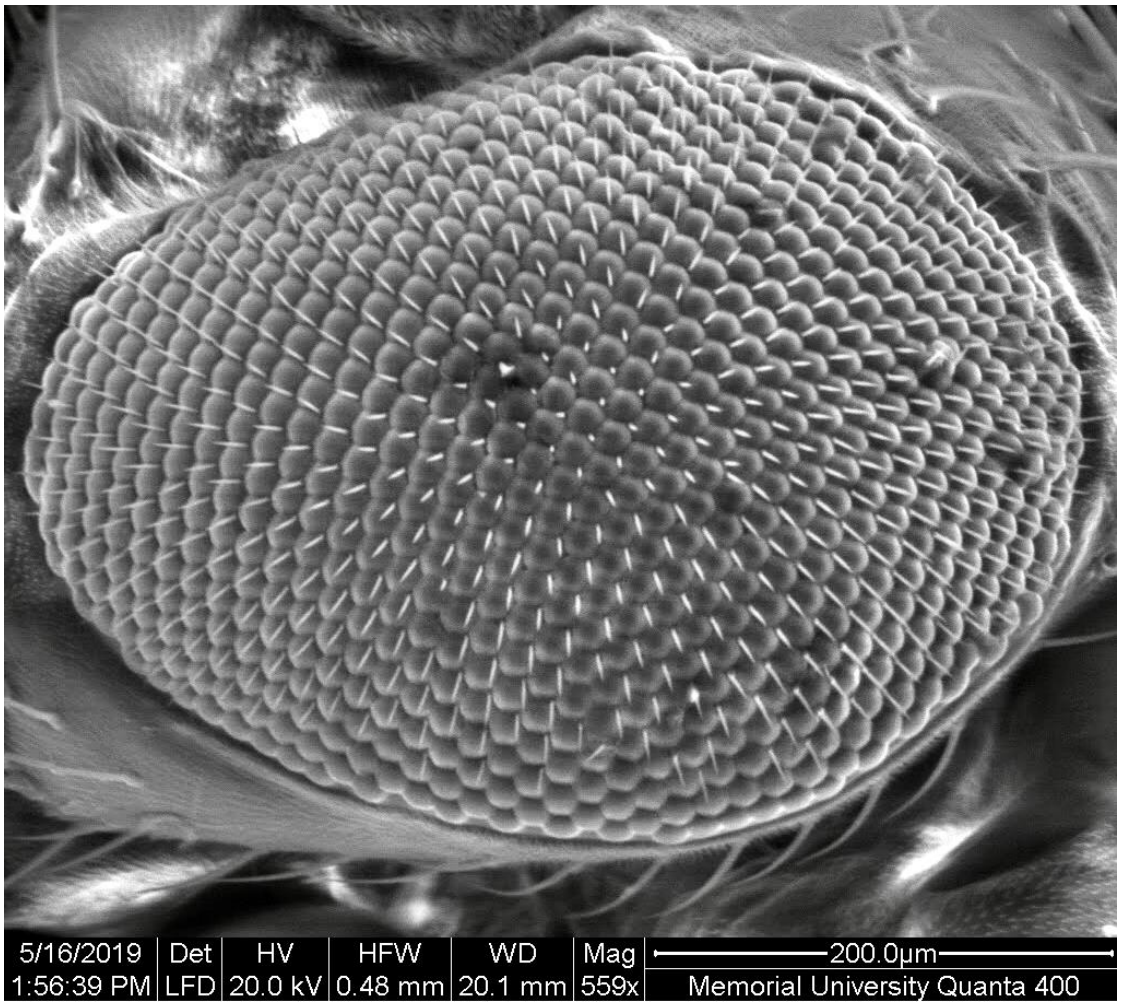

Figure 1. *Drosophila melanogaster* eye: a scanning electron micrograph of *GMR-Gal4; UAS-lacZ*. The genotype of the induvial picture is *GMR-Gal4; UAS-lacZ*. Even shaped ommatidia and a number of interommatidial bristles can be observed via this image of a healthy fly taken by FEI MLA 650F scanning electron microscope (500x magnification).

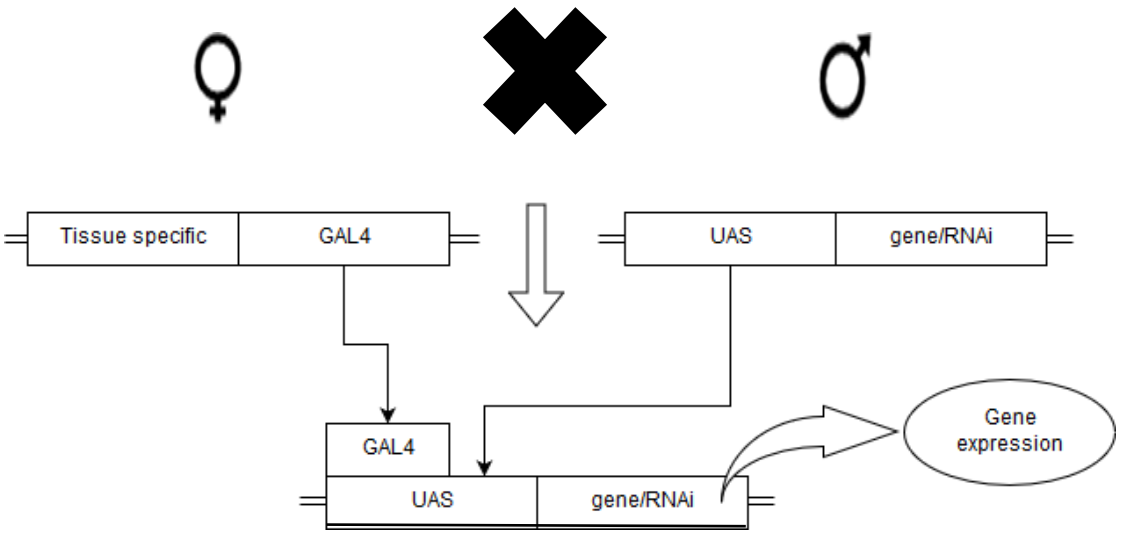

Figure 2. The Gal4/UAS two part directed expression transgenic system. A line encoding the yeast transcription activator protein Gal4 is crossed with a derivative line bearing the Upstream Activation Sequence (*UAS*); Gal4 protein specifically binds to this sequence to activate gene transcription. Gene expression is regulated in a time-specific and tissue-specific manner by promoter or enhancer sequences upstream of Gal4, and the progeny will correspondingly express the gene downstream of the *UAS* sequences (Neckameyer & Argue, 2012). Image was created in draw.io program.

PTPRH* homologues in *Drosophila melanogaster

When the desired gene has been identified as a disease gene, bioinformatics searches of the well-characterized genome of *D. melanogaster* can easily recognize one or more potential homologues (Staveley, 2012). *Ptp10D* and *Ptp4E* are two homologues of *PTPRH* in *D. melanogaster* which are the product of gene duplication. They are characterized by the presence of three to eight FN III repeats as well as three immunoglobulins in extracellular domain, a single PTP cytoplasmic domain, and a single transmembrane domain (Oliva et al., 2016). Following their similarity, Ptp10D and Ptp4E share 89% identity in their catalytic domains which is reduced to 40% compared to other RPTPs (Oliva & Hassan, 2017). Both genes are located on the X chromosome and *Ptp4E* has one less intron than *Ptp10D*. *Ptp4E* is duplicated from *Ptp10D* and is peculiar to drosophilid species. Non-drosophilid species have only one RPTP matching to *Ptp4E/Ptp10D* which is more similar to the ancestral gene, *Ptp10D* (Jeon, Nguyen, Bahri, & Zinn, 2008). Potential common functions are likely due to the similarity in the proteins' structures.

There are six RPTP genes in *D. melanogaster* which are all expressed in CNS neurons (Sun, Bahri, Schmid, Chia, & Zinn, 2000). RPTPs and tyrosine kinases (TKs) are essential in the pathways related to cell growth and neuronal growth cone guidance (Arzan Zarin & Labrador, 2019). However, they regulate these pathways in the opposite way. In cell growth pathways, TKs are receptors and phosphatases are cytoplasmic modulators, while their role in neuronal guidance pathways is vice versa (Jeon et al., 2008). *Ptp4E* is ubiquitously expressed in late stages of embryonic development, whereas *Ptp10D* expression is limited to CNS axons in late embryos (Yang, Seow,

Bahri, Oon, & Chia, 1991). It is found that Ptp4E protein is closely related to Ptp10D due to their partial functional redundancy especially for nervous system phenotypes (Tao et al., 2019). It has been shown that knockdown of *Ptp10D* alone in *Drosophila* has not shown any defects in the embryo. Whereas, double mutants with other members of RPTP family, Ptp69D, produces LOF phenotypes in motor axon guidance which is a crucial step of neural development. Moreover, triple and quadruple LOF mutation of Ptp10D with other RPTP shows severe defects in motor neurons (Arzan Zarin & Labrador, 2019). Later studies have shown that there are no visible phenotypes in *Ptp4E* single mutants which can be explained by compensation by *Ptp10D*. However, double mutant embryos in which *Ptp10D* and *Ptp4E* both are genetically removed have not shown viability and died at hatching stage, but specific phenotypes related to CNS and tracheal cells have been detected (Jeon et al., 2008). These deficiencies have been observed in the formation of longitudinal axons which can be recovered by *Ptp4E* expression in neurons (Oliva & Hassan, 2017). Existing evidence for Ptp4E and Ptp10D having roles in neural growth and development is of great importance in studying PD etiology.

A recent study with the emphasis of identification of new PD candidate genes, by using loss of function RNAi stocks for *Ptp10D* and *Ptp4E* within the Drosophila *α-synuclein* transgenic model system, provided classical LOF alleles for both genes. By screening the results, severe effects on α-synuclein-induced degeneration in the retina were observed in *Ptp10D/RNAi* lines. Although, just one of two available RNAi lines for *Ptp4E* met their threshold criteria (Jansen, et al., 2017). Interestingly, heterozygosity of each gene in isolation did not show an increase in *α-synuclein* dependent retinal

degeneration but trans-heterozygosity for strong alleles showed a substantial enhancement which is consistent with the overlapping functions of these two genes in *D. melanogaster* (Jansen, et al., 2017). It is necessary to investigate both genes to understand the association with PD.

Goals and objectives

The central goal of this study is to explore the association between the *Ptp10D* and *Ptp4E* genes and Parkinson disease by means of a variety of techniques: bioinformatics analyses to examine the conservation of the PTPRH protein and, therefore, likely conserved function, biometric analyses of the eye to determine if a neurodevelopmental affect can be assigned to altered expression, and longevity and locomotor ability over time to evaluate the potential to model PD in flies with altered PTPRH activity.

Materials and methods

Bioinformatics analysis

Identification of the homologue of human *PTPRH* in *Drosophila melanogaster*

The National Center for Biotechnology Information (NCBI) database (*https://www.ncbi.nlm.nih.gov*) was used to identify the amino acid sequence of human PTPRH (Accession number: XP_016882545). In the next step, by using the retrieved protein query from NCBI in tBLASTn search tool (*https://blast.ncbi.nlm.nih.gov/*), two homologues in *Drosophila melanogaster* were identified as Ptp4E and Ptp10D. The accession numbers are respectively NP_001162671.2 and NP_001259453.1.

Identification of additional homologues and conserved domains and creation of a multiple alignment

Since two homologues were found for *PTPRH* in *D. melanogaster*, just *Ptp10D* was considered in the multiple alignments due to its longer sequence. Besides, it has been shown that *Ptp10D* is the ancestor gene (Jeon et al., 2008). The FASTA format of *Drosophila melanogaster* Ptp10D protein query with the accession number of AGB95296.1 was obtained from the National Center for Biotechnology Information (NCBI). tBLASTn, which is one of the basic local alignment search tools, was employed to recognize the homologues of *D. melanogaster Ptp10D* in vertebrates and invertebrates. Amongst the available isoforms, the one with the highest coverage percentage in the query and highest total score was chosen as the homologue of this

gene. By using the Clustal Omega program (*https://www.ebi.ac.uk/Tools/msa/clustalo/*) a multiple sequence alignment was done to show the similarity among the proteins. Conserved domains for each sequence were identified by NCBI conserved domains database and Pfam (Sanger Institute) (*https://pfam.xfam.org*).The accession numbers of protein queries used in the alignment are as following: *Drosophila melanogaster Ptp10D* (accession number NP_001259453), *Homo sapiens PTPRH* (accession number XP_016882545.1), *Mus musculus PTPRH* (accession number NP_997153.2), *Pan troglodytes PTPRH* (accession number XP_009434687.3), *Culex quinquefasciatus Ptp10D* (accession number XP_001847466.1), and *Aedes aegypti Ptp10D* (accession number XP_021705337.1).

D. melanogaster **culturing and crosses**

D. melanogaster **stocks**

In this study the control responder line, *UAS-lacZ*, and all the *Gal4*-bearing transgenic lines, which are *GMR-Gal4*, *TH-Gal4*, *DDC-Gal4*, and *D42-Gal4*, were obtained from the Bloomington Drosophila Stock Center (Indiana University, IN, USA). There were five experimental lines related to *Ptp10D* gene; one overexpression line and four inhibition lines, including *UAS-Ptp10D-RNA*^{v8010} *(II)*, *UAS-Ptp10D-RNAi*^{v1104}, and *UAS-Ptp10D-RNAi*^{KK101775} were purchased from Vienna Drosophila Resource Center in Vienna, Austria. For *Ptp4E*, the two inhibition lines were obtained from Bloomington Drosophila Stock Centre.

D. melanogaster media

A standard Drosophila medium was used to keep *Drosophila melanogaster* stocks properly. This media consists of 65g/L cornmeal, 15 g/L yeast, 5.5 g/L agar and 50ml/L fancy grade molasses in water with 5 ml of 0.1 g/mL methyl paraben in ethanol and 2.5 mL of propionic acid to prevent mold growth. Afterward, 7 ml of medium was poured to each vial to solidify and then stored at 4 to 6°C. The medium was produced by Dr. Brian E. Staveley approximately twice a month.

Table 2: Genotypes of all stocks used in this research

Genotype	Abbreviation	Expression Pattern	Reference
Control line			
w; UAS-lacZ^{4-1-2}	*UAS-lacZ*	---	(Brand & Perrimon, 1993)
Experimental lines			
w[1118] P{w[+mC]=EP}Ptp10D[EP1172]	*UAS-Ptp10D^{EP1172}*	---	(Rorth et al., 1998)
y[1] sc[*] v[1]; P{y[+t7.7] v[+t1.8]=TRiP.HMS01917}attP2	*UAS-Ptp10D-RNAi^{HMS01917}*	---	(Perkins, et al., 2015)
P{KK101775}VIE-260B	*UAS-Ptp10D-RNAi^{KK101775}*	---	(Dietzl et al., 2007)
w[1118]; P{GD115}v1104/TM3	*UAS-Ptp10D-RNAi^{v1104}*	---	(Dietzl et al., 2007)
w[1118]; P{GD2611}v8010	*UAS-Ptp10D-RNA^{v8010}*	---	(Dietzl et al., 2007)
y[1] sc[*] v[1]; P{y[+t7.7] v[+t1.8]=TRiP.HMS01838}attP2	*UAS-Ptp4E-RNAi^{HMS01838}*	---	(Dietzl et al., 2007)
y[1] v[1]; P{y[+t7.7] v[+t1.8]=TRiP.HMS05000}attP40	*UAS-Ptp4E-RNAi^{HMS05000}*		(Perkins, et al., 2015)
Transgenic lines			
w; GMR-GAL4^{12}	*GMR-Gal4*	Eye	(Freeman, 1996)
w^{1118}; P{Ddc-GAL4.L}$^{4.3D}$	*DDC-Gal4*	Neuron	(Li, Chaney, Forte, & Hirsh, 2000)
w*; P{ple-GAL4.F}^{3}	*TH-Gal4*	Dopaminergic neuron	(Friggi-Grelin, Iche, & Birman, 2003)
w[*]; P{w[+mW.hs]=GawB}D42	*D42-Gal4*	Motor neuron	(Yeh, Gustafson, & Boulianne, 1995)

Drosophila melanogaster crosses

The appropriate temperature for storing the stocks is room temperature (typically 20 to 22°C). The desired genotype, often composed of UAS or Gal4, was considered when choosing the male and female *Drosophila melanogaster* for breeding. For all the crosses virgin females and males were obtained respectively from experimental *UAS*-bearing responder l lines and *Gal4*-containing transgenic lines. Matings were carried out upon fresh media after virgin females were isolated, every 8 to 12 hours and males were 24 hours. For the mating process, 3 to 5 females and 2 to 3 males were introduced to each mating vial. Flies were then transferred onto fresh media three times for every 2 to 3 days for more productive matings. As soon as eclosion had taken place, paternal flies were discarded, and the male progeny of the critical class were collected. Since a *UAS-Ptp4E-RNAi*^{HMS05000} bearing line possesses the *CyO* balancer chromosome, careful consideration was given when collecting respective critical class males, and the progenies with *Curly* wings were all discarded.

Biometric analysis of the *Drosophila melanogaster* compound eye

The effects on the number of ommatidia and interommatidial bristles were determined by detailed biometric analysis of the *D. melanogaster* compound eye. As eclosure occurs, the critical class male progeny resulted from the selected crosses were collected and matured for 3 to 5 days in groups of 20 or less upon standard Drosophila medium at room temperature. The flies were frozen at -80°C, and eventually thawed and finally placed upon aluminium Scanning Electron Microscopy studs. Using forceps, the

flies were carefully placed on their right side so that the left eye would face upwards. Approximately 20 flies of each critical class were prepared and imaged. Scanning electron microscope photography was carried out after 48 hours of sample desiccation. The Mineral Liberation Analyzer 650F was employed to scan the left eye of every single male fly. Ten images were chosen as a sample for each cross, which had the best quality and clarity, and then the image analysis was done by the software program ImageJ (*https://imagej.nih.gov/ij/*) by counting the number of ommatidia and interommatidial bristles with cell counter. Graphpad Prism 8 (Graphpad Software Inc.) was used in order to analyze obtained data as well as the calculation of mean ± standard error of the mean. Parametric statics were utilized for the analysis since the data was obtained randomly from a normal distribution. By means of unpaired T-test (two-tailed), significant differences between crosses were determined. Results were considered statistically significant where the p-value was less than 0.05.

Behavioural Assays

Ageing assay

To study the life span of selected critical class flies in comparison with control (unaffected) flies, a survival analysis was carried out. Initially, the male progeny of the critical classes were collected from each cross under gaseous carbon dioxide (CO_2) on a daily basis. The flies were maintained under ideal conditions, with up to 20 flies per vial to prevent overcrowding and on fresh standard medium at 25°C. This process continued until the collection of approximately 300 male critical class flies per cross

which typically took one to three weeks depending on the experiment. On the second day after the collection of flies the observation began in which the number of dead flies was recorded. Flies are considered to be dead when there was no movement detected (Staveley et al., 1990). The vials were scored every two days until the last fly in the cohort was dead. The medium was changed whenever there was a dead fly in the vial as well as no less than twice a week to maintain ideal condition for all remaining flies. All the data then transferred to Graphpad Prism 8 (Graphpad Software Inc.) and then survival curves were analyzed by using the log-rank test with significance considered at $p < 0.05$ with Bonferroni correction.

Locomotion assay

The motor control of flies was studied during their life span through a locomotor analysis which involved collecting 70 critical class male progeny flies from each breeding on the same day of eclosure, distributing and maintaining in seven vials (ten flies per each vial) and then transferring them to a new medium twice a week over the period the experiment. To maintain ideal conditions, all the vials were kept at 25°C. Beginning with one week after collection; the ability of flies to climb was assessed every seven days. Each group consisting of ten flies per genotype underwent ten trials to make a total of 500 trials per week. Each trial lasted for 10 seconds during which I actively observed the tube to record the data. A 1.5-cm diameter glass tube with a length of 30 cm was used to determine climbing ability which was gauged by reaching or surpassing 2 cm intervals of the glass tube, as described by Todd and Staveley, 2008. The

measurement of climbing ability was repeated every seven days. The index was calculated through the equation: Climbing index = Σ nm/N where n is the number of flies at a given level, m is the score of the level which is between one and five and N is the total number of flies climbed in that trial. These data were analyzed by the software GraphPad Prism 8 (GraphPad Software Inc.). Finally, a nonlinear regression curve was used to show the analysis of 5-climbing index as a function of time for each genotype with 95% confidence intervals within a graph. The decrease in climbing ability is shown when there is a slope in the graph and the initial climbing ability is represented by Y-intercept. Both parameters are calculated for each curve. Slopes of the curves were compared using a 95% confidence interval and they were considered statistically significant where the p-value was ≤ 0.05.

Results

Bioinformatics analysis

Identification of *PTPRH* homologues in *Drosophila melanogaster* and conserved domains

The amino acid sequence of *Homo sapiens* PTPRH protein was obtained from NCBI (XP_016882545.1). A tBLASTn search was conducted on the *D. melanogaster* genome and *PTP10D* and *PTP4E* genes, which are the product of a gene duplication, were identified as the most similar ones compared to *PTPRH*. The alignment shows that the percentage of query covered by the database sequence for Ptp10D and PTP4E proteins are 90% and 89%, respectively. The highest percent identity of the queries for Ptp10D is 44.03%, and for Ptp4E it is 43.97%. The multiple alignment of these three sequences in Clustal Omega shows that the Protein-tyrosine phosphatase (PTP) domain and Fibronectin type III (FN3) domains are conserved between each of these proteins in *D. melanogaster* and PTPRH in human (Figures 3 & 4).

The PTPRH protein is conserved between vertebrates and invertebrates

To conduct a multiple alignment of the PTPRH proteins from vertebrates and invertebrates, sequences from *D. melanogaster* (NP_001259453), *Culex quinquefasciatus* (XP_001847466.1), *Aedes aegypti* (XP_021705337.1), *Homo sapiens* (XP_016882545.1), *Mus musculus* (NP_997153.2), and *Pan troglodytes* (XP_009434687.3) were used. These sequences were identified by tBLASTn search. The alignment shows that the Protein-tyrosine phosphatase (PTP) domain and FN(III)

domains are conserved in both vertebrates and invertebrates. However, there are some domains related to FN3 repeats that were specific to either invertebrates or vertebrates (Figure 5). The illustration in Figure 6 shows the conserved domain between the PTPRH protein in *H. sapiens* and its homologues in *D. melanogaster*: Ptp10D and Ptp4E. Ptp10D is the longest protein (1653 aa) with nine FN3 domains and one PTP domain, which is the longest domain and is completely conserved between all species. Ptp4E with 1615 aa length has eight FN3 domains and one PTP domain. PTPRH is the shortest protein (1137 aa) with six FN3 domains and one PTP domain.

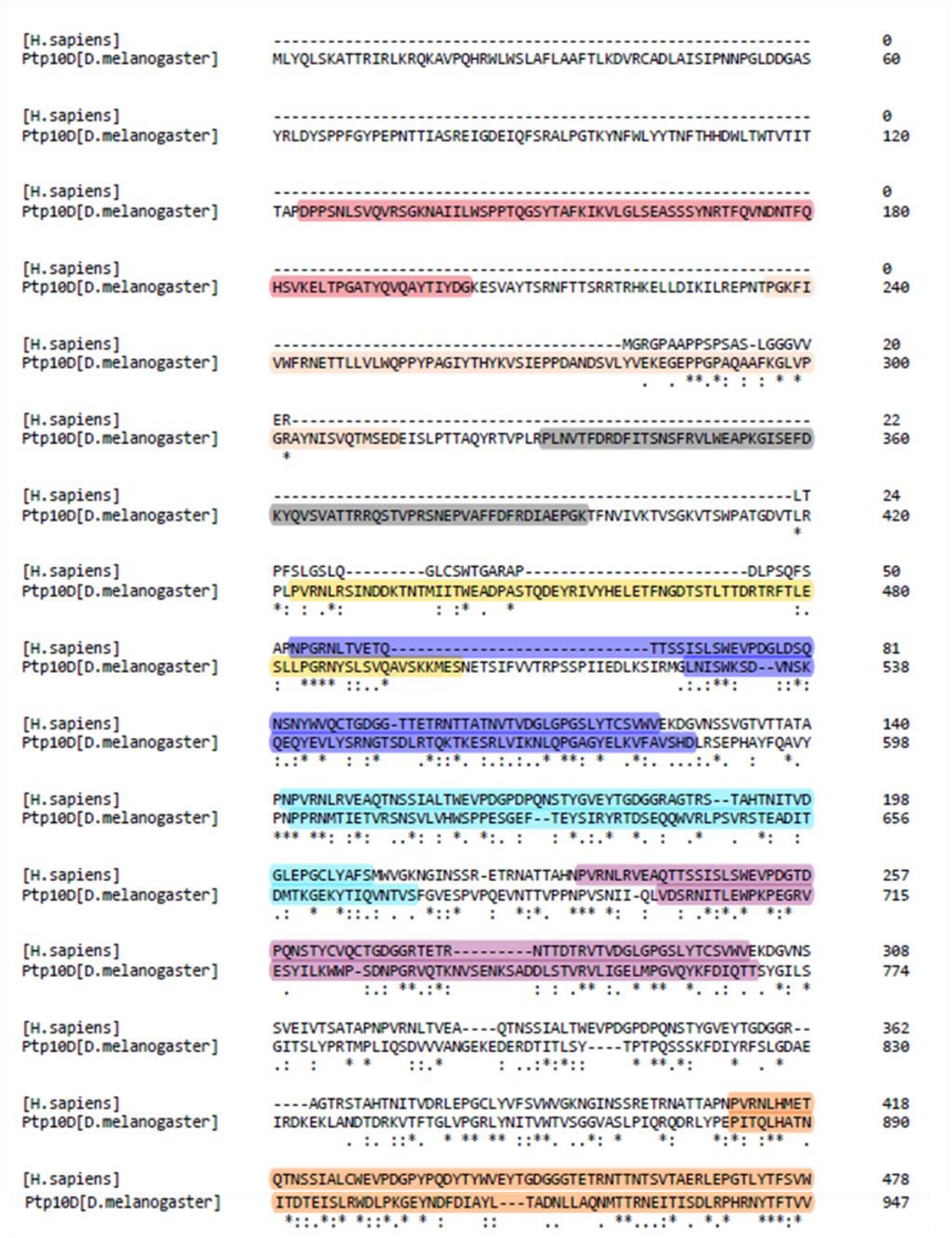
[H.sapiens]
Ptp10D[D.melanogaster]
0
60
120
180
240
20
300
22
360
24
420
50
480
81
538
140
598
198
656
257
715
308
774
362
830
418
890
478
947

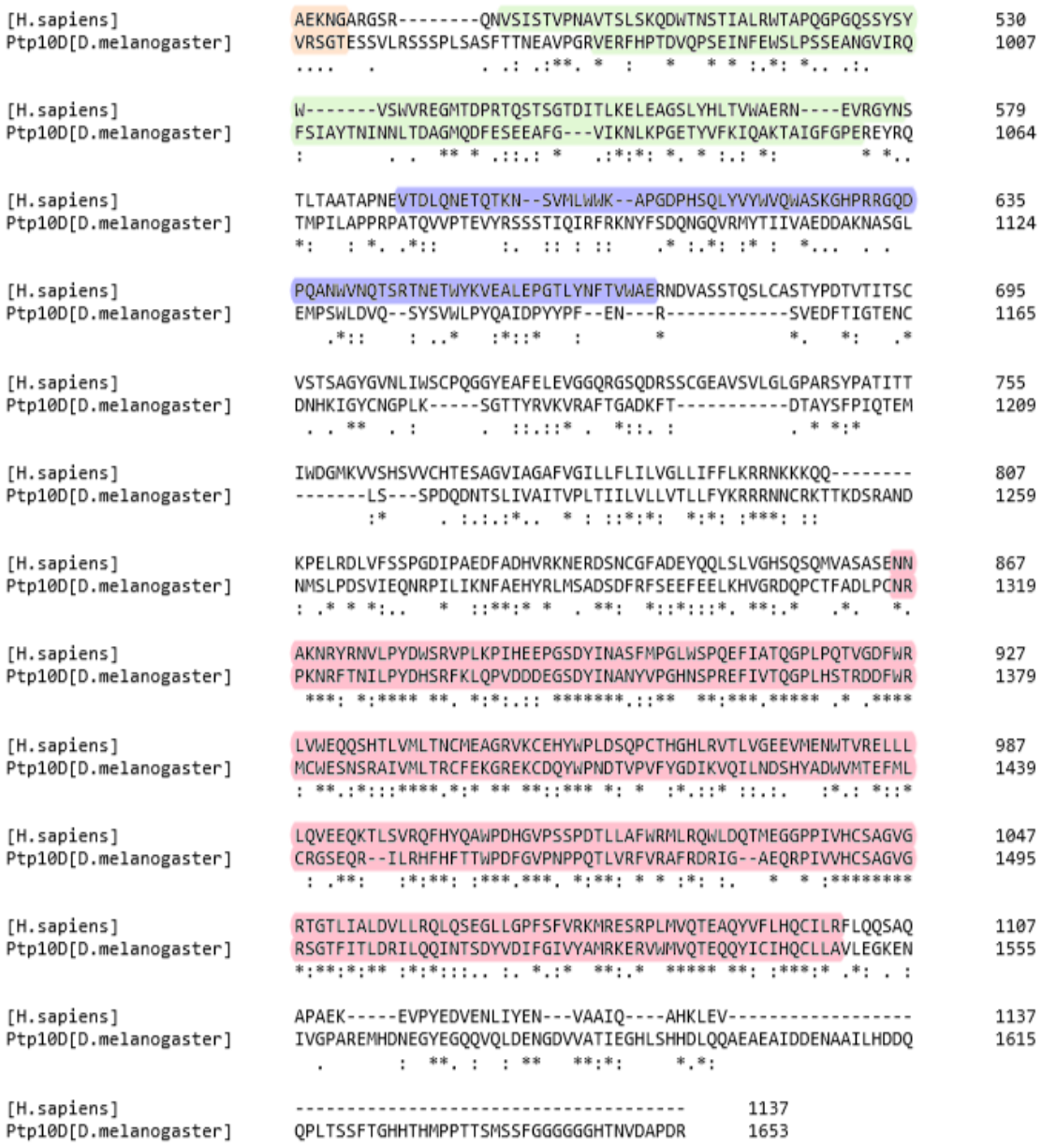

Figure 3: Alignment of human PTPRH with *Drosophila melanogaster* Ptp10D
Highlighted regions represent fibronectin type III (FN3) domains except the last highlighted region (pink) which is protein tyrosine phosphatase (PTP) domain. Protein sequences obtained from BLAST and conserved domains of each sequence obtained from Pfam. ‘‘*’’ indicates fully conserved amino acids in aligned sequences. ‘‘:’’ indicates conserved amino acid with less similar properties and ‘‘.’’ indicates semi-conserved substitutions.


[H.sapiens] ---------- 0
Ptp4E[D.melanogaster] MDCATRKQQQLRAHHQQQQIQIQTHGRKRQQLQKQRHNHHHYYQNSQQQQKHFVWLVVGI 60
[H.sapiens] ---------- 0
Ptp4E[D.melanogaster] LTIFLAQHANAADLVINVPNASSNANAFYRIDYSPPFGFPEPNTTIPASDIGKDIKFSRA 120
[H.sapiens] ---------- 0
Ptp4E[D.melanogaster] LPGTEYNFWLYYTNSTHREQLTWTVNITTAPDPPANLSVQLRSSKSAFITWRPPGSGRYS 180
[H.sapiens] ---------- 0
Ptp4E[D.melanogaster] GFRIRVLGLTDLPFERSYSLEGNETLQLSAKELTPGGSYQVQAYSVYQGKESVAYTSRNF 240
[H.sapiens] ---------- 0
Ptp4E[D.melanogaster] TTKPNTPGKFIVWFRNETTLLVLWQPPFPAGIYTHYRVSITPDDAIQSVLYVEREGEPPG 300
[H.sapiens] ---------- 0
Ptp4E[D.melanogaster] PAQAAFKGLVPGREYNISVQTVSEDETSSVPTTARYLTVPERVLNVTFDEAYTTSSSFRV 360
[H.sapiens] ---------- 0
Ptp4E[D.melanogaster] RWEPPRTYSEFDAYQVMLSTSRRIFNVPRAANGDSVYFDYPDILEPGRTYEVVVKTIADN 420
[H.sapiens] -----MGRGPAAPPSPSASLGGGVVER---------- 22
Ptp4E[D.melanogaster] VNSWPASGEVTLRPRPVRSLGGFLDDRSNALHISWEPAETGRQDSYRISYHEQTNASEVP 480
[H.sapiens] --------------LTPFSLGSLQGLCSW----------TGARAPDLPSQFSAPNPGRNL 58
Ptp4E[D.melanogaster] APFPVAAESQITTNLTEYTLDSLLAGRRYLIAVQALSKGVASNASDIT-RYTR--PAAPL 537
[H.sapiens] TVE-TQTTSSISLSWEVPDGLDSQNSNYWVQCTGDGGTT-ETRNTTATNVTVDGLGPGSL 116
Ptp4E[D.melanogaster] IQELRSIDQGLMLSWRSD--VNSRQDRYEVHYQRNGTREERTMATNETSLTIHYLHPGSG 595
[H.sapiens] YTCSVWVEKDGVNSSVGTVTTATAPNPVRNLRVEAQTNSSIALTWEVPDGPDPQNSTYGV 176
Ptp4E[D.melanogaster] YEVKVHAISHGVRSEPHSYFQAVFPKPPQNLTLQTVHTNLVVLHWQAPEGSDFS--EYVV 653
[H.sapiens] EYTGDGGRAGTRSTAHTN-ITVDGLEPGCLYAFSMWVGKNGINSSRET-RNATTAHNPVR 234
Ptp4E[D.melanogaster] RYRTDASPWQRISGLHENEARIKDMHYGERYLVQVNTVSFGVESPHPLELNVTMPPQPVS 713
[H.sapiens] NLRVEAQTTSSISLSWEVPDGTDPQNSTYCVQCTGDGGR--------TETRNTTDTRVTV 286
Ptp4E[D.melanogaster] NV-VPLVDSRNLTLEWPRPDGHVDFYTLKWWP-TDEEDRVEFKNVTQLEDLSSPSVRIPI 771
[H.sapiens] DGLGPGSLYTCSVWVEKDGVNSSVEIVTSATAPNPVRNLT-----VEAQTNSSIALTWEV 341
Ptp4E[D.melanogaster] EDLSPGRQYRFEVQASSNGIRSGTTHLSTRTMPLIQSDVFIANAGHEQGQDETITLSYT- 830
[H.sapiens] PDGPDPQNSTYGVEYT---GD---GGRAGTRSTAHTNITVDRLEPGCLYVFSVWVGKNGI 395
Ptp4E[D.melanogaster] ---PTPADSTRFDIYRFSMGDPTIKDKEKLANDTERKLSFSGLTPGKLYNVTVWTVSGGV 887
[H.sapiens] NSSRETRNATTAPNPVRNLHMETQTNSSIALCWEVPDGPYPQDYTYWVEYTGDGGGTETR 455
Ptp4E[D.melanogaster] ASLPVQRLYRLHPLPISDLKAIQVAAREITLHWTAPAGEYTDFELQYLSADEEAPQLLQN 947

Figure 4: Alignment of human PTPRH with *Drosophila melanogaster* Ptp4E
Highlighted regions represent fibronectin type III (FN3) domains except the last highlighted region (pink) which is protein tyrosine phosphatase (PTP) domain. Protein sequences obtained from BLAST and conserved domains of each sequence obtained from Pfam. ‘‘*’’ indicates fully conserved amino acids in aligned sequences. ‘‘:’’ indicates conserved amino acid with less similar properties and ‘‘.’’ indicates semi-conserved substitutions.

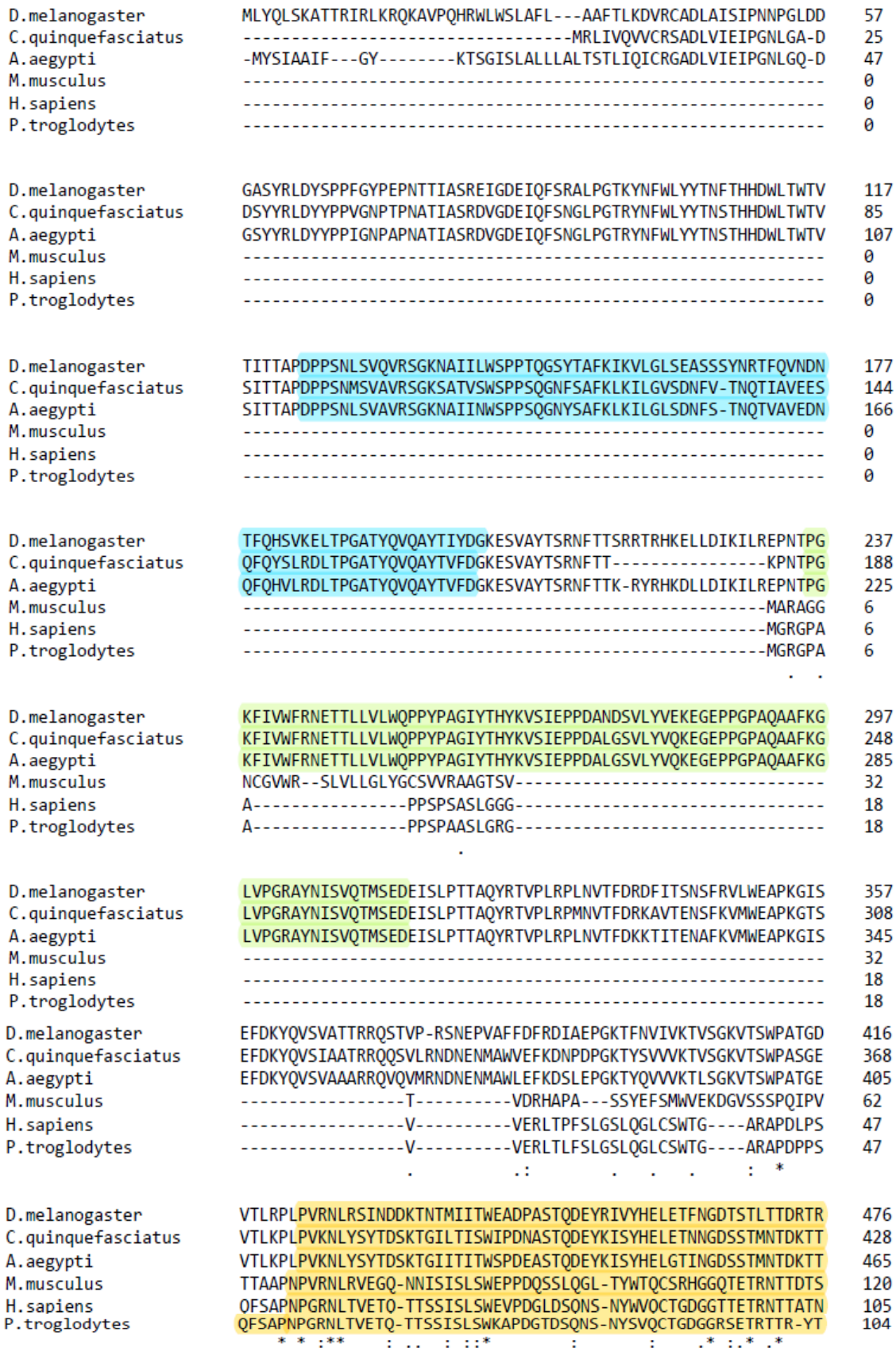
D.melanogaster MLYQLSKATTRIRLKRQKAVPQHRWLWSLAFL---AAFTLKDVRCADLAISIPNNPGLDD 57
C.quinquefasciatus ----------MRLIVQVVCRSADLVIEIPGNLGA-D 25
A.aegypti -MYSIAAIF---GY--------KTSGISLALLLALTSTLIQICRGADLVIEIPGNLGQ-D 47
M.musculus 0
H.sapiens 0
P.troglodytes 0
D.melanogaster GASYRLDYSPPFGYPEPNTTIASREIGDEIQFSRALPGTKYNFWLYYTNFTHHDWLTWTV 117
C.quinquefasciatus DSYYRLDYYPPVGNPTPNATIASRDVGDEIQFSNGLPGTRYNFWLYYTNSTHHDWLTWTV 85
A.aegypti GSYYRLDYYPPIGNPAPNATIASRDVGDEIQFSNGLPGTRYNFWLYYTNSTHHDWLTWTV 107
M.musculus 0
H.sapiens 0
P.troglodytes 0
D.melanogaster TITTAPDPPSNLSVQVRSGKNAIILWSPPTQGSYTAFKIKVLGLSEASSSYNRTFQVNDN 177
C.quinquefasciatus SITTAPDPPSNMSVAVRSGKSATVSWSPPSQGNFSAFKLKILGVSDNFV-TNQTIAVEES 144
A.aegypti SITTAPDPPSNLSVAVRSGKNAIINWSPPSQGNYSAFKLKILGLSDNFS-TNQTVAVEDN 166
M.musculus 0
H.sapiens 0
P.troglodytes 0
D.melanogaster TFQHSVKELTPGATYQVQAYTIYDGKESVAYTSRNFTTSRRTRHKELLDIKILREPNTPG 237
C.quinquefasciatus QFQYSLRDLTPGATYQVQAYTVFDGKESVAYTSRNFTT----------KPNTPG 188
A.aegypti QFQHVLRDLTPGATYQVQAYTVFDGKESVAYTSRNFTTK-RYRHKDLLDIKILREPNTPG 225
M.musculus ----------MARAGG 6
H.sapiens ----------MGRGPA 6
P.troglodytes ----------MGRGPA 6
D.melanogaster KFIVWFRNETTLLVLWQPPYPAGIYTHYKVSIEPPDANDSVLYVEKEGEPPGPAQAAFKG 297
C.quinquefasciatus KFIVWFRNETTLLVLWQPPYPAGIYTHYKVSIEPPDALGSVLYVQKEGEPPGPAQAAFKG 248
A.aegypti KFIVWFRNETTLLVLWQPPYPAGIYTHYKVSIEPPDALGSVLYVQKEGEPPGPAQAAFKG 285
M.musculus NCGVWR--SLVLLGLYGCSVVRAAGTSV---------- 32
H.sapiens A----------PPSPSASLGGG---------- 18
P.troglodytes A----------PPSPAASLGRG---------- 18
D.melanogaster LVPGRAYNISVQTMSEDEISLPTTAQYRTVPLRPLNVTFDRDFITSNSFRVLWEAPKGIS 357
C.quinquefasciatus LVPGRAYNISVQTMSEDEISLPTTAQYRTVPLRPMNVTFDRKAVTENSFKVMWEAPKGTS 308
A.aegypti LVPGRAYNISVQTMSEDEISLPTTAQYRTVPLRPLNVTFDKKTITENAFKVMWEAPKGIS 345
M.musculus ---------- 32
H.sapiens ---------- 18
P.troglodytes ---------- 18
D.melanogaster EFDKYQVSVATTRRQSTVP-RSNEPVAFFDFRDIAEPGKTFNVIVKTVSGKVTSWPATGD 416
C.quinquefasciatus EFDKYQVSIAATRRQQSVLRNDNENMAWVEFKDNPDPGKTYSVVVKTVSGKVTSWPASGE 368
A.aegypti EFDKYQVSVAAARRQVQVMRNDNENMAWLEFKDSLEPGKTYQVVVKTLSGKVTSWPATGE 405
M.musculus ----------T----------VDRHAPA---SSYEFSMWVEKDGVSSSPQIPV 62
H.sapiens ----------V----------VERLTPFSLGSLQGLCSWTG----ARAPDLPS 47
P.troglodytes ----------V----------VERLTLFSLGSLQGLCSWTG----ARAPDPPS 47
D.melanogaster VTLRPLPVRNLRSINDDKTNTMIITWEADPASTQDEYRIVYHELETFNGDTSTLTTDRTR 476
C.quinquefasciatus VTLKPLPVKNLYSYTDSKTGILTISWIPDNASTQDEYKISYHELETNNGDSSTMNTDKTT 428
A.aegypti VTLKPLPVKNLYSYTDSKTGIITITWSPDEASTQDEYKISYHELGTINGDSSTMNTDKTT 465
M.musculus TTAAPNPVRNLRVEGQ-NNISISLSWEPPDQSSLQGL-TYWTQCSRHGGQTETRNTTDTS 120
H.sapiens QFSAPNPGRNLTVETQ-TTSSISLSWEVPDGLDSQNS-NYWVQCTGDGGTTETRNTTATN 105
P.troglodytes QFSAPNPGRNLTVETQ-TTSSISLSWKAPDGTDSQNS-NYSVQCTGDGGRSETRTTR-YT 104

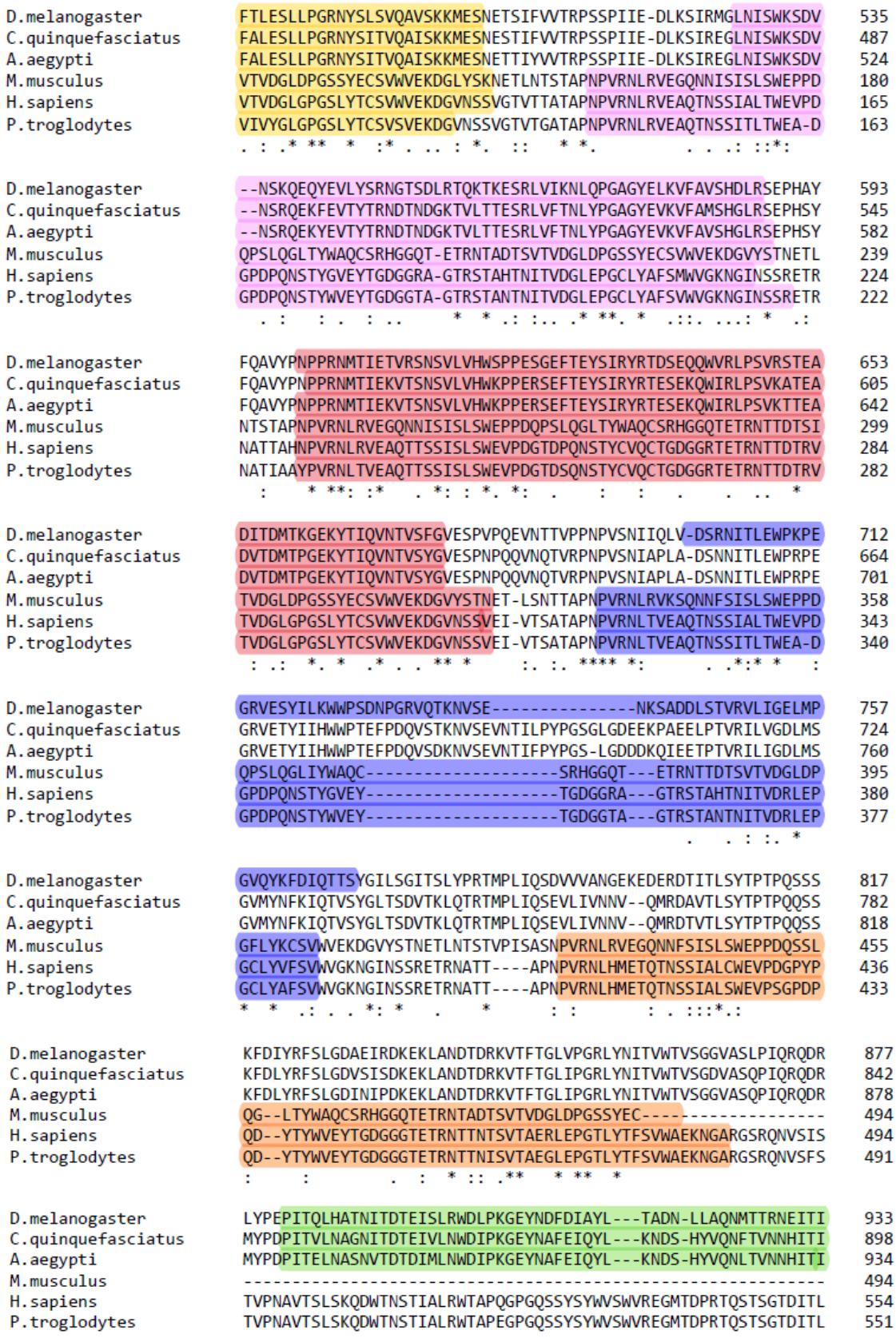
D.melanogaster FTLESLLPGRNYSLSVQAVSKKMESNETSIFVVTRPSSPIIE-DLKSIRMGLNISWKSDV 535
C.quinquefasciatus FALESLLPGRNYSITVQAISKKMESNESTIFVVTRPSSPIIE-DLKSIREGLNISWKSDV 487
A.aegypti FALESLLPGRNYSITVQAISKKMESNETTIYVVTRPSSPIIE-DLKSIREGLNISWKSDV 524
M.musculus VTVDGLDPGSSYECSVWVEKDGLYSKNETLNTSTAPNPVRNLRVEGQNNISISLSWEPPD 180
H.sapiens VTVDGLGPGSLYTCSVWVEKDGVNSSVGTVTTATAPNPVRNLRVEAQTNSSIALTWEVPD 165
P.troglodytes VIVYGLGPGSLYTCSVSVEKDGVNSSVGTVTGATAPNPVRNLRVEAQTNSSITLTWEA-D 163
--NSKQEQYEVLYSRNGTSDLRTQKTKESRLVIKNLQPGAGYELKVFAVSHDLRSEPHAY 593
--NSRQEKFEVTYTRNDTNDGKTVLTTESRLVFTNLYPGAGYEVKVFAMSHGLRSEPHSY 545
--NSRQEKYEVTYTRNDTNDGKTVLTTESRLVFTNLYPGAGYEVKVFAVSHGLRSEPHSY 582
QPSLQGLTYWAQCSRHGGQT-ETRNTADTSVTVDGLDPGSSYECSVWVEKDGVYSTNETL 239
GPDPQNSTYGVEYTGDGGRA-GTRSTAHTNITVDGLEPGCLYAFSMWVGKNGINSSRETR 224
GPDPQNSTYWVEYTGDGGTA-GTRSTANTNITVDGLEPGCLYAFSVWVGKNGINSSRETR 222
FQAVYPNPPRNMTIETVRSNSVLVHWSPPESGEFTEYSIRYRTDSEQQWVRLPSVRSTEA 653
FQAVYPNPPRNMTIEKVTSNSVLVHWKPPERSEFTEYSIRYRTESEKQWIRLPSVKATEA 605
FQAVYPNPPRNMTIEKVTSNSVLVHWKPPERSEFTEYSIRYRTESEKQWIRLPSVKTTEA 642
NTSTAPNPVRNLRVEGQNNISISLSWEPPDQPSLQGLTYWAQCSRHGGQTETRNTTDTSI 299
NATTAHNPVRNLRVEAQTTSSISLSWEVPDGTDPQNSTYCVQCTGDGGRTETRNTTDTRV 284
NATIAAYPVRNLTVEAQTTSSISLSWEVPDGTDSQNSTYCVQCTGDGGRTETRNTTDTRV 282
DITDMTKGEKYTIQVNTVSFGVESPVPQEVNTTVPPNPVSNIIQLV-DSRNITLEWPKPE 712
DVTDMTPGEKYTIQVNTVSYGVESPNPQQVNQTVRPNPVSNIAPLA-DSNNITLEWPRPE 664
DVTDMTPGEKYTIQVNTVSYGVESPNPQQVNQTVRPNPVSNIAPLA-DSNNITLEWPRPE 701
TVDGLDPGSSYECSVWVEKDGVYSTNET-LSNTTAPNPVRNLRVKSQNNFSISLSWEPPD 358
TVDGLGPGSLYTCSVWVEKDGVNSSVEI-VTSATAPNPVRNLTVEAQTNSSIALTWEVPD 343
TVDGLGPGSLYTCSVWVEKDGVNSSVEI-VTSATAPNPVRNLTVEAQTNSSITLTWEA-D 340
GRVESYILKWWPSDNPGRVQTKNVSE---------------NKSADDLSTVRVLIGELMP 757
GRVETYIIHWWPTEFPDQVSTKNVSEVNTILPYPGSGLGDEEKPAEELPTVRILVGDLMS 724
GRVETYIIHWWPTEFPDQVSDKNVSEVNTIFPYPGS-LGDDDKQIEETPTVRILIGDLMS 760
QPSLQGLIYWAQC-------------------SRHGGQT---ETRNTTDTSVTVDGLDP 395
GPDPQNSTYGVEY-------------------TGDGGRA---GTRSTAHTNITVDRLEP 380
GPDPQNSTYWVEY-------------------TGDGGTA---GTRSTANTNITVDRLEP 377
GVQYKFDIQTTSYGILSGITSLYPRTMPLIQSDVVVANGEKEDERDTITLSYTPTPQSSS 817
GVMYNFKIQTVSYGLTSDVTKLQTRTMPLIQSEVLIVNNV--QMRDAVTLSYTPTPQQSS 782
GVMYNFKIQTVSYGLTSDVTKLQTRTMPLIQSEVLIVNNV--QMRDTVTLSYTPTPQQSS 818
GFLYKCSVWVEKDGVYSTNETLNTSTVPISASNPVRNLRVEGQNNFSISLSWEPPDQSSL 455
GCLYVFSVWVGKNGINSSRETRNATT----APNPVRNLHMETQTNSSIALCWEVPDGPYP 436
GCLYAFSVWVGKNGINSSRETRNATT----APNPVRNLHMETQTNSSIALSWEVPSGPDP 433
KFDIYRFSLGDAEIRDKEKLANDTDRKVTFTGLVPGRLYNITVWTVSGGVASLPIQRQDR 877
KFDLYRFSLGDVSISDKEKLANDTDRKVTFTGLIPGRLYNITVWTVSGDVASQPIQRQDR 842
KFDLYRFSLGDINIPDKEKLANDTDRKVTFTGLIPGRLYNITVWTVSGGVASQPIQRQDR 878
QG--LTYWAQCSRHGGQTETRNTADTSVTVDGLDPGSSYEC----------------- 494
QD--YTYWVEYTGDGGGTETRNTTNTSVTAERLEPGTLYTFSVWAEKNGARGSRQNVSIS 494
QD--YTYWVEYTGDGGGTETRNTTNISVTAEGLEPGTLYTFSVWAEKNGARGSRQNVSFS 491
LYPEPITQLHATNITDTEISLRWDLPKGEYNDFDIAYL---TADN-LLAQNMTTRNEITI 933
MYPDPITVLNAGNITDTEIVLNWDIPKGEYNAFEIQYL---KNDS-HYVQNFTVNNHITI 898
MYPDPITELNASNVTDTDIMLNWDIPKGEYNAFEIQYL---KNDS-HYVQNLTVNNHITI 934
---------- 494
TVPNAVTSLSKQDWTNSTIALRWTAPQGPGQSSYSYWVSWVREGMTDPRTQSTSGTDITL 554
TVPNAVTSLSKQDWTNSTIALRWTAPEGPGQSSYSYWVSWVREGMTDPRTQSTSGTDITL 551

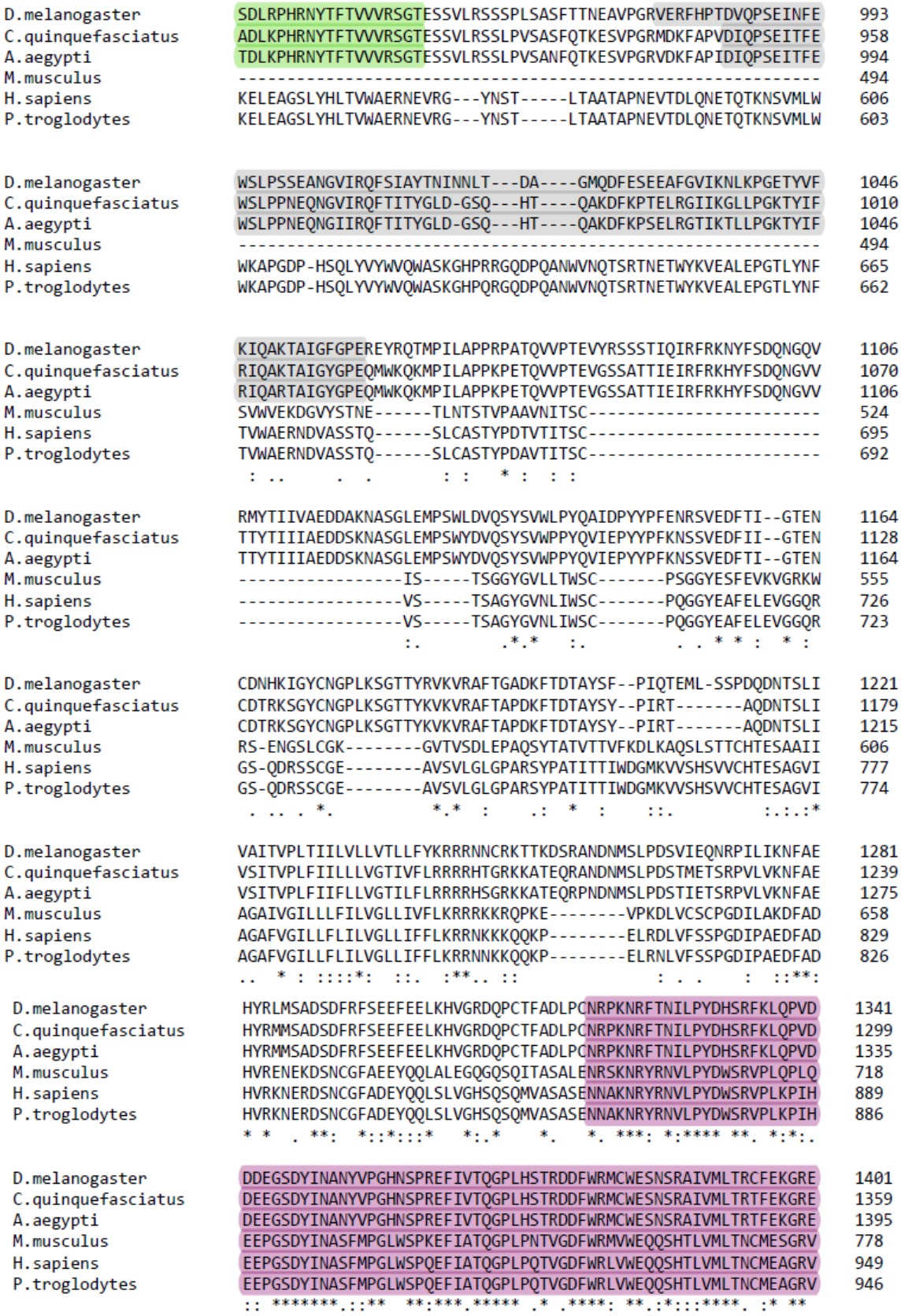
D.melanogaster SDLRPHRNYTFTVVVRSGTESSVLRSSSPLSASFTTNEAVPGRVERFHPTDVQPSEINFE 993
C.quinquefasciatus ADLKPHRNYTFTVVVRSGTESSVLRSSLPVSASFQTKESVPGRMDKFAPVDIQPSEITFE 958
A.aegypti TDLKPHRNYTFTVVVRSGTESSVLRSSLPVSANFQTKESVPGRVDKFAPIDIQPSEITFE 994
M.musculus ---------- 494
H.sapiens KELEAGSLYHLTVWAERNEVRG---YNST-----LTAATAPNEVTDLQNETQTKNSVMLW 606
P.troglodytes KELEAGSLYHLTVWAERNEVRG---YNST-----LTAATAPNEVTDLQNETQTKNSVMLW 603
D.melanogaster WSLPSSEANGVIRQFSIAYTNINNLT---DA----GMQDFESEEAFGVIKNLKPGETYVF 1046
C.quinquefasciatus WSLPPNEQNGVIRQFTITYGLD-GSQ---HT----QAKDFKPTELRGIIKGLLPGKTYIF 1010
A.aegypti WSLPPNEQNGIIRQFTITYGLD-GSQ---HT----QAKDFKPSELRGTIKTLLPGKTYIF 1046
M.musculus ---------- 494
H.sapiens WKAPGDP-HSQLYVYWVQWASKGHPRRGQDPQANWVNQTSRTNETWYKVEALEPGTLYNF 665
P.troglodytes WKAPGDP-HSQLYVYWVQWASKGHPQRGQDPQANWVNQTSRTNETWYKVEALEPGTLYNF 662
D.melanogaster KIQAKTAIGFGPEREYRQTMPILAPPRPATQVVPTEVYRSSSTIQIRFRKNYFSDQNGQV 1106
C.quinquefasciatus RIQAKTAIGYGPEQMWKQKMPILAPPKPETQVVPTEVGSSATTIEIRFRKHYFSDQNGVV 1070
A.aegypti RIQARTAIGYGPEQMWKQKMPILAPPKPETQVVPTEVGSSATTIEIRFRKHYFSDQNGVV 1106
M.musculus SVWVEKDGVYSTNE------TLNTSTVPAAVNITSC---------- 524
H.sapiens TVWAERNDVASSTQ------SLCASTYPDTVTITSC---------- 695
P.troglodytes TVWAERNDVASSTQ------SLCASTYPDAVTITSC---------- 692
D.melanogaster RMYTIIVAEDDAKNASGLEMPSWLDVQSYSVWLPYQAIDPYYPFENRSVEDFTI--GTEN 1164
C.quinquefasciatus TTYTIIIAEDDSKNASGLEMPSWYDVQSYSVWPPYQVIEPYYPFKNSSVEDFII--GTEN 1128
A.aegypti TTYTIIIAEDDSKNASGLEMPSWYDVQSYSVWPPYQVIEPYYPFKNSSVEDFTI--GTEN 1164
M.musculus ----------IS-----TSGGYGVLLTWSC-------PSGGYESFEVKVGRKW 555
H.sapiens ----------VS-----TSAGYGVNLIWSC-------PQGGYEAFELEVGGQR 726
P.troglodytes ----------VS-----TSAGYGVNLIWSC-------PQGGYEAFELEVGGQR 723
D.melanogaster CDNHKIGYCNGPLKSGTTYRVKVRAFTGADKFTDTAYSF--PIQTEML-SSPDQDNTSLI 1221
C.quinquefasciatus CDTRKSGYCNGPLKSGTTYKVKVRAFTAPDKFTDTAYSY--PIRT-------AQDNTSLI 1179
A.aegypti CDTRKSGYCNGPLKSGTTYKVKVRAFTAPDKFTDTAYSY--PIRT-------AQDNTSLI 1215
M.musculus RS-ENGSLCGK--------GVTVSDLEPAQSYTATVTTVFKDLKAQSLSTTCHTESAAII 606
H.sapiens GS-QDRSSCGE--------AVSVLGLGPARSYPATITTIWDGMKVVSHSVVCHTESAGVI 777
P.troglodytes GS-QDRSSCGE--------AVSVLGLGPARSYPATITTIWDGMKVVSHSVVCHTESAGVI 774
D.melanogaster VAITVPLTIILVLLVTLLFYKRRRNNCRKTTKDSRANDNMSLPDSVIEQNRPILIKNFAE 1281
C.quinquefasciatus VSITVPLFIILLLVGTIVFLRRRRHTGRKKATEQRANDNMSLPDSTMETSRPVLVKNFAE 1239
A.aegypti VSITVPLFIIFLLVGTILFLRRRRHSGRKKATEQRPNDNMSLPDSTIETSRPVLVKNFAE 1275
M.musculus AGAIVGILLLFILVGLLIVFLKRRRKKRQPKE--------VPKDLVCSCPGDILAKDFAD 658
H.sapiens AGAFVGILLFLILVGLLIFFLKRRNKKKQQKP--------ELRDLVFSSPGDIPAEDFAD 829
P.troglodytes AGAFVGILLFLILVGLLIFFLKRRNNKKQQKP--------ELRNLVFSSPGDIPAEDFAD 826
D.melanogaster HYRLMSADSDFRFSEEFEELKHVGRDQPCTFADLPCNRPKNRFTNILPYDHSRFKLQPVD 1341
C.quinquefasciatus HYRMMSADSDFRFSEEFEELKHVGRDQPCTFADLPCNRPKNRFTNILPYDHSRFKLQPVD 1299
A.aegypti HYRMMSADSDFRFSEEFEELKHVGRDQPCTFADLPCNRPKNRFTNILPYDHSRFKLQPVD 1335
M.musculus HVRENEKDSNCGFAEEYQQLALEGQGQSQITASALENRSKNRYRNVLPYDWSRVPLQPLQ 718
H.sapiens HVRKNERDSNCGFADEYQQLSLVGHSQSQMVASASENNAKNRYRNVLPYDWSRVPLKPIH 889
P.troglodytes HVRKNERDSNCGFADEYQQLSLVGHSQSQMVASASENNAKNRYRNVLPYDWSRVPLKPIH 886
D.melanogaster DDEGSDYINANYVPGHNSPREFIVTQGPLHSTRDDFWRMCWESNSRAIVMLTRCFEKGRE 1401
C.quinquefasciatus DEEGSDYINANYVPGHNSPREFIVTQGPLHSTRDDFWRMCWESNSRAIVMLTRTFEKGRE 1359
A.aegypti DEEGSDYINANYVPGHNSPREFIVTQGPLHSTRDDFWRMCWESNSRAIVMLTRTFEKGRE 1395
M.musculus EEPGSDYINASFMPGLWSPKEFIATQGPLPNTVGDFWRMVWEQQSHTLVMLTNCMESGRV 778
H.sapiens EEPGSDYINASFMPGLWSPQEFIATQGPLPQTVGDFWRLVWEQQSHTLVMLTNCMEAGRV 949
P.troglodytes EEPGSDYINASFMPGLWSPQEFIATQGPLPQTVGDFWRLVWEQQSHTLVMLTNCMEAGRV 946

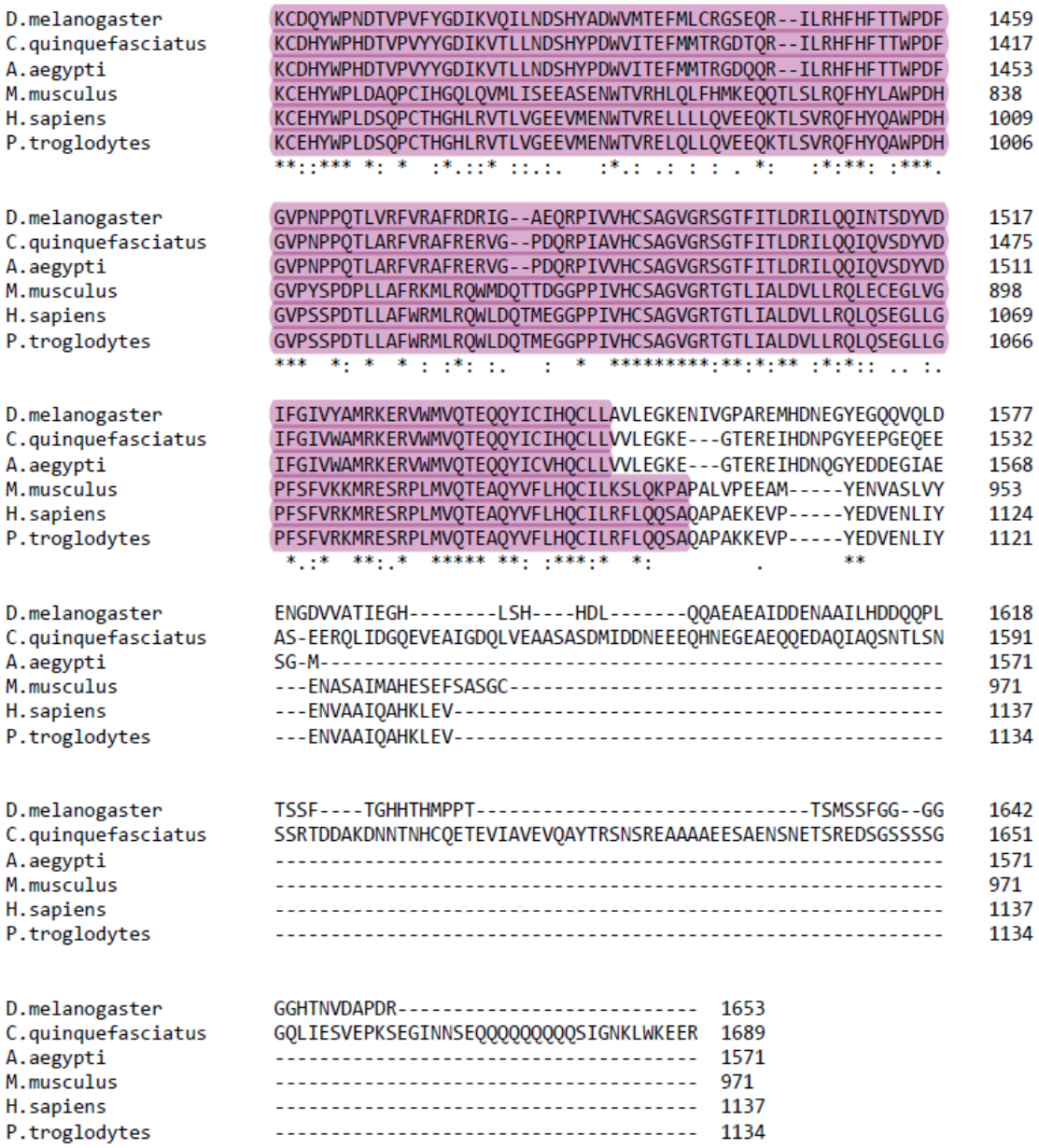

Figure 5: PTPRH is well-conserved in vertebrates and invertebrates. Clustal Omega multiple alignment of PTPRH protein in vertebrates and Ptp10D in invertebrates. Highlighted regions are FN3 domains except the last region in pink which is the longest domain is PTP domain. "*" indicates amino acids that are identical in all sequences in the alignment. ":" indicates conserved substitutions. "." indicates semi-conserved substitutions.

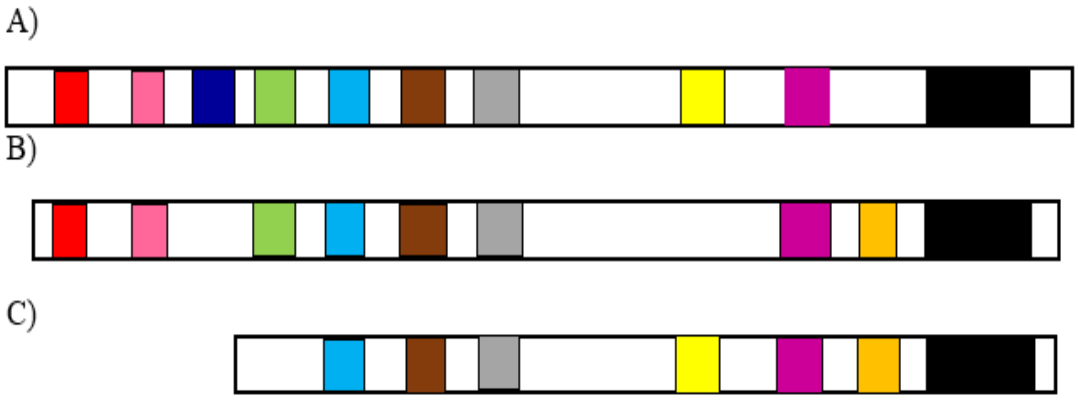

Figure 6: Comparison of *D. melanogaster* Ptp10D (A), Ptp4E (B) proteins, with *Homo sapiens* PTPRH protein (C) with coloured conserved domains. Coloured rectangles represent fibronectin type III (FN3) domains except for the last highlighted region (black) which is protein tyrosine phosphatase (PTP) domain.

Biometric analysis of the compound eye

Effects of the inhibition and overexpression of *Ptp10D* and inhibition of *Ptp4E* during development of eye of *D. melanogaster*

The eye of *D. melanogaster* is a highly effective model system to use to analyze molecular interactions and developmental mechanisms of the nervous system (Arzu, et al., 2013). It is made up of approximately 800 units designated as ommatidia under normal developmental conditions. Measuring the neurodegeneration is feasible through the eye structure due to the existence of a large number of neurons, more than 6000, make it very convenient for observing changes in phenotypes (Frankfort, et al., 2002). By using the *GMR* transgene in the *Gal4/UAS* system, we can inhibit or overexpress our desired gene in the eye of *D. melanogaster* and analyze the results. Certain parameters can be analyzed to study the impacts of changes in the development process including the ommatidia number, interommatidial bristle number, ommatidia area, and eye area. To determine the phenotypic changes in the eye due to altering *Ptp10D* and *Ptp4E* expression, a biometric analysis was carried out (Figure 8 & 9). Changes in the numbers of ommatidia and bristles for each derivative line were compared to the control (*GMR-Gal4; UAS-lacZ*). A summary of the ommatidia and bristle numbers is shown in Table 3 & 4, respectively. Biometric analysis of the scanning electron micrographs showed that eye-specific inhibition of *Ptp10D* and *Ptp4E* decreased the number of ommatidia in eye (Figure 8). Inhibition of $RNAi^{kk101775}$ had the most significant decrease amongst other *Ptp10D* inhibition transgenic lines (ommatidia mean number per eye: 666.4 ± 8.713). Between two available inhibition lines for *Ptp4E*, $RNAi^{HMS01838}$, with a median

ommatidia number of 648.8 ± 8.155 had the most substantial decrease. This is compared to the control *UAS-lacZ* in which the median number of ommatidia per eye was 710.3 ± 3.330. There is only one RNAi line, *RNAi* ^{v8010}, for *Ptp10D* which did not have significant changes based on its p-value. The number of ommatidia per eye for this transgenic line was 695.9 ± 7.213 (Table 3).

The inhibition of *Ptp4E* and *Ptp10D* with the transgene *GMR-GAL4* led to a significant decrease in interommatidial bristle number (Figure 9). The range of the average bristle number per eye was from 221.5 ± 40.26 to 577.2 ± 8.711 for inhibition lines of *Ptp10D* in which the most significant decrease belonged to *RNAi*^{HMS01917}. The average bristle number for *Ptp4E-RNAi*^{HMS01838} and *Ptp4E-RNAi*^{HMS05000} were 105 ± 10.36 and 344.9 ± 9.914, respectively. These were compared to the control line, *UAS-lacZ*, where the average number of bristle per eye were631.2 ± 6.93 (Table 4). The overexpression of *Ptp10D* significantly decreased the ommatidia and bristle number. By using *Ptp10D*^{EP1172}, the overexpression line under the control of the *GMR-Gal4* transgene, the average number of ommatidia and bristle number per eye decreased to a median value of 662.2 ± 4.800 and 300 ± 8.955, respectively, compared to 710.3 ± 3.330 and 631.2 ± 6.93, which were the average number of ommatidia and interommatidial bristle, respectively, for the control *UAS-lacZ*.

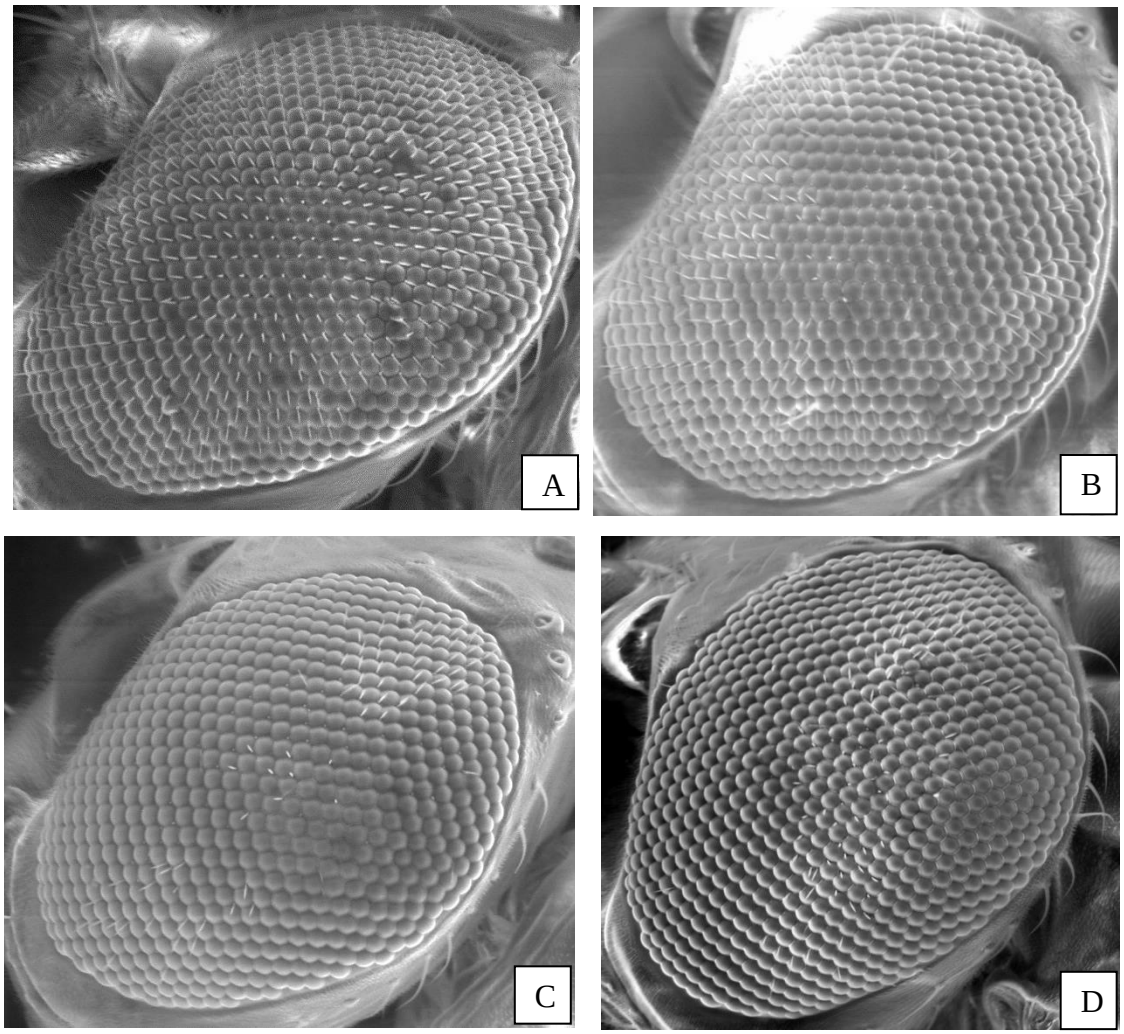

Figure 7: Inhibition and overexpression of *Ptp10D* and inhibition of *Ptp4E* significantly decreased the number of ommatidia and interommatidial bristles of *D. melanogaster*. Scanning electron micrographs of A: *GMR-GAL4; UAS-lacZ*, B: *GMR-Gal4; UAS-Ptp10D*^{EP1172} C*: GMR-Gal4; UAS-Ptp4E-RNAi*^{HMS01838}, and D: *GMR-Gal4; UAS-Ptp10D-RNAi* ^{HMS01917}.

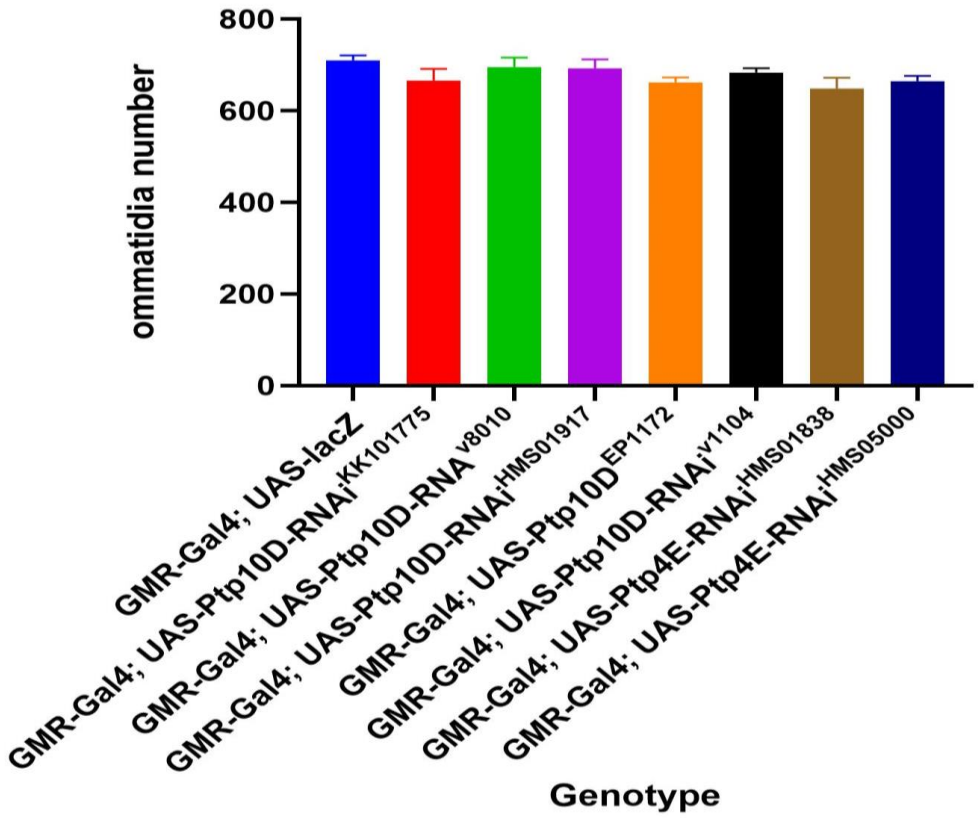

Figure 8: Biometric analysis of the consequences of inhibition and overexpression of *Ptp10D* and inhibition of *Ptp4E* during development of the *D. melanogaster Drosophila* compound eye. Inhibition of *Ptp10D* (four lines) and *Ptp4E* (two lines) significantly decreased ommatidia number in the compound eye. There is only one overexpression line for *Ptp10D* which showed a significant decrease as well. The changes in ommatidia number are not significant in the inhibition line *UAS-Ptp10D-RNAi* ^{v8010}. Significance is $p<0.05$ as compared to control group *UAS-lacZ*.

Table 3. Summary of the biometric analysis of ommatidia number when *Ptp10D* is inhibited and overexpressed and *Ptp4E* is inhibited during the development of the compound eye directed by *GMR-Gal4*.

Genotype	**Sample Size (n)**	**Mean ± SEM**	**P-value compared to control**	**Significant**
GMR-Gal4; UAS-lacZ (control)	10	710.3 ± 3.330	N/A	N/A
GMR-Gal4; UAS-Ptp10D-RNAi^{kk101775} (inhibition)	10	666.4 ± 8.713	<0.0001	Yes
GMR-Gal4; UAS-Ptp10D-RNAi ^{v8010} (inhibition)	10	695.9 ± 7.213	0.0613	No
GMR-Gal4; UAS-Ptp10D-RNAi ^{HMS01917} (inhibition)	10	692.7 ± 6.987	0.0215	Yes
GMR-Gal4; UAS-Ptp10D-RNAi ^{v1104} (inhibition)	10	683.4 ± 4.445	<0.0001	Yes
GMR-Gal4; UAS-Ptp10D^{EP1172} (overexpression)	10	662.2 ± 4.800	<0.0001	Yes
GMR-Gal4; UAS-Ptp4E-RNAi^{HMS01838} (inhibition)	10	648.8 ± 8.155	<0.0001	Yes
GMR-Gal4; UAS-Ptp4E-RNAi^{HMS05000} (inhibition)	10	665.3 ± 4.789	<0.0001	Yes

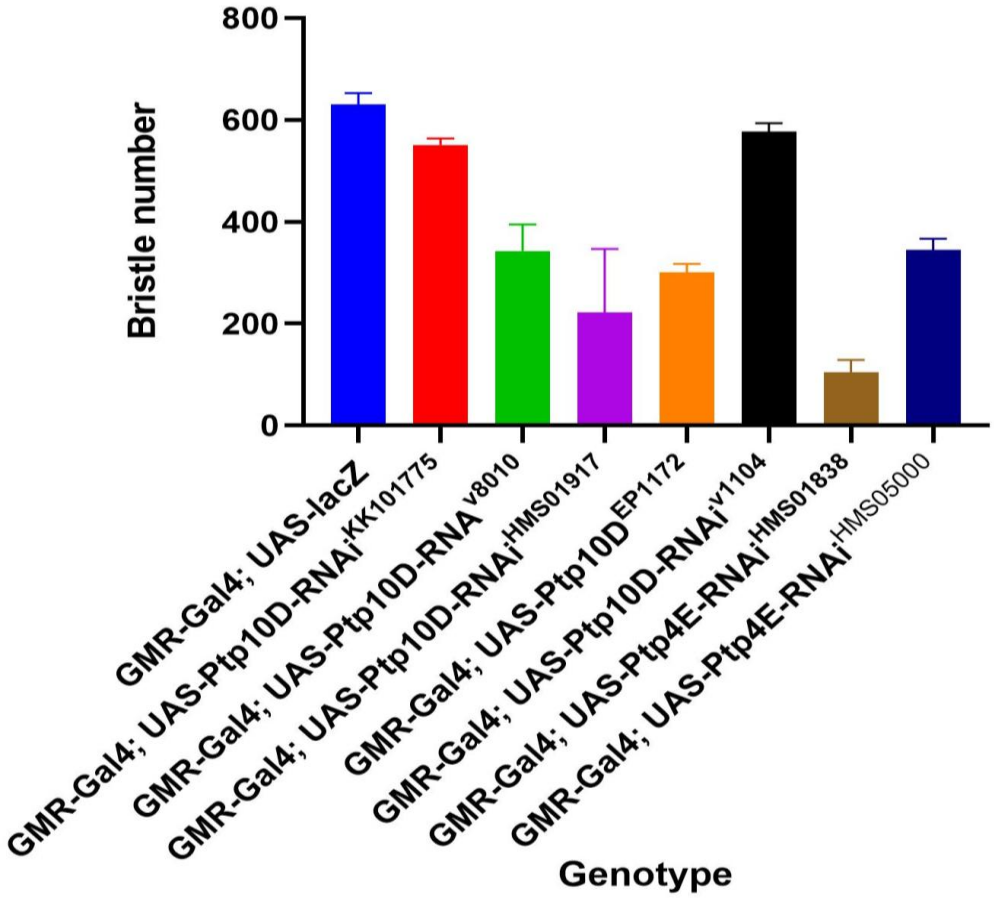

Figure 9: The effect of inhibition and overexpression of *Ptp10D* and inhibition of *Ptp4E* upon the development of interommatidial bristle number in the *Drosophila* compound eye. Loss-of-function of *Ptp10D* and *Ptp4E* lead to a significant decrease in interommatidial bristle number compared to the control *UAS-lacZ* in all experimental liness. Overexpression of *Ptp10D* also resulted in a significant decrease in bristle number. Based on t-tests, which were used to analyzing data, p-values less than 0.05 were considered significant. Error bars show the standard error of the mean.

Table 4. Summary of the biometric analysis of interommatidial bristle number when *Ptp10D* is inhibited and overexpressed and *Ptp4E* is inhibited during the development of the compound eye.

Genotype	Sample Size (n)	Mean ± SEM	P-value compared to control	Significant
GMR-Gal4; UAS-lacZ (control)	10	631.2 ± 6.93	N/A	N/A
GMR-Gal4; UAS-Ptp10D-RNAi^{kk101775} (inhibition)	10	551 ± 7.993	<0.0001	Yes
GMR-Gal4; UAS-Ptp10D-RNAi ^{v8010} (inhibition)	10	342.8 ± 17.89	<0.0001	Yes
GMR-Gal4; UAS-Ptp10D-RNAi ^{HMS01917} (inhibition)	10	221.5 ± 40.26	<0.0001	Yes
GMR-Gal4; UAS-Ptp10D-RNAi ^{v1104} (inhibition)	10	577.2 ± 8.711	<0.0001	Yes
GMR-Gal4; UAS-Ptp10D^{EP1172} (overexpression)	10	300 ± 8.955	<0.0001	Yes
GMR-Gal4; UAS-Ptp4E-RNAi^{HMS01838} (inhibition)	10	105 ± 10.36	<0.0001	Yes
GMR-Gal4; UAS-Ptp4E-RNAi^{HMS05000} (inhibition)	10	344.9 ± 9.914	<0.0001	Yes

Table 5. Summary of biometric analyses of ommatidia and interommatidial bristle number. For these analyses an eye-specific transgenic line *GMR-Gal4* was crossed to *Ptp10D* and *Ptp4E* responder lines.

Responder lines	**Transgenic line**	
Inhibition	*GMR-Gal4*	
	Ommatidia number	Bristle number
UAS-Ptp10D-RNAi^{kk101775}	Significant Decrease	Significant Decrease
UAS-Ptp10D-RNAi ^{v8010}	No significant change	Significant Decrease
UAS-Ptp10D-RNAi ^{HMS01917}	Significant Decrease	Significant Decrease
UAS-Ptp10D-RNAi ^{v1104}	Significant Decrease	Significant Decrease
Overexpression		
UAS-Ptp10D^{EP1172}	Significant Decrease	Significant Decrease
Inhibition		
UAS-Ptp4E-RNAi^{HMS01838}	Significant Decrease	Significant Decrease
UAS-Ptp4E-RNAi ^{HMS05000}	Significant Decrease	Significant Decrease

Effects of the inhibition of *Ptp10D* on *D. melanogaster*

Inhibition of *Ptp10D* decreases climbing ability and lifespan

The main hallmark of PD is a progressive degeneration of dopaminergic neurons. Using different kinds of drivers allows us to study the effects of *Ptp10D* on selected dopaminergic neurons. To investigate the impact of the LOF of *Ptp10D* on the climbing ability and lifespan of *D. melanogaster*, the motor neuron specific transgenic line *D42-Gal4*, the neuron-specific transgenic line *DDC-Gal4*, and the dopaminergic neuron-specific transgenic line *TH-Gal4* were used in the *Gal4/UAS* system. The ageing assay was carried out in parallel with climbing analysis for all drivers to identify the changes in the climbing ability due to premature senescence. The survival curves in Figure 10 show that the loss of function of Ptp10D using *D42-Gal4* transgene significantly decreased the lifespan, except for *Ptp10D-RNAi*^{kk101775} flies in which the changes were not considerably different (P-value: 0.1860) compared to the *lacZ*-expressing controls. The median lifespan for *Ptp10D-RNAi*^{v1104}, *Ptp10D-RNAi* ^{v8010}, and *Ptp10D-RNAi* ^{HMS0191} were 50, 54, and 58 days, respectively. While the control flies live for an average of 66 days (Table 6). The climbing ability for these experimental lines significantly differed from the control *UAS-lacZ* when using the motor neuron specific driver *D42-GAL4* with a P-value of <0.0001 for all lines (Figure 11). The most significantly different climbing curve belonged to *D42-Gal4; UAS-Ptp10D-RNAi* ^{HMS01917} with a 95% confidence interval of 0.03173 – 0.04704 compared to 0.03699 – 0.04897 for *D42-Gal4; UAS-lacZ* (Table 7).

When different inhibition lines of Ptp10D were expressed in flies through the *DDC-Gal4* transgene, which is a neuron-specific line, extensive changes occurred in their lifespan (Figure 12). The median survival for control flies, *DDC-Gal4; UAS-lacZ*, was 72 while it decreased to 56, 54, and 50 for *Ptp10D-RNAi* ^{v8010}, *Ptp10D-RNAi* ^{v1104}, and *Ptp10D-RNAi* ^{HMS01917} flies, respectively (Table 8). Interestingly, *DDC-Gal4; UAS-Ptp10D-RNAi* ^{HMS01917} flies with the shortest median lifespan showed the lowest climbing ability amongst all *Ptp10D* inhibition lines as well (Figure 13). The 95% confidence intervals for this line was 0.02649 – 0.0371 compared to 0.04563 – 0.05455 for *DDC-Gal4; UAS-lacZ* (Table 9). The p-value for all lines were <0.0001 except for *DDC-Gal4; UAS-Ptp10D-RNAi*^{kk101775} which was 0.0084 and less significant than the others.

Survival curves for transgenic lines with dopaminergic neuron specificity shows significant differences between experimental lines and the control line *TH-Gal4; UAS-lacZ* (Figure 14). The Median survival for the control group was 72 and it decreased to 68, 60, 62, and 58 for *Ptp10D-RNAi*^{kk101775}, *Ptp10D-RNAi* ^{HMS01917}, *Ptp10D-RNAi* ^{v8010}, and *Ptp10D-RNAi* ^{v1104}, respectively (Table 10). By comparing the median lifespan between *DDC* and *TH* inhibition lines, it becomes clear that the decrease in the flies' lifespan is more significant when it comes to *DDC* transgene considering that the median survival was 72 days for the control group of both drivers. The climbing curves indicate that all transgenic flies using the *TH* transgene experienced a decrease in their climbing ability in which *Ptp10D-RNAi* ^{HMS01917} had the most significant decrease compared to

the control line (Figure 15). The 95% confidence intervals for this line was 0.03984 – 0.05256 in comparison to 0.04104 – 0.05848 in control flies (Table 11).

Effects of the overexpression of *Ptp10D*

Overexpression of *Ptp10D* decreases climbing ability and longevity

To assess the effects of the overexpression of *Ptp10D* on the longevity and climbing ability of *D. melanogaster*, the motor neuron-specific transgenic line *D42-Gal4*, the neuron-specific transgenic line *DDC-Gal4*, and the dopaminergic neuron-specific transgenic line *TH-Gal4* were used. When using *D42-Gal4* transgene a significant decrease was observed in the lifespan of flies (Figure 16). In this overexpression line, *D42-Gal4; UAS- Ptp10D*^{EP1172}, the median lifespan decreased to 54 from 66 in *D42-Gal4; UAS-lacZ* (Table 12). In addition to longevity, the climbing ability was reduced significantly (Figure 17). As is shown in Table 13 the 95% confidence intervals for *UAS-lacZ* and *Ptp10D*^{EP1172} were 0.03699 – 0.04897 and 0.02972 – 0.04550, respectively.

The most significant change in the longevity of Ptp10D overexpressing flies was related to the neuron-specific transgenic line *DDC-Gal4* (Figure 18). The median survival in *DDC-Gal4; UAS-lacZ* was 72 days which remarkably decreased to 46 in *DDC-Gal4; UAS-Ptp10D*^{EP1172} (Table 14). Moreover, the decreases in climbing ability by using the *DDC-Gal4* transgenic line can be seen in Figure 19. Based on the t-test analysis the 95% confidence intervals for *Ptp10D*^{EP1172} was 0.03409 – 0.04520

compared to 0.04563 – 0.05455 for *UAS-lacZ* (Table 15). The climbing and ageing assay for the overexpression of *Ptp10D* were repeated with the *TH-Gal4* transgene which led to a significant decrease in both parameters. (Figure 20 and 21). The median lifespan of *TH-Gal4; UAS-Ptp10D*^{EP1172} was 54 days based on the log-rank analysis compared to 72 days in control flies (Table 16).

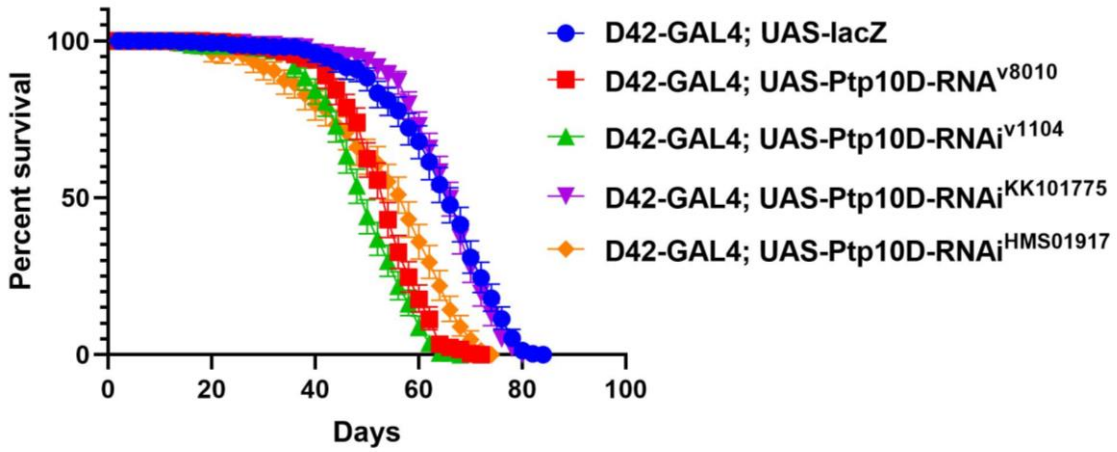

Figure 10: Inhibition of *Ptp10D* using a motor neuron-specific transgene (*D42-Gal4*) causes a significant decrease in longevity. Four different inhibition lines were used. All of them except *Ptp10D-RNAi^{kk101775} (II)* were significant compared to control *D42-Gal4; UAS-lacZ*. Longevity is shown by percent survival. Significance is $p < 0.05$ and error bars shows the standard error of the mean.

Table 6. Comparison of the longevity of flies for the inhibition of *Ptp10D* in motor neurons by Mantel-Cox Log-rank statistics. Chi-square values and p-values were calculated using *UAS-lacZ* controls.

Genotype	Number of flies	Median Survival (days)	Chi – square value	P-value	Significant
D42-Gal4; UAS-lacZ	306	66	N/A	N/A	N/A
D42-Gal4; UAS-Ptp10D-RNAi^{kk101775}	332	66	1.749	0.1882	No
D42-Gal4; UAS-Ptp10D-RNAi ^{v8010}	300	54	239.2	<0.0001	Yes
D42-Gal4; UAS-Ptp10D-RNAi HMS01917	292	58	106.0	<0.0001	Yes
D42-Gal4; UAS-Ptp10D-RNAi ^{v1104}	324	50	331.0	<0.0001	Yes

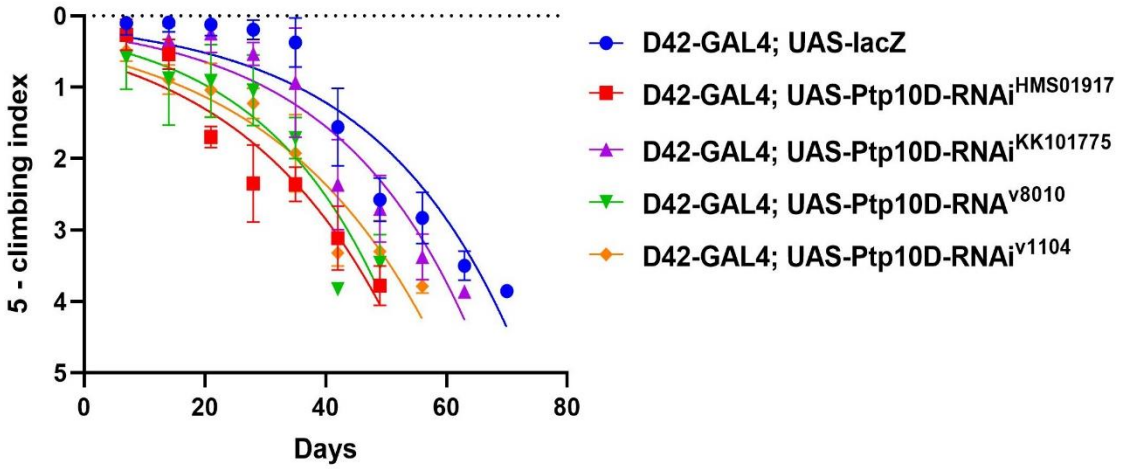

Figure 11: Inhibition of *Ptp10D* using a motor neuron specific transgenic line (*D42-Gal4*) causes a significant decrease in flies climbing ability over time. Four different inhibition lines were used. All of them were significant compared to control *D42-Gal4; UAS-lacZ*. Data was analyzed by a non-linear curve fit with 95% confidence intervals to determine significance. Error bars represent standard error of the mean.

Table 7. Comparison of the climbing ability of flies for the inhibition of *Ptp10D* in motor neurons by using a non-linear regression curve for each inhibition line.

Genotype	**95% Confidence Intervals**	**R^2**	**P-value**	**Significant**
D42-Gal4; UAS-lacZ	0.03699 – 0.04897	0.8735	N/A	N/A
D42-Gal4; UAS-Ptp10D-RNAi^{kk101775}	0.03761 – 0.05105	0.8653	<0.0001	Yes
D42-Gal4; UAS-Ptp10D-RNAi ^{v8010}	0.03737 – 0.06007	0.7700	<0.0001	Yes
D42-Gal4; UAS-Ptp10D-RNAi ^{HMS01917}	0.03173 – 0.04704	0.8262	<0.0001	Yes
D42-Gal4; UAS-Ptp10D-RNAi ^{v1104}	0.03130 – 0.04244	0.8642	<0.0001	Yes

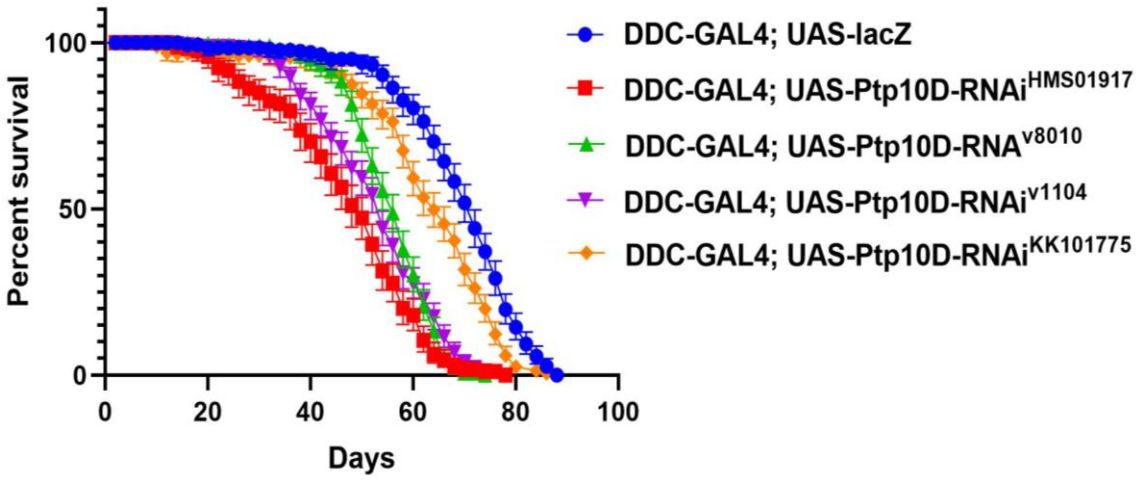

Figure 12: Inhibition of *Ptp10D* using a neuron-specific transgenic line (*DDC-Gal4*) causes a significant decrease in longevity. Four different inhibition lines were used and all of them were significant compared to control *DDC-Gal4; UAS-lacZ*. Longevity is shown by percent survival. Significance is $p < 0.05$ and error bars shows the standard error of the mean.

Table 8. Comparison of the longevity of flies for the inhibition of *Ptp10D DDC-Gal4* expressing in neurons by Mantel-Cox Log-rank statistics. Chi-square values and p-values were calculated using *UAS-lacZ* controls.

Genotype	Number of flies	Median Survival (days)	Chi – square value	P-value	Significant
DDC-Gal4; UAS-lacZ	299	72	N/A	N/A	N/A
DDC-Gal4; UAS-Ptp10D-RNAi^{kk101775}	356	64	44.01	<0.0001	Yes
DDC-Gal4; UAS-Ptp10D-RNAi ^{v8010}	300	56	305.2	<0.0001	Yes
DDC-Gal4; UAS-Ptp10D-RNAi HMS01917	237	50	342.2	<0.0001	Yes
DDC-Gal4; UAS-Ptp10D-RNAi ^{v1104}	348	54	306.6	<0.0001	Yes

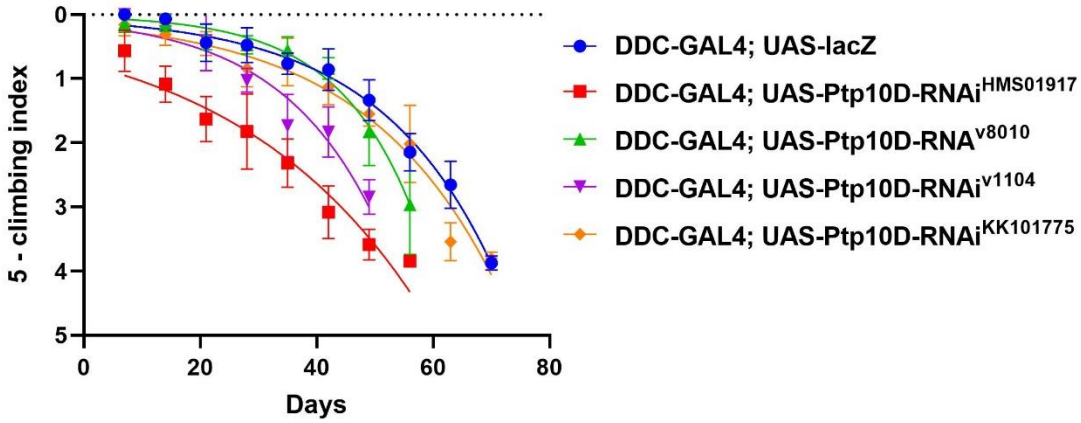

Figure 13: Inhibition of *Ptp10D* using a neuron-specific transgenic line (*DDC-Gal4*) causes a significant decrease in flies climbing ability over time. Four different inhibition lines were used. All of them were significant compared to control *DDC-Gal4; UAS-lacZ*. Data was analyzed by a non-linear curve fit with 95% confidence intervals to determine significance. Error bars represent standard error of the mean.

Table 9. Comparison of the climbing ability of flies for the inhibition of *Ptp10D* in neurons by using a non-linear regression curve for each inhibition line.

Genotype	**95% Confidence Intervals**	**R^2**	**P-value**	**Significant**
DDC-Gal4; UAS-lacZ	0.04563 – 0.05455	0.9533	N/A	N/A
DDC-Gal4; UAS-Ptp10D-RNAi^{kk101775}	0.03929 – 0.04888	0.9262	0.0084	Yes
DDC-Gal4; UAS-Ptp10D-RNAi ^{v8010}	0.06274 – 0.09120	0.8831	<0.0001	Yes
DDC-Gal4; UAS-Ptp10D-RNAi ^{HMS01917}	0.02649 – 0.03571	0.8662	<0.0001	Yes
DDC-Gal4; UAS-Ptp10D-RNAi ^{v1104}	0.04799 – 0.07268	0.8224	<0.0001	Yes

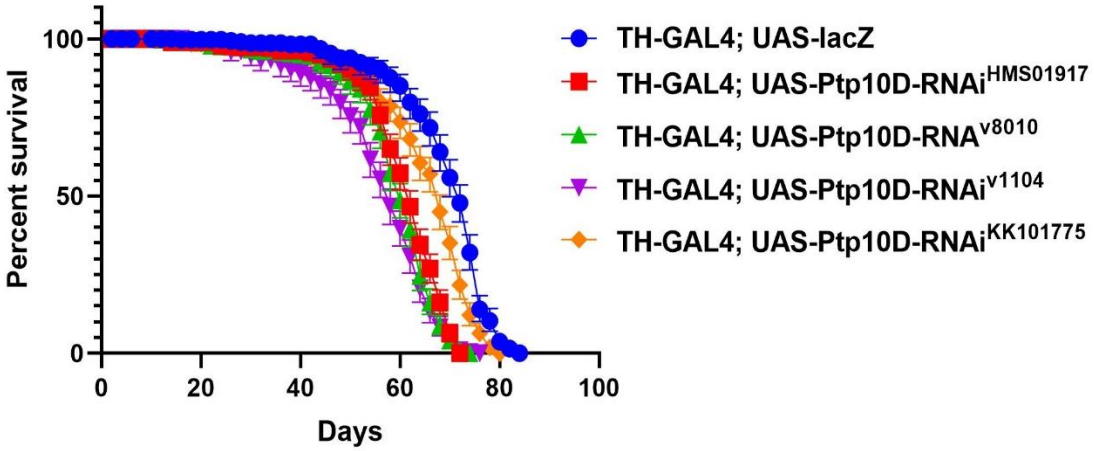

Figure 14: Inhibition of *Ptp10D* using a dopaminergic neuron specific driver (*TH-Gal4*) causes a significant decrease in longevity. Four different inhibition lines were used and all of them were significant compared to control *TH-Gal4; UAS-lacZ*. Longevity is shown by percent survival. Significance is $p < 0.05$ and error bars shows the standard error of the mean.

Table 10. Comparison of the longevity of flies for the inhibition of *Ptp10D* in dopaminergic neurons by Mantel-Cox Log-rank statistics. Chi-square values and p-values were calculated using *UAS-lacZ* controls.

Genotype	Number of flies	Median Survival (days)	Chi–square value	P-value	Significant
TH-Gal4; UAS-lacZ	272	72	N/A	N/A	N/A
TH-Gal4; UAS-Ptp10D-RNAi kk101775	314	68	44.76	<0.0001	Yes
TH-Gal4; UAS-Ptp10D-RNAi v8010	321	60	257.4	<0.0001	Yes
TH-Gal4; UAS-Ptp10D-RNAi HMS01917	365	62	233.6	<0.0001	Yes
TH-Gal4; UAS-Ptp10D-RNAi v1104	300	58	272.6	<0.0001	Yes

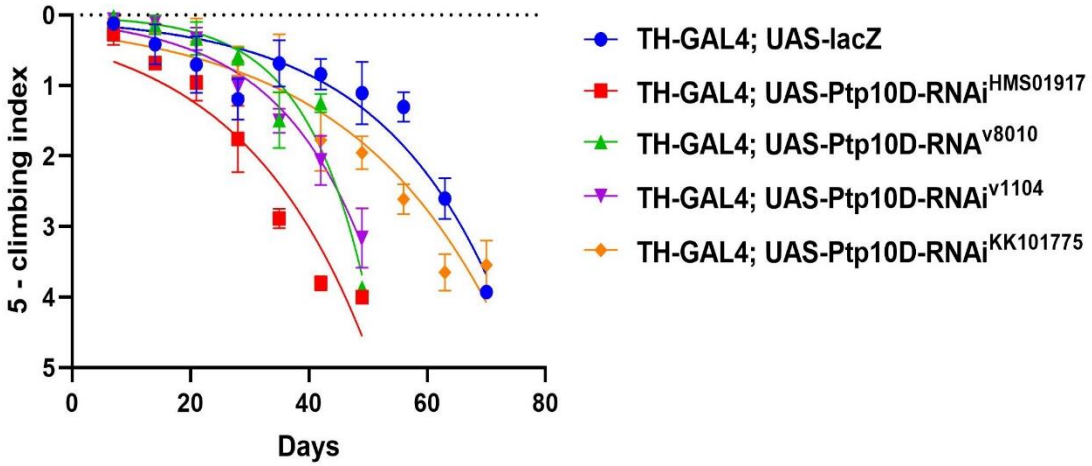

Figure 15: Inhibition of *Ptp10D* using a dopaminergic neuron specific transgenic line (*TH-Gal4*) causes a significant decrease in flies climbing ability over time. Four different inhibition lines were used. All of them were significant compared to control *TH-Gal4; UAS-lacZ*. Data were analyzed by a non-linear curve fit with 95% confidence intervals to determine significance. Error bars represent standard error of the mean.

Table 11. Comparison of the climbing ability of flies for the inhibition of *Ptp10D* in dopaminergic neurons by using a non-linear regression curve for each inhibition line.

Genotype	**95% Confidence Intervals**	**R^2**	**P-value**	**Significant**
TH-Gal4; UAS-lacZ	0.04104 – 0.05848	0.8594	N/A	N/A
TH-Gal4; UAS-Ptp10D-RNAi^{kk101775}	0.03413 – 0.04385	0.8933	0.0001	Yes
TH-Gal4; UAS-Ptp10D-RNAi ^{v8010}	0.07946 – 0.1160	0.9149	<0.0001	Yes
TH-Gal4; UAS-Ptp10D-RNAi ^{HMS01917}	0.03984 – 0.05256	0.9024	<0.0001	Yes
TH-Gal4; UAS-Ptp10D-RNAi ^{v1104}	0.05782 – 0.07365	0.9370	<0.0001	Yes

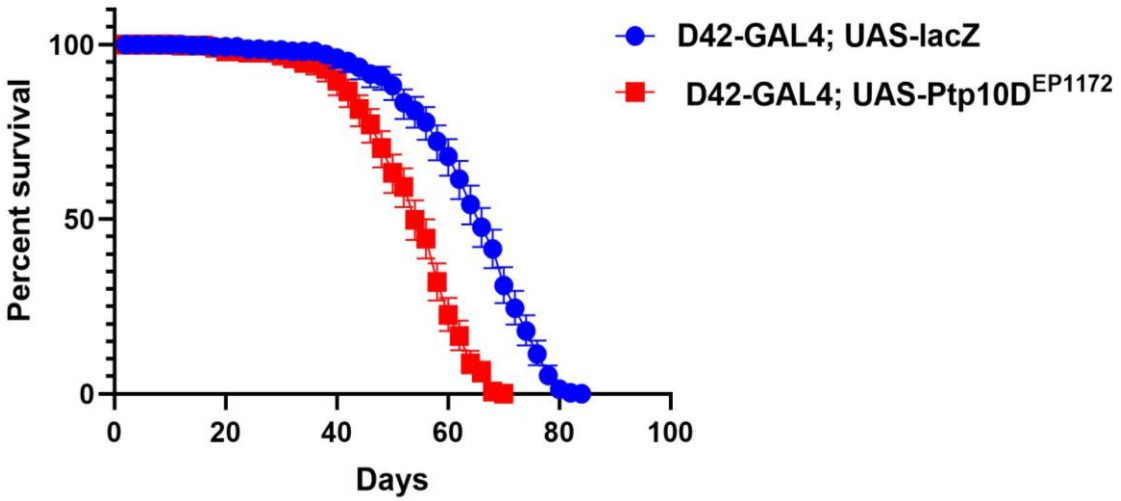

Figure 16: Overexpression of *Ptp10D* using a motor neuron specific transgenic line (*D42-Gal4*) causes a significant decrease in longevity. Flies expressing *UAS-Ptp10D^{EP1172}(X)* were significant compared to control *D42-Gal4; UAS-lacZ*. Longevity is shown by percent survival. Significance is $p < 0.05$ and error bars shows the standard error of the mean.

Table 12. Comparison of the longevity of flies for the overexpression of *Ptp10D* in motor neurons by Mantel-Cox Log-rank statistics. Chi-square values and p-values were calculated using *UAS-lacZ* controls.

Genotype	Number of flies	Median Survival (days)	Chi – square value	P-value	Significant
D42-Gal4; UAS-lacZ	306	66	N/A	N/A	N/A
D42-Gal4; UAS-Ptp10D^{EP1172}	297	54	205.9	<0.0001	Yes

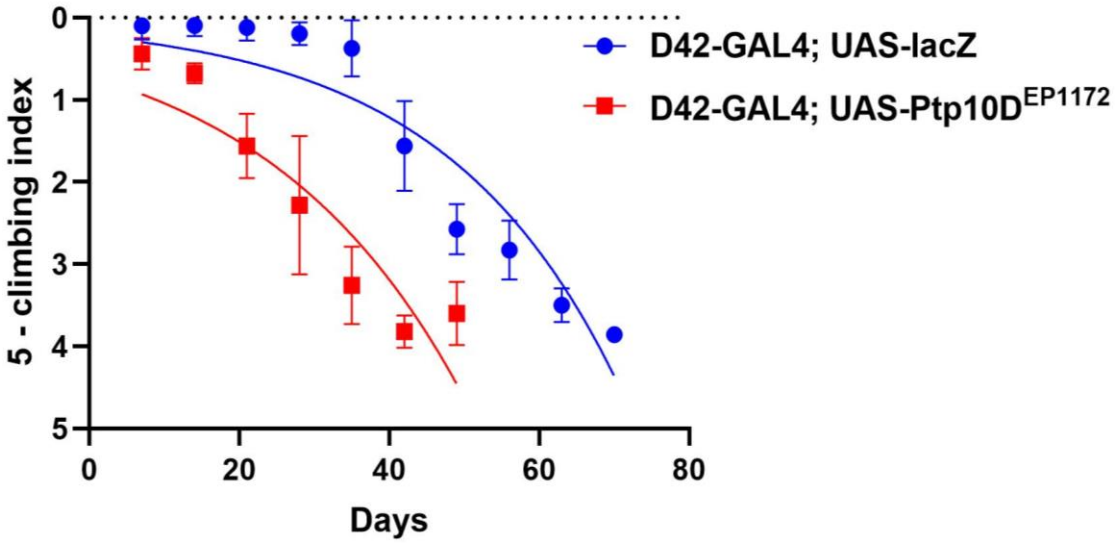

Figure 17: Overexpression of *Ptp10D* using a motor neuron specific transgenic line (*D42-Gal4*) causes a significant decrease in flies climbing ability over time. Four different inhibition lines were used. All of them were significant compared to control *D42-Gal4; UAS-lacZ*. Data was analyzed by a non-linear curve fit with 95% confidence intervals to determine significance. Error bars represent standard error of the mean.

Table 13. Comparison of the climbing ability of flies for the overexpression of *Ptp10D* in motor neurons by using a non-linear regression curve for each inhibition line.

Genotype	**95% Confidence Intervals**	**R^2**	**P-value**	**Significant**
D42-Gal4; UAS-lacZ	0.03699 – 0.04897	0.8735	N/A	N/A
D42-Gal4; UAS-Ptp10D^{EP1172}	0.02972 – 0.04550	0.7840	<0.0001	Yes

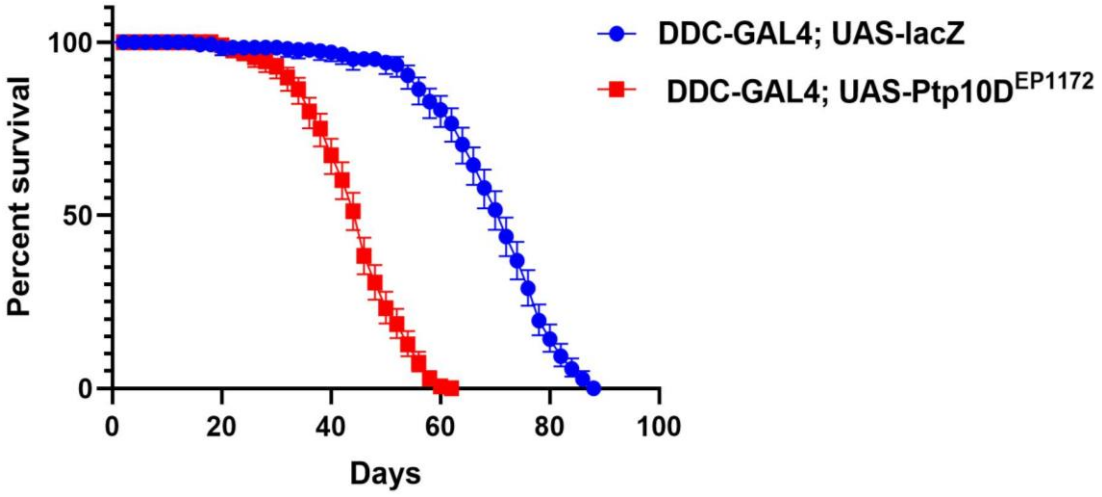

Figure 18: Overexpression of *Ptp10D* using a neuron specific transgenic line (*DDC-Gal4*) causes a significant decrease in longevity. Flies expressing *UAS-Ptp10D*^{EP1172} were significant compared to control *DDC-Gal4; UAS-lacZ.* Longevity is shown by percent survival. Significance is $p < 0.05$ and error bars shows the standard error of the mean.

Table 14. Comparison of the longevity of flies for the overexpression of *Ptp10D* in neurons by Mantel-Cox Log-rank statistics. Chi-square values and p-values were calculated using *UAS-lacZ* controls.

Genotype	Number of flies	Median Survival (days)	Chi – square value	P-value	Significant
DDC-Gal4; UAS-lacZ	299	72	N/A	N/A	N/A
DDC-Gal4; UAS-Ptp10D^{EP1172}	324	46	556.5	<0.0001	Yes

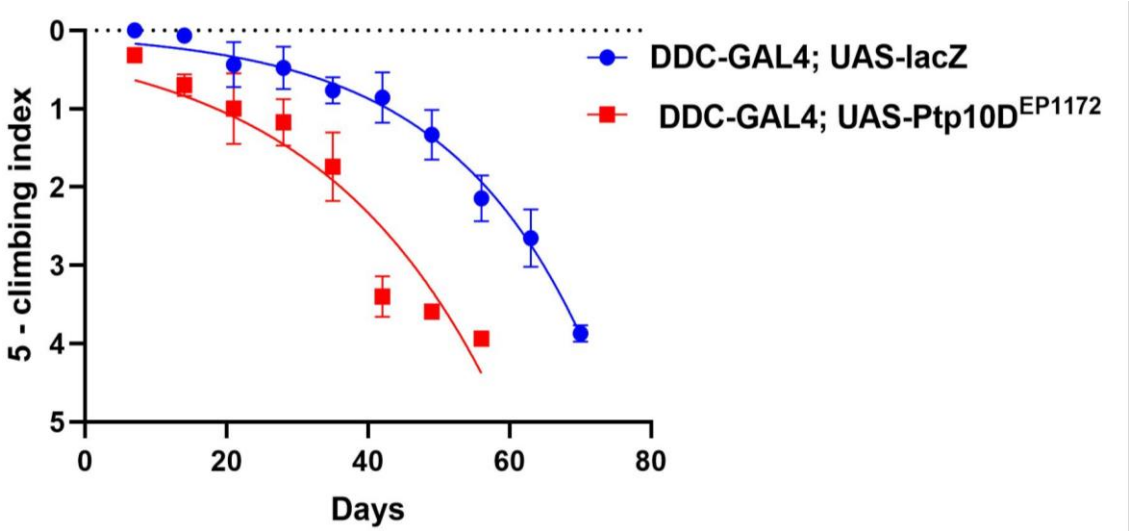

Figure 19: Overexpression of *Ptp10D* using a neuron specific transgenic line (*DDC-Gal4*) causes a significant decrease in flies climbing ability over time. Four different inhibition lines were used. All of them were significant compared to control *DDC-Gal4; UAS-lacZ*. Data was analyzed by a non-linear curve fit with 95% confidence intervals to determine significance. Error bars represent standard error of the mean.

Table 15. Comparison of the climbing ability of flies for the overexpression of *Ptp10D* in neurons by using a non-linear regression curve for each inhibition line.

Genotype	**95% Confidence Intervals**	**R^2**	**P-value**	**Significant**
DDC-Gal4; UAS-lacZ	0.04563 – 0.05455	0.9533	N/A	N/A
DDC-Gal4; UAS-Ptp10D^{EP1172}	0.03409 – 0.04520	0.8846	<0.0001	Yes

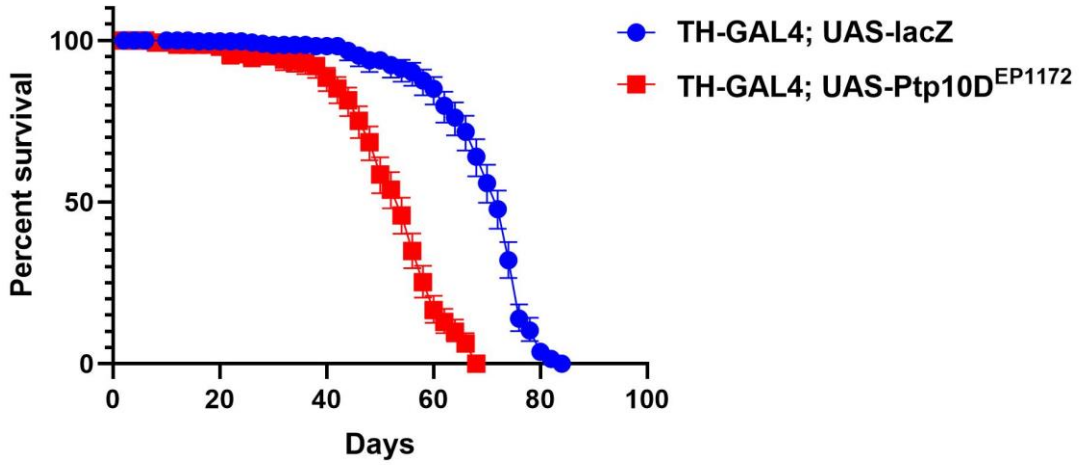

Figure 20: Overexpression of *Ptp10D* using a dopaminergic neuron specific transgenic line (*TH-Gal4*) causes a significant decrease in longevity. Flies expressing *UAS-Ptp10D*^{EP1172} were significant compared to control *TH-Gal4; UAS-lacZ*. Longevity is shown by percent survival. Significance is $p < 0.05$ and error bars shows the standard error of the mean.

Table 16. Comparison of the longevity of flies for the overexpression of *Ptp10D* in dopaminergic neurons by Mantel-Cox Log-rank statistics. Chi-square values and p-values were calculated using *UAS-lacZ* controls.

Genotype	Number of flies	Median Survival (days)	Chi – square value	P-value	Significant
TH-Gal4; UAS-lacZ	272	72	N/A	N/A	N/A
TH-Gal4; UAS-Ptp10D^{EP1172}	301	54	383.5	<0.0001	Yes

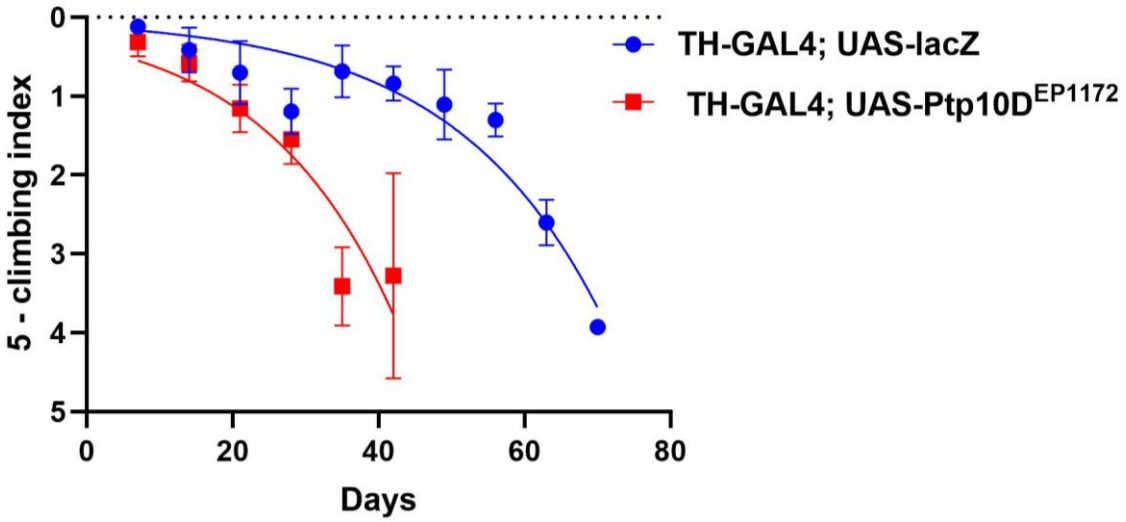

Figure 21: Overexpression of *Ptp10D* using a dopaminergic neuron-specific transgenic line (*TH-Gal4*) causes a significant decrease in flies climbing ability over time. Four different inhibition lines were used. All of them were significant compared to control *TH-Gal4; UAS-lacZ*. Data were analyzed by a non-linear curve fit with 95% confidence intervals to determine significance. Error bars represent standard error of the mean.

Table 17. Comparison of the climbing ability of flies for the overexpression of *Ptp10D* in dopaminergic neurons by using a non-linear regression curve for each inhibition line.

Genotype	**95% Confidence Intervals**	**R^2**	**P-value**	**Significant**
TH-Gal4; UAS-lacZ	0.04104 – 0.05848	0.8594	N/A	N/A
TH-Gal4; UAS-Ptp10D^{EP1172}	0.04122 – 0.07112	0.7479	<0.0001	Yes

Effects of the inhibition of *Ptp4E* in *D. melanogaster*

Loss of function of *Ptp4E* results in a reduction in longevity and climbing ability

To identify the effect of *Ptp4E* inhibition in *D. melanogaster*, three different transgenic lines were used in the *Gal4/UAS* system: the motor neuron-specific transgene *D42-Gal4*, the neuron-specific transgene *DDC-Gal4*, and the dopaminergic neuron-specific transgene *TH-Gal4*. When using the *D42-Gal4* transgenic line, the most significant change in both ageing and climbing ability was for the *Ptp4E-RNAi*^{HMS01838} inhibition line (Figure 22 & 23). As can be seen in Table 18, the median survival for *Ptp4E-RNAi*^{HMS01838} was 54 days, while for *Ptp4E-RNAi* ^{HMS05000} it was 64 compared to *D42-Gal4; UAS-lacZ*, which was 66 days. As is shown in Table 19, the 95% confidence interval was 0.03410 – 0.04619 for *RNAi*^{HMS01838} in comparison to 0.03699 – 0.04897 for the control group.

The inhibition of *Ptp4E* using the neuron-specific transgene *DDC-Gal4* led to a significant decrease in lifespan and climbing ability (Figure 24 & 25). The median lifespan for flies with the inhibition of *Ptp4E-RNAi*^{HMS01838} and *Ptp4E-RNAi* ^{HMS05000} with transgenic line *DDC-Gal4* was 58 and 56, respectively, which is shorter than the control *UAS-lacZ* whose median lifespan was 72 (Table 20). The changes in climbing ability were also significant as the 95% confidence interval was 0.02234 – 0.03361 and 0.05021 – 0.07713 for *Ptp4E-RNAi*^{HMS01838} and *Ptp4E-RNAi* ^{HMS05000}, which was compared to 0.04563 – 0.05455 for *UAS-lacZ* (Table 21).

Consistent with the above results for *D42-Gal4* and *DDC-Gal4* drivers, the inhibition of *Ptp4E-RNAi*^{HMS01838} with the dopaminergic neuron-specific *TH-Gal4* transgene resulted in the most significant decrease in longevity and climbing ability (Figure 26 & 27). The reduction for the other inhibition line of *Ptp4E* was also substantial. The median survival decreased from 72 in *TH-Gal4; UAS-lacZ* to 54 and 62 in *Ptp4E-RNAi*^{HMS01838} and *Ptp4E-RNAi* ^{HMS05000}, respectively (Table 22). Based on Figure 27, *Ptp4E-RNAi*^{HMS01838} flies significant change, in which the 95% confidence interval was 0.03115 – 0.04695 in comparison to the control group with 0.04104 – 0.05848 (Table 23). A summary of ageing and climbing analyses is provided in Table 24 which suggests that all results except for one were significantly important.

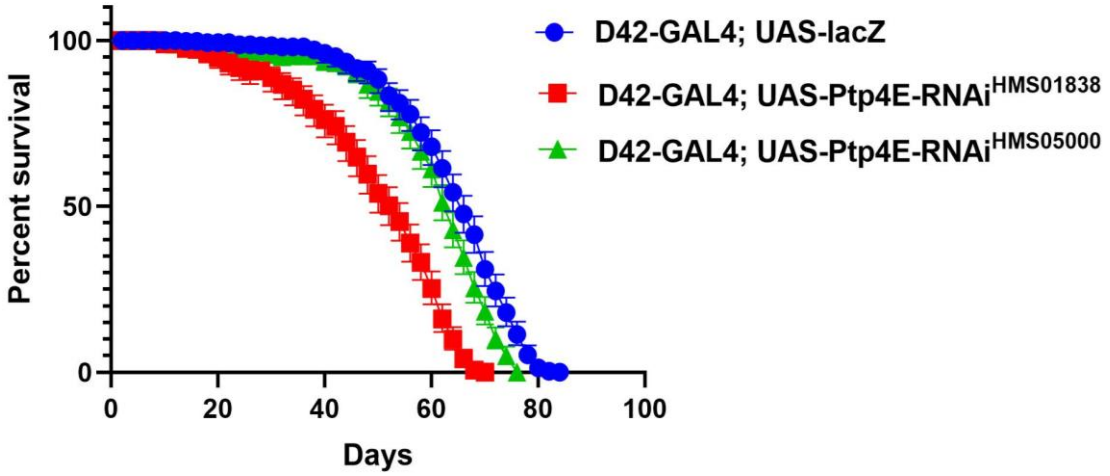

Figure 22: Inhibition of *Ptp4E* using a motor neuron specific transgenic line (*D42-Gal4*) causes a significant decrease in longevity. Two different inhibition lines were used and both were significant compared to the control *D42-Gal4; UAS-lacZ*. Longevity is shown by percent survival. Significance is $p < 0.05$ and error bars shows the standard error of the mean.

Table 18. Comparison of the longevity of flies for the inhibition of *Ptp4E* in motor neurons by Mantel-Cox Log-rank statistics. Chi-square values and p-values were calculated using *UAS-lacZ* controls.

Genotype	**Number of flies**	**Median Survival (days)**	**Chi – square value**	**P-value**	**Significant**
D42-Gal4; UAS-lacZ	306	66	N/A	N/A	N/A
D42-Gal4; UAS-Ptp4E-RNAi^{HMS01838}	293	54	1.749	<0.0001	Yes
D42-Gal4; UAS-Ptp4E-RNAi ^{HMS05000}	338	64	31.82	<0.0001	Yes

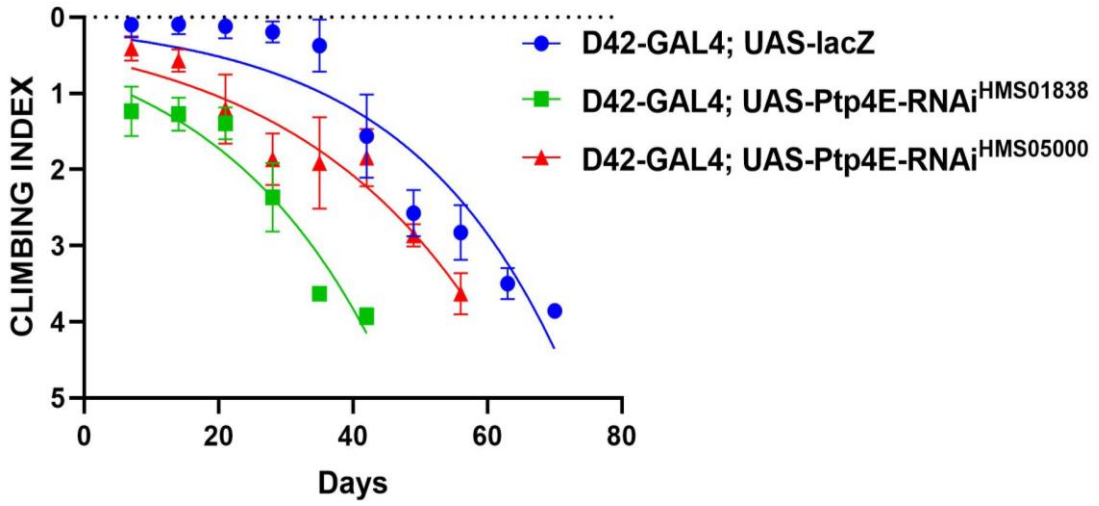

Figure 23: Inhibition of *Ptp4E* using a motor neuron specific transgenic line (*D42-Gal4*) causes a significant decrease in flies climbing ability over time. Two different inhibition lines were used. Both were significant compared to the control *D42-Gal4; UAS-lacZ*. Data were analyzed by a non-linear curve fit with 95% confidence intervals to determine significance. Error bars represent standard error of the mean.

Table 19. Comparison of the climbing ability of flies for the inhibition of *Ptp4E* in motor neurons by using a non-linear regression curve for each inhibition line.

Genotype	**95% Confidence Intervals**	**R^2**	**P-value**	**Significant**
D42-Gal4; UAS-lacZ	0.03699 – 0.04897	0.8735	N/A	N/A
D42-Gal4; UAS-Ptp4E-RNAi^{HMS01838}	0.03410 – 0.04619	0.8930	<0.0001	Yes
D42-Gal4; UAS-Ptp4E-RNAi ^{HMS05000}	0.02919 – 0.04020	0.8536	<0.0001	Yes

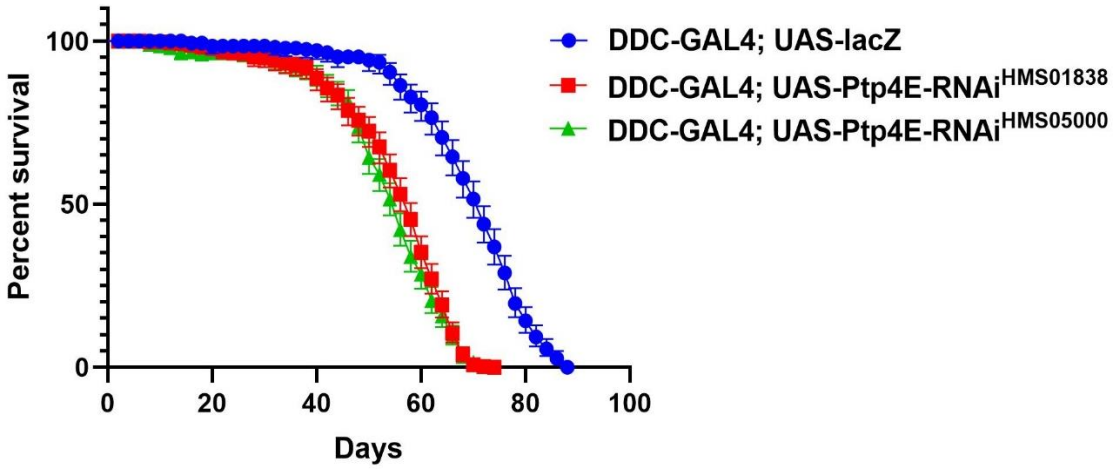

Figure 24: Inhibition of *Ptp4E* using a neuron-specific transgenic line (*DDC-Gal4*) causes a significant decrease in longevity. Two different inhibition lines were used and both were significant compared to control *DDC-Gal4; UAS-lacZ*. Longevity is shown by percent survival. Significance is $p < 0.05$ and error bars shows the standard error of the mean.

Table 20. Comparison of the longevity of flies for the inhibition of *Ptp4E* in neurons by Mantel-Cox Log-rank statistics. Chi-square values and p-values were calculated using *UAS-lacZ* controls.

Genotype	Number of flies	Median Survival (days)	Chi – square value	P-value	Significant
DDC-Gal4; UAS-lacZ	299	72	N/A	N/A	N/A
DDC-Gal4; UAS-Ptp4E-RNAi^{HMS01838}	366	58	302.6	<0.0001	Yes
DDC-Gal4; UAS-Ptp4E-RNAi ^{HMS05000}	386	56	31.82	<0.0001	Yes

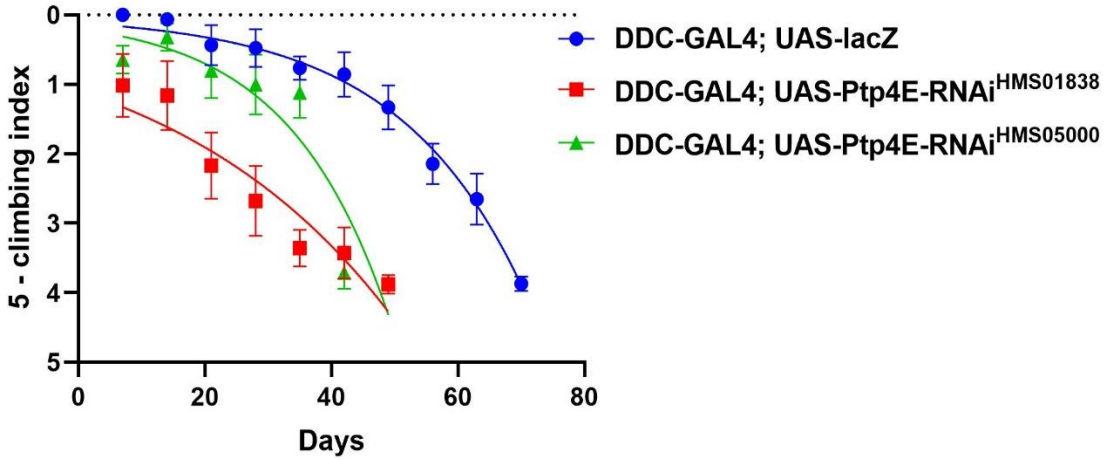

Figure 25: Inhibition of *Ptp4E* using a neuron-specific transgenic line (*DDC-Gal4*) causes a significant decrease in flies climbing ability over time. Two different inhibition lines were used. Both were significant compared to the control *DDC-Gal4; UAS-lacZ*. Data were analyzed by a non-linear curve fit with 95% confidence intervals to determine significance. Error bars represent standard error of the mean.

Table 21. Comparison of the climbing ability of flies for the inhibition of *Ptp4E* in neurons by using a non-linear regression curve for each inhibition line.

Genotype	**95% Confidence Intervals**	**R^2**	**P-value**	**Significant**
DDC-Gal4; UAS-lacZ	0.04563 – 0.05455	0.9533	N/A	N/A
DDC-Gal4; UAS-Ptp4E-RNAi^{HMS01838}	0.02234 – 0.03361	0.7874	<0.0001	Yes
DDC-Gal4; UAS-Ptp4E-RNAi ^{HMS05000}	0.05021 – 0.07713	0.8203	<0.0001	Yes

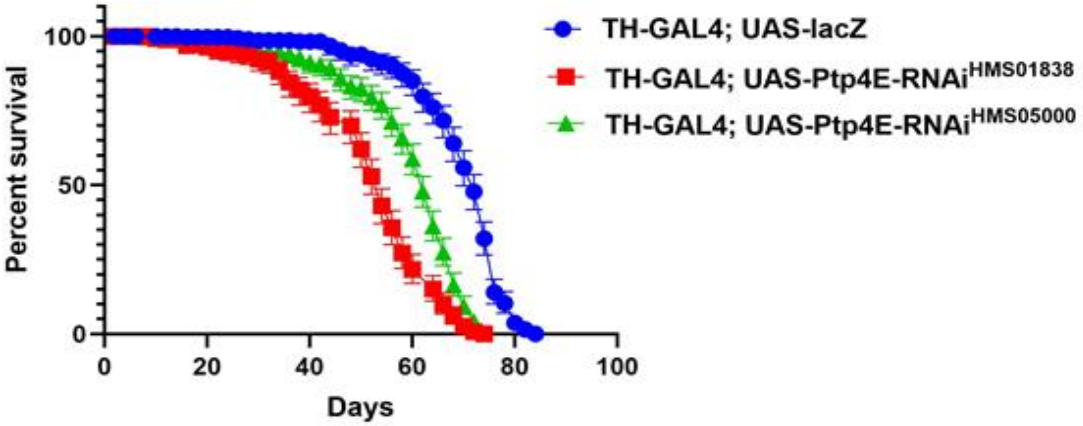

Figure 26: Inhibition of *Ptp4E* using a dopaminergic neuron-specific transgenic line (*TH-Gal4*) causes a significant decrease in longevity. Two different inhibition lines were used and both were significant compared to the control *TH-Gal4; UAS-lacZ*. Longevity is shown by percent survival. Significance is $p < 0.05$ and error bars shows the standard error of the mean.

Table 22. Comparison of the longevity of flies with inhibition of *Ptp4E* in motor neurons by Mantel-Cox Log-rank statistics. Chi-square values and p-values were calculated using *UAS-lacZ* control.

Genotype	Number of flies	Median Survival (days)	Chi – square value	P-value	Significant
TH-Gal4; UAS-lacZ	272	72	N/A	N/A	N/A
TH-Gal4; UAS-Ptp4E-RNAi^{HMS01838}	272	54	322.9	<0.0001	Yes
TH-Gal4; UAS-Ptp4E-RNAi ^{HMS05000}	353	62	210.3	<0.0001	Yes

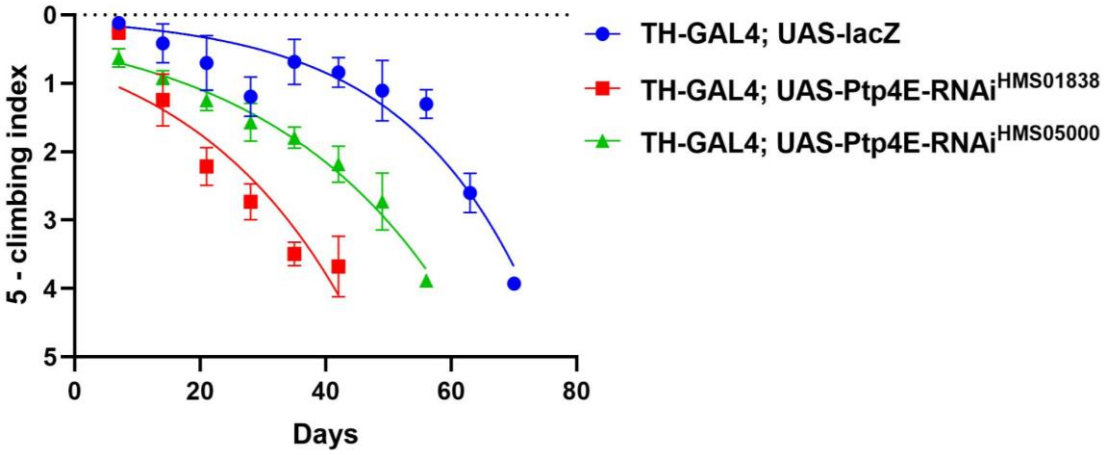

Figure 27: Inhibition of *Ptp4E* using a dopaminergic specific transgenic line (*TH-Gal4*) causes a significant decrease in flies climbing ability over time. Two different inhibition lines were used. Both were significant compared to the control *TH-Gal4; UAS-lacZ*. Data were analyzed by a non-linear curve fit with 95% confidence intervals to determine significance. Error bars represent standard error of the mean.

Table 23. Comparison of the climbing ability of flies with inhibition of *Ptp4E* in dopaminergic neurons by using a non-linear regression curve for each inhibition line.

Genotype	**95% Confidence Intervals**	**R^2**	**P-value**	**Significant**
TH-Gal4; UAS-lacZ	0.04104 – 0.05848	0.8594	N/A	N/A
TH-Gal4; UAS-Ptp4E-RNAi^{HMS01838}	0.03115 – 0.04695	0.8185	<0.0001	Yes
TH-Gal4; UAS-Ptp4E-RNAi ^{HMS05000}	0.03109 – 0.03732	0.9469	<0.0001	Yes

Table 24. A comparison summary of ageing and climbing analyses. *Ptp10D* and *Ptp4E* responder lines were crossed to *D42-Gal4*, *DDC-Gal4*, and *TH-Gal4* transgenic lines**.**

Responder lines	**Transgenic lines**					
Inhibition	*D42*		*DDC*		*TH*	
	Ageing	Climbing	Ageing	Climbing	Ageing	Climbing
UAS-Ptp10D-RNAi^{kk101775}	-	↓	↓	↓	↓	↓
UAS-Ptp10D-RNAi ^{v8010}	↓	↓	↓	↓	↓	↓
UAS-Ptp10D-RNAi ^{HMS01917}	↓	↓	↓	↓	↓	↓
UAS-Ptp10D-RNAi ^{v1104}	↓	↓	↓	↓	↓	↓
Overexpression						
UAS-Ptp10D^{EP1172}	↓	↓	↓	↓	↓	↓
Inhibition						
UAS-Ptp4E-RNAi^{HMS01838}	↓	↓	↓	↓	↓	↓
UAS-Ptp4E-RNAi ^{HMS05000}	↓	↓	↓	↓	↓	↓

↓ is significant decrease and – is no significant change.

Discussion

Parkinson Disease (PD) is a movement disorder that is considered to be among the most widely-occurring neurodegenerative diseases. The risk of having this disease increases with age, as 1 to 2% of the human population over the age of 65 years suffers from PD and this proportion increases with advanced age (Schapira, 1995). Commonly, it is known that resting tremors, rigidity, bradykinesia, and postural instability are the main motor symptoms of PD. Neuronal dysfunction or loss in the *substantia nigra* of the midbrain, to cause dopamine deficiency in the striatum, and intracellular aggregation of α-synuclein are the most noted neuropathological hallmarks of Parkinson Disease (Trinh et al., 2014). Multiple signal transduction pathways and sub-cellular mechanisms are involved in the underlying molecular pathogenesis of the disease: α-synuclein proteostasis, mitochondrial function, oxidative stress, calcium homeostasis, axonal transport, and neuroinflammation (Poewe et al., 2017). Understanding the functions of genes that have been found to lead to hereditary forms of PD can reveal the involvement of newly implicated cellular pathways and provide great insights into the disease etiology and reveal new cellular pathways.

Growing knowledge of the genetic basis of some forms of PD has led to the identification of a number of genetic loci that cause familial PD or increase the risk for PD. *PTPRH*, via its Drosophila homologues, is the gene of interest selected to be the focus of this study due to its potential role in signalling to the mitochondria. Moreover, it has been found that inhibition of *PTPRH* in neuroblastoma cell lines as an *in vitro*

model leads to changes in mitochondrial morphology (Jansen et al., 2017). Potential *PTPRH* homologues in *D. melanogaster* have not been extensively studied in *Drosophila* models of PD. Two potential homologues have been identified in *D. melanogaster* (Jansen et al., 2017). *Ptp10D* and *Ptp4E*, two homologues of *PTPRH*, are the result of gene duplication. Partial functional redundancy of these two genes, especially in the nervous system, encouraged my research group to study the consequences of altered expression of these genes while exploiting the *D. melanogaster* organism model. To assess the effects of *Ptp10D* and *Ptp4E* on cell growth, cell death, longevity, and climbing ability, they were ectopically inhibited and overexpressed in *D. melanogaster* by using the *Gal4/UAS* system.

***Drosophila Ptp10D* and *Ptp4E* are conserved across vertebrates and invertebrates**

The similarities between the potential homologues of *PTPRH* in vertebrates and invertebrates were determined by performing bioinformatics analysis. Alignment of the protein sequence of *Homo sapiens PTPRH* and *D. melanogaster Ptp10D* and *Ptp4E* shows that the PTPRH protein should share functional similarities with the products of the *Drosophila* homologues with a number of conserved domains present in these proteins (Figure 3 & 4). Fibronectin type III (FN3) repeats and the proteins tyrosine phosphatase (PTP) domain are conserved in Ptp10D and Ptp4E in *Drosophila* and PTPRH in humans. Although the PTP region is highly conserved, the placement of FN3 domains may vary between proteins as do the differences in number of amino acid

residues in these proteins as human PTPRH is much smaller than either *Drosophila* Ptp10D or Ptp4E.

Ptp10D, as the longer of the two *Drosophila* proteins contains nine FN3 domains, while Ptp4E has eight and PTPRH has six. It is interesting to note that in addition to the PTP domain, four domains amongst six FN3 domains in PTPRH are well conserved in these three proteins. Of the remaining FN3 domains, one is conserved between PTPRH and Ptp10D, and another one is maintained between PTPRH and Ptp4E. In *D. melanogaster*, the Ptp10D and Ptp4E proteins share seven conserved FN3 domains and one PTP domain. Clearly, the presence of conserved domains in human PTPRH and *D. melanogaster* Ptp10D and Ptp4E suggests that these proteins have a shared ancestor as well as comparable functions in the two species. While the number of FN3 repeats in vertebrates and PTPRH varies from six to eight (Figure 3 & 4), the range is seven to 12 among invertebrates (Figure 5). The comparison of Ptp10D and Ptp4E protein structures and sequences shows that they are 54% identical along the whole length of the protein and thus are very similar in function (Chicote, DeSalle, & García-España, 2017). There is only one copy of *Ptp4E/Ptp10D* in non-drosophilid species, which is more similar to *Ptp10D* (Matozaki et al., 2010). This provide further evidence that *Ptp10D* is the ancestral gene. Therefore, the Ptp10D sequence has been used in the multiple alignment for vertebrates and invertebrates (Figure 5). The multiple alignment indicates that, as mentioned before, PTP, which acts as a negative regulator for integrin-mediated signalling, is a highly conserved motif among vertebrates and invertebrates and might be associated with the inhibition of cell growth and motility.

Effects of RNAi-induced knockdown of *Ptp10D* in *D. melanogaster*

The compound eye structure provides a valuable model system for studying neural tissue-related diseases for two main reasons: first, key signalling pathways that control basic developmental processes are conserved between humans and flies, and second, its unique structure allows any changes due to defects in neurodevelopment to be quantified. The *D. melanogaster* compound eye is made of 700 to 800 subunits called ommatidia and is a complex comprised largely of neural tissue (Frankfort & Mardon, 2002). Thus, the presence of more than 6000 neurons in each eye makes the measurement of neurodevelopmental defects feasible even in cases in which only slight abnormalities are apparent.

In a recent study, the inhibition of *Ptp10D* along with the co-expression of *α-synuclein* was shown to enhance retinal degeneration, whereas the mutant allele in *α-synuclein* null flies through *Rhodopsin1-Gal4* does not cause significant α-synuclein toxicity (Jansen et al., 2017). In this experiment, I inhibited *Ptp10D* directly in the eye of *D. melanogaster* through eye-specific expression, utilizing the *GMR-Gal4* transgenic line. The results demonstrate a decrease in both the number of ommatidia and interommatidial bristles. It should be noted that the reduced ommatidia number is slight but significant, while the decline in bristle number is relatively substantial (Table 3 & 4). In addition to the three RNAi lines used in Jansen et al.'s study, I experimented with the *Ptp10D-RNAi*^{HMS01917} transgene which produced the most significant reduction in bristle number (Figure 10). Despite the uncertainty about the underlying reasons for this reduction, the decrease in the ommatidia and bristle numbers may be due to a reduction

in cell death or a decrease in cell growth (Brachmann & Cagan, 2003). Since there is a possibility for Ptp10D, being a subset of RPTP, to act as a cytoplasmic modulator in cell growth pathways, it may be inferred that the reduction in Ptp10D may lead to the disruption of cell growth pathways and therefore a reduction in ommatidia and interommatidial bristle number.

Since a shorter lifespan is one of the characteristics of PD-associated phenotypes, longevity assays were carried out to recognize the impact of *Ptp10D* inhibition on the lifespans of critical class Drosophila. Four distinct inhibition lines were crossed to three directed expression *Gal4*-bearing transgenic lines, each of which had a specific profile of tissue of expression. Three out of four inhibition transgenes resulted in a significant decrease in lifespan when guided by the motor neuron-specific transgene *D42-Gal4* (Figure 11). Based on statistical comparison, *D42-Gal4; UAS-Ptp10D-RNAi*^{v1104} produced the most significant reduction in which the number of median survival days decreases by 16 (see Table 6). Correspondingly, this transgene resulted in the largest decrease of all inhibition transgenes directed by the dopaminergic neuron-specific transgene *TH-Gal4* (Table 10). It should be added that all the lines had a significant decrease in lifespan, but the decrease was the largest for *Ptp10D-RNAi* ^{v1104} with a median lifespan of 14 days. The experiment was repeated with a neuron-specific transgene *DDC-Gal4*, which caused a decrease in all used inhibition lines. The most significant reduction in longevity was 22 days, in *DDC-Gal4; UAS-Ptp10D-RNAi* ^{HMS01917}, critical class males and the second most significant decrease was 18 days for the *DDC-Gal4; Ptp10D-RNAi* ^{v1104} flies (Table 8). No other studies have been done to

analyze longevity and climbing ability through the manipulation of *Ptp10D* and *Ptp4E*. An apoptotic death of DA neurons, may lead to a decrease in cell survival (Lev, Melamed, & Offen, 2003) and consequently a shorter lifespan in transgenic flies in which *Ptp10D* is inhibited. Moreover, the Ptp10D protein probably has roles in cell growth pathways, which means its inhibition may lead to a disruption in cell growth pathways and, subsequently, earlier cell death and a shorter life span.

Based on the above results regarding the deleterious effects of the inhibition of *Ptp10D* upon compound eye morphology and longevity, it was hypothesised that loss of *Ptp10D* activity may have adverse effects on climbing ability throughout the life of the flies. Moreover, the climbing assays are of great importance due to the nature of Parkinson Disease, which is linked with diminished locomotor ability during life. Therefore, locomotor analyses were conducted to examine the climbing ability of *Drosophila* over time. As expected, there is a noticeable decrease in the climbing ability of flies with the inhibition of *Ptp10D* when crossed with *D42-Gal4*, *DDC-Gal4*, and *TH-Gal4* transgenic lines. Experiments on four inhibition lines with these different drivers have produced consistent results in which the *UAS-Ptp10D-RNAi*^{HMS01917} inhibition line had the most significant decrease in climbing ability (Table 7, 9, and 11).

This is the first time the effect of *Ptp10D* manipulation on the climbing ability of *D. melanogaster* has been studied, so the precise role of this protein in pathways related to climbing ability is unclear. However, there is evidence that supports the role of *Ptp10D* in CNS development, as the expression of this gene is limited to the axons of CNS in late embryos in flies (Yang, Seow, Bahri, Oon, & Chia, 1991). Furthermore, a

recent study showed that *Ptp10D* has a role in motor axon guidance (Oliva & Hassan, 2017). The inhibition of this gene activity may strengthen the production of the LOF phenotype in motor axon guidance, which is crucial in neural development. The deleterious effects of *Ptp10D* inhibition on neurons and then the longevity and climbing ability suggest that the LOF of *Ptp10D* produces PD-like phenotypes.

Effects of the overexpression of *Ptp10D* in *D. melanogaster*

The overexpression of *Ptp10D* under the control of the eye-specific transgene, *GMR-Gal4*, has led to a significant reduction in the number of ommatidia and interommatidial bristles in the compound eye of *D. melanogaster*. Through biometric analysis, it has been shown that the decrease in bristle number compared to the control line is larger than the ommatidia reduction. Up to this point, there has been no previous research on the effects of the overexpression of *Ptp10D* in the eye of *Drosophila*. The observed decrease in the number of ommatidia and bristles suggests a significant reduction in cell number during eye development. A reduction of cell number can be due to either increased cell death or decreased cell growth (Kramer et al., 2003). From this, it may be inferred that the overexpression of *Ptp10D* might cause the inhibition of cell proliferation required for normal eye development.

In my experiment, the overexpression of *Ptp10D* influences the longevity of *D. melanogaster*. When the overexpression transgene *UAS-Ptp10D*^{EP1172} was directed by the motor neuron-specific transgene (*D42-Gal4*), dopaminergic neuron-specific

transgene (*TH-Gal4*), and neuron-specific transgene (*DDC-Gal4*), a fairly consistent phenotype was achieved. All the critical classes derived from specifically designed crosses have given rise to a significant reduction in longevity. To be specific, the median survival of critical class flies directed by *D42-Gal4*, *TH-Gal4*, and *DDC-Gal4* was shown to decrease by 12, 18, and 26 days, respectively. As was the case with the results of the inhibition of *Ptp10D* through longevity assays, the most significant reduction occurred when the *DDC-Gal4* transgenic line was used (Table 14). Although a similar experiment has not been done on the overexpression of *Ptp10D* to compare the results, one study has shown that *PTPRH* overexpression led to apoptotic cell death in the fibroblast cell line, which is used as an *in vitro* PD model, through inhibiting the survival signalling pathways and activating the cellular pro-apoptotic pathways (Takada et al., 2002). There is a strong probability that *PTPRH* has a key role in cell proliferation, survival, and cell apoptosis. As a consequence of *Ptp10D* being a potential homologue of *PTPRH* in *D. melanogaster*, it can be speculated that the overexpression of *Ptp10D* may increase apoptosis and/or decrease cell survival and therefore shorten the lifespan.

The potential role of *Ptp10D* in cell survival encouraged the study of the potential effects of *Ptp10D* overexpression upon one of the most important neurological characteristics of PD, diminishment of locomotor ability over time. This study demonstrates that the overexpression of *Ptp10D* leads to a significant reduction in the climbing ability of critical class flies during the life of ageing flies. Similar to previous experiments, the overexpression line was crossed to three different tissue-specific transgenic lines to produce critical class males. The overexpression of *Ptp10D*, either in

motor neurons, dopaminergic neurons or a subset of neurons including the serotonergic and dopaminergic neurons results in lower climbing ability compared to the control group. Based upon the previous discussion, it seems that *Ptp10D* may have a crucial role in cell growth and survival and is essential for intact neural development. However, an optimal amount of gene activity is required for maintained locomotor activity as either too high or too low level of activity of *Ptp10D* has the demonstrated deleterious effects.

Effects of *Ptp4E* inhibition in *D. melanogaster*

The other possible homologue of *PTPRH*, *Ptp4E*, was inhibited specifically in the eye of *Drosophila* to determine if loss of function could lead to PD-like phenotypes. Two distinct RNAi transgenic lines were employed, and each led to deleterious effects upon the morphology of the *Drosophila* eye. Both methods of inhibition revealed a significant decrease in the number of ommatidia and bristles. In accordance with other results, the changes in bristle number were extreme and significant. Results similar to the inhibition of *Ptp10D* were to be expected due to the potential of functional redundancy between *Ptp10D* and *Ptp4E*. The assumption that Ptp4E may play a role in nervous system development, as it is expressed in the late embryo in a ubiquitous manner (Yang et al., 1991). However, a recent experiment produced a contrasting result (Jansen et al., 2017), as inhibition of *Ptp4E* in the developing eye through the directing *Rhodobdin1-Gal4* transgene with two distinct inhibitory RNAi transgenes did not find significant retinal degeneration.

In further analysis, the effect of *Ptp4E* inhibition upon the longevity of critical class male flies was investigated. Two available *Ptp4E-RNAi* lines were crossed to different *Gal4*-bearing transgenic lines, including the motor neuron-specific transgene (*D42-Gal4*), dopaminergic neuron-specific transgene (*TH-Gal4*), and neuron-specific transgene (*DDC-Gal4*). The inhibition of *Ptp4E* results in a significant decrease in the lifespan of flies, as the median survival is decreased by 18 days in *TH-Gal4; UAS-Ptp4E-RNAi*^{HMS01838}critical class males, which lead to the most significant decrease in life span compared to the control group (Table 22). The *Ptp4E-RNAi*^{HMS01838} inhibition transgene caused a decline of 14 and 12 days in lifespan when directed by *DDC-Gal4* and *D42-Gal4*, respectively (Table 20 & 18). Due to the similarity between *Ptp10D* and *Ptp4E* in their function, it can be inferred that the inhibition of *Ptp4E* in flies may cause a decrease in cell survival to lead to a decrease in longevity. Consistent with the ageing results, *Ptp4E-RNAi*^{HMS01838} had the most significant decrease in climbing ability when directed by all three Gal4 transgenes used in the climbing assays. Since the climbing results for both *Ptp4E-RNAi* transgenes when they were under the direction of *D42-Gal4*, *DDC-Gal4*, and *TH-Gal4* were significant, it can be inferred that the inhibition of *Ptp10D* results in the production of PD-like phenotypes in *D. melanogaster*.

Conclusion

In this study, I have demonstrated that *PTPRH* has two homologues in *D. melanogaster*: *Ptp10D* and *Ptp4E*. Through bioinformatics analyses, it has been

suggested that these protein encoding genes, in *Homo sapiens* and *Drosophila melanogaster*, may have been functionally conserved due to the high level of sequence conservation, especially the presence of conserved domains including FN3 and PTP. To provide further justifications, the LOF and GOF of these two genes were studied through biometric, longevity, and climbing over lifetime assays. In addition, the inhibition of *Ptp10D* and *Ptp4E* through *RNAi* results in a significant reduction in ommatidia and bristle number, longevity, and climbing ability. The inhibition of each gene leads to a novel PD model. The overexpression of *Ptp10D* was analyzed through the same assays by one available overexpression line, and consistent results were obtained through the analyses of gene inhibition. Thus, in this experiment, the GOF of *Ptp10D* produced a PD-like phenotype as well. However, it would be worthwhile to further the study with additional overexpression lines of *Ptp10D* as well as *Ptp4E*.

One of the most important objectives that may be accomplished in a follow up to the current study is the execution of an experiment with simultaneous knockdown and overexpression of both genes to eliminate any potential compensation due to redundancy in function of the orthologous gene and then compare the severity of phenotypes compared to those of this study. Moreover, due to the close association of *PTPRH* with a well-established PD gene *FBXO7*, the interaction of *Ptp10D* and/or *Ptp4E* with *FBXO7* should be of great interest to study. Further studies to complement these genetic studies could be conducted, from a molecular and cellular point of view, to investigate the potential roles of *Ptp10D* and *Ptp4E* in cell growth and development.

References

Agrawal, N., Dasaradhi, P.V., Mohmmed, A., Malhotra, P., Bhatnagar, R.K., & Mukherjee, S.K. (2003). RNA interference: biology, mechanism, and applications. *Microbiology and Molecular Biology Reviews, 67*(4), 657-685.

Andersen, J.N., Jansen, P.G., Echwald, S.M., Mortensen, O.H., Fukada, T., Del Vecchio, R., Tonks, N.K., & Møller, N.P.H. (2004). A genomic perspective on protein tyrosine phosphatases: gene structure, pseudogenes, and genetic disease linkage. *The FASEB Journal, 18*(1), 8-30.

Armstrong, J.D., Texada, M.J., Munjaal, R., Baker, D.A, & Beckingham, K.M. (2006). Gravitaxis in *Drosophila melanogaster*: a forward genetic screen. *Genes, Brain and Behavior, 5*(3), 222-239.

Aryal, B., & Lee, Y. (2019). Disease model organism for Parkinson disease: *Drosophila melanogaster*. *BMB Reports, 52*(4), 250-258.

Arzan Zarin, A., & Labrador, J.P. (2019). Motor axon guidance in Drosophila. *Seminars in Cell & Developmental Biology*, 85, 36-47.

Baig, M.H., Ahmad, K., Rabbani, G., & Choi, I. (2018). Use of peptides for the management of Alzheimer's Disease: Diagnosis and Inhibition. *Frontiers in Aging Neuroscience, 10*, 21.

Baker, N.E., Li, K., Quiquand, M., Ruggiero, R., & Wang, L. (2014). Eye development. *Methods, 68*(1), 252-259.

Bekris, L.M., Mata, I.F., & Zabetian, C.P. (2010). The genetics of Parkinson disease. *Journal of Geriatric Psychiatry and Neurology, 23*(4), 228-242.

Bernstein, E., Caudy, A.A., Hammond, S.M., & Hannon, G.J. (2001). Role for a bidentate ribonuclease in the initiation step of RNA interference. *Nature, 409*(6818), 363.

Bose, A., & Beal, M.F. (2016). Mitochondrial dysfunction in Parkinson's disease. *Journal of Neurochemistry, 139*, 216-231.

Brachmann, C.B., & Cagan, R.L. (2003). Patterning the fly eye: the role of apoptosis. *TRENDS in Genetics, 19*(2), 91-96.

Brand, A.H., & Perrimon,N. (1993). Targeted gene expression as a means of altering cell fates and generating dominant phenotypes. *Development (Cambridge, England), 118*(2), 401-415.

Bujko, M., Kober, P., Statkiewicz, M., Mikula, M., Grecka, E., Rusetska, N., Ligaj, M., Ostrowski, J., & Siedlecki, J.A. (2017). Downregulation of PTPRH (sap-1) in colorectal tumors. *International Journal of Oncology, 51*(3), 841-850.

Burchell, V.S., Nelson, D.E., Sanchez-Martinez, A., Delgado-Camprubi, M., Ivatt, R.M., Pogson, J. H., Randle, S.J., Wray, S., Lewis, P.A., Houlden, H., Abramov, A.Y., Hardy, J., Wood, N.W., Whitworth, A.J., Laman, H., & Plun-Favreau, H. (2013). The Parkinson's disease–linked proteins Fbxo7 and Parkin interact to mediate mitophagy. *Nature Neuroscience, 16*(9), 1257.

Cagan, R. (2009). Principles of Drosophila eye differentiation. *Current Topics in Developmental Biology, 89*, 115-135.

Charcot, J. (1872). Leçons sur les maladies du systeme nerveux. 3 vols. *Paris: Bureaux Du Progres Médical, 87*.

Chaudhuri, K.R., Healy, D.G., & Schapira, A.H. (2006). Non-motor symptoms of Parkinson's disease: diagnosis and management. *The Lancet Neurology, 5*(3), 235-245.

Chicote, J.U., DeSalle, R., & García-España, A. (2017). Phosphotyrosine phosphatase R3 receptors: Origin, evolution and structural diversification. *Public Library of Science, 12*(3), e0172887.

Dawson, T.M., & Dawson, V.L. (2010). The role of parkin in familial and sporadic Parkinson's disease. *Movement Disorders, 25*(S1), S32-S39.

De Lau, L.M., & Breteler, M.M. (2006). Epidemiology of Parkinson's disease. *The Lancet Neurology, 5*(6), 525-535.

Del Rey, N.L., Quiroga-Varela, A., Garbayo, E., Carballo-Carbajal, I., Fernández-Santiago, R., Monje, M.H.G., Trigo-Damas, I., Blanco-Prieto, M.J., & Blesa, J. (2018). Advances in Parkinson's Disease: 200 years later. *Frontiers in Neuroanatomy, 12:*113.

Deng, H., Wang, P., & Jankovic, J. (2018). The genetics of Parkinson disease. *Ageing Research Reviews, 42*, 72-85.

Devi, L., Raghavendran, V., Prabhu, B.M., Avadhani, N.G., & Anandatheerthavarada, H.K. (2008). Mitochondrial import and accumulation of alpha-synuclein impair complex I in human dopaminergic neuronal cultures and Parkinson disease brain. *The Journal of Biological Chemistry, 283*(14), 9089-9100.

Devoto, V.M. P., & Falzone, T.L. (2017). Mitochondrial dynamics in Parkinson's disease: A role for α-synuclein? *Disease Models & Mechanisms, 10*(9), 1075-1087.

Dietzl, G., Chen, D., Schnorrer, F., Su, K., Barinova, Y., Fellner, M. Gasser, B., Kinsey, K., Oppel, S., Scheiblauer, S., Couto, A., Marra, V., Keleman, K., & Dickson, B.J. (2007). A genome-wide transgenic RNAi library for conditional gene inactivation in Drosophila. *Nature, 448*(7150), 151.

Du, Y., & Grandis, J. R. (2015). Receptor-type protein tyrosine phosphatases in cancer. *Chinese Journal of Cancer, 34*(2), 61-69.

Erkkinen, M.G., Kim, M., & Geschwind, M.D. (2018). Clinical neurology and epidemiology of the major neurodegenerative diseases. *Cold Spring Harbor Perspectives in Biology, 10*(4), a033118.

Fearnley, J.M., & Lees, A.J. (1991). Ageing and Parkinson's disease: *substantia nigra* regional selectivity. *Brain, 114*(5), 2283-2301.

Frankfort, B.J., & Mardon, G. (2002). R8 development in the Drosophila eye: A paradigm for neural selection and differentiation. *Development (Cambridge, England), 129*(6), 1295-1306.

Freeman, M. (1996). Reiterative use of the EGF receptor triggers differentiation of all cell types in the Drosophila eye. *Cell, 87*(4), 651-660.

Friggi-Grelin, F., Iche, M., & Birman, S. (2003). Tissue-specific developmental requirements of Drosophila tyrosine hydroxylase isoforms. *Genesis, 35*(3), 175-184.

Gasser, T. (2009). Mendelian forms of Parkinson's disease. *Biochimica Biophysica Acta (BBA)-Molecular Basis of Disease, 1792*(7), 587-596.

Goedert, M. (2001). Alpha-synuclein and neurodegenerative diseases. *Nature Reviews Neuroscience, 2*(7), 492-501.

Goetz, C. G. (2011). The history of Parkinson's Disease: Early clinical descriptions and neurological therapies. *Cold Spring Harbor Perspectives in Medicine, 1*(1), a008862.

Gonzalez, C. (2013). Drosophila melanogaster: a model and a tool to investigate malignancy and identify new therapeutics. *Nature Reviews Cancer, 13*(3), 172-183.

Heigwer, F., Port, F., & Boutros, M. (2018). RNA interference (RNAi) screening in Drosophila. *Genetics, 208*(3), 853-874.

Hendriks, W.J., Elson, A., Harroch, S., & Stoker, A.W. (2008). Protein tyrosine phosphatases: Functional inferences from mouse models and human diseases. *The FEBS Journal, 275*(5), 816-830.

Hernandez, D.G., Reed, X., & Singleton, A.B. (2016). Genetics in Parkinson disease: Mendelian versus non-Mendelian inheritance. *Journal of Neurochemistry, 139*, 59-74.

Hirtz, D., Thurman, D., Gwinn-Hardy, K., Mohamed, M., Chaudhuri, A., & Zalutsky, R. (2007). How common are the "common" neurologic disorders? *Neurology, 68*(5), 326-337.

Hourani, M., Mendes, A., Berretta, R., & Moscato, P. (2007). Genetic biomarkers for brain hemisphere differentiation in Parkinson's disease. Paper presented at the *AIP Conference Proceedings, 952*(1) 207-216.

Hunter, T. (1998). The croonian lecture 1997. The phosphorylation of proteins on tyrosine: Its role in cell growth and disease. *Philosophical Transactions of the Royal Society of London.Series B: Biological Sciences, 353*(1368), 583-605.

Iyer, J., Wang, Q., Le, T., Pizzo, L., Gronke, S., Ambegaokar, S.S., Imai, Y., Srivastava, A., Troisí, B.L., Mardon, G., Artero, R., Jackson, G.R., Isaacs, A.M., Partridge, L., Lu, B., Kumar, J.P., & Girirajan, S. (2016). Quantitative assessment of eye phenotypes for functional genetic studies using Drosophila melanogaster. *G3 (Bethesda, Md.), 6*(5), 1427-1437.

Jansen, I. E., Ye, H., Heetveld, S., Lechler, M.C., Michels, H., Seinstra, R.I., Lubbe, S.J., Drouet, V., Lesage, S., Majounie, E., Gibbs, J.R., Nalls, M.A., Ryten, M., Botia, J.A., Vandrovcova, J., Simon-Sanchez, J., Castillo-Lizardo, M., Rizzu, P., Blauwendraat, C., Chouhan, A.K., Li, Y., Yogi, P., Amin, N., van Duijn, C.M., International Parkinson's Disease Genetics Consortium (IPGDC), Morris, H.R., Brice, A., Singleton, A.B., David, D.C., Nollen, E.A., Jain, S., Shulman, J.M., & Heutink, P. (2017). Discovery and functional prioritization of Parkinson's disease candidate genes from large-scale whole exome sequencing. *Genome Biology, 18*(1), 22.

Jeibmann, A., & Paulus, W. (2009). Drosophila melanogaster as a model organism of brain diseases. *International Journal of Molecular Sciences, 10*(2), 407-440.

Jennings, B. H. (2011). Drosophila–a versatile model in biology & medicine. *Materials Today, 14*(5), 190-195.

Jeon, M., Nguyen, H., Bahri, S., & Zinn, K. (2008). Redundancy and compensation in axon guidance: Genetic analysis of the Drosophila Ptp10D/Ptp4E receptor tyrosine phosphatase subfamily. *Neural Development, 3*(1), 3.

Karbowski, M., & Neutzner, A. (2012). Neurodegeneration as a consequence of failed mitochondrial maintenance. *Acta Neuropathologica, 123*(2), 157-171.

Karimi-Moghadam, A., Charsouei, S., Bell, B., & Jabalameli, M.R. (2018). Parkinson disease from mendelian forms to genetic susceptibility: New molecular insights into the neurodegeneration process. *Cellular and Molecular Neurobiology, 38*(6), 1153-1178.

Keene, A.C., & Waddell, S. (2007). Drosophila olfactory memory: Single genes to complex neural circuits. *Nature Reviews Neuroscience, 8*(5), 341-354.

Kitada, T., Asakawa, S., Hattori, N., Matsumine, H., Yamamura, Y., Minoshima, S., Yokochi, M., Mizuno, Y., & Shimizu, N. (1998). Mutations in the parkin gene cause autosomal recessive juvenile parkinsonism. *Nature, 392*(6676), 605-608.

Koopman, W.J., Visch, H., Smeitink, J.A., & Willems, P.H. (2006). Simultaneous quantitative measurement and automated analysis of mitochondrial morphology, mass, potential, and motility in living human skin fibroblasts. *Cytometry Part A: The Journal of the International Society for Analytical Cytology, 69*(1), 1-12.

Kraut, R., Menon, K., & Zinn, K. (2001). A gain-of-function screen for genes controlling motor axon guidance and synaptogenesis in Drosophila. *Current Biology, 11*(6), 417-430.

Lambrechts, R., Faber, A., & Sibon, O. (2018). Modelling in miniature: Using drosophila melanogaster to study human neurodegeneration. *Drug Discovery Today: Disease Models, 25,* 3-10.

Leroy, E., Boyer, R., Auburger, G., Leube, B., Ulm, G., Mezey, E., Harta, G., Brownstein, M.J., Jonnalagada, S., Chernova. T., Dehejia, A., Lavedan, C., Gasser, T., Steinbach, P.J., Wilkinson, K.D., & Polymeropoulos, M.H., (1998). The ubiquitin pathway in Parkinson's disease. *Nature, 395*(6701), 451-452.

Lev, N., Melamed, E., & Offen, D. (2003). Apoptosis and Parkinson's disease. *Progress in Neuro-Psychopharmacology and Biological Psychiatry, 27*(2), 245-250.

Li, H., Chaney, S., Forte, M., & Hirsh, J. (2000). Ectopic G-protein expression in dopamine and serotonin neurons blocks cocaine sensitization in Drosophila melanogaster. *Current Biology, 10*(4), 211-214.

Liu, G., Zhang, C., Yin, J., Li, X., Cheng, F., Li, Y., Yang, H., Uéda, K., & Chan, P., Yu, S. (2009). Alpha-synuclein is differentially expressed in mitochondria from different rat brain regions and dose-dependently down-regulates complex I activity. *Neuroscience Letters,* 454(3), 187-192.

Ma, C. (2004). Animal models of disease in vivo assays are not usually performed until or after lead optimization is complete. *Modern Drug Discovery, 7,* 30-36.

Marín, I. (2006). The Parkinson disease gene LRRK2: Evolutionary and structural insights. *Molecular Biology and Evolution, 23*(12), 2423-2433.

Matozaki, T., & Kasuga, M. (1996). Roles of protein-tyrosine phosphatases in growth factor signalling. *Cellular Signalling, 8*(1), 13-19.

Matozaki, T., Murata, Y., Mori, M., Kotani, T., Okazawa, H., & Ohnishi, H. (2010). Expression, localization, and biological function of the R3 subtype of receptor-type protein tyrosine phosphatases in mammals. *Cellular Signalling, 22*(12), 1811-1817.

Matozaki, T., Suzuki, T., Uchida, T., Inazawa, J., Ariyama, T., Matsuda, K., Horita, K., Noguchi, H., Mizuno, H., & Sakamoto, C. (1994). Molecular cloning of a human transmembrane-type protein tyrosine phosphatase and its expression in gastrointestinal cancers. *The Journal of Biological Chemistry, 269*(3), 2075-2081.

Moon, H.E., & Paek, S.H. (2015). Mitochondrial dysfunction in Parkinson's disease. *Experimental Neurobiology, 24*(2), 103-116.

Moura, M., & Conde, C. (2019). Phosphatases in mitosis: Roles and regulation. *Biomolecules, 9*(2), 55.

Nagano, H., Noguchi, T., Inagaki, K., Yoon, S., Matozaki, T., Itoh, H., Kasuga, M., & Hayashi, Y. (2003). Downregulation of stomach cancer-associated protein tyrosine phosphatase-1 (SAP-1) in advanced human hepatocellular carcinoma. *Oncogene, 22*(30), 4656-4663.

Nass, R., & Przedborski, S. (2011). *Parkinson's disease: Molecular and therapeutic insights from model systems* Elsevier.

Neckameyer, W.S., & Argue, K.J. (2012). Comparative approaches to the study of physiology: Drosophila as a physiological tool. *American Journal of Physiology-Regulatory, Integrative and Comparative Physiology, 304*(3), R177-R188.

Ni, J., Zhou, R., Czech, B., Liu, L., Holderbaum, L., Yang-Zhou, D., Shim, H.S., Tao, R., Handler, D., Karpowicz, P., Binari, R., Booker, M., Brennecke, J., Perkins, L.A., Hannon, G.J., & Perrimon, N. (2011). A genome-scale shRNA resource for transgenic RNAi in Drosophila. *Nature Methods, 8*(5), 405-407.

Noguchi, T., Tsuda, M., Takeda, H., Takada, T., Inagaki, K., Yamao, T., Fukunaga, K., Matozaki, T., & Kasuga, M. (2001). Inhibition of cell growth and spreading by stomach cancer-associated protein-tyrosine phosphatase-1 (SAP-1) through dephosphorylation of p130cas. *The Journal of Biological Chemistry, 276*(18), 15216-15224.

Nussbaum, R.L., & Polymeropoulos, M.H. (1997). Genetics of Parkinson's disease. *Human Molecular Genetics, 6*(10), 1687-1691.

Oliva, C., Soldano, A., Mora, N., De Geest, N., Claeys, A., Erfurth, M. L., Sierralta, J., Ramaekers, A., Dascenco, D., Ejsmont, R. K., Schmucker, D., Sanchez-Soriano, N., & Hassan, B. A. (2016). Regulation of Drosophila brain wiring by neuropil interactions via a slit-robo-RPTP signaling complex. *Developmental Cell, 39*(2), 267-278.

Paisán-Ruíz, C., Jain, S., Evans, E.W., Gilks, W.P., Simón, J., Van Der Brug, & M., Khan, N. (2004). Cloning of the gene containing mutations that cause PARK8-linked Parkinson's disease. *Neuron, 44*(4), 595-600.

Pandey, U.B., & Nichols, C.D. (2011). Human disease models in Drosophila melanogaster and the role of the fly in therapeutic drug discovery. *Pharmacological Reviews, 63*(2), 411-436.

Parkinson, J. (1817). An essay on the shaking palsy. london, whittingham and rowland. *James Parkinson (1755–1824),* 145-218.

Perkins, L., Holderbaum, L., & Perrimon, N. (2009). *Update to TRiP Stock Collection,*

Phelps, C.B., & Brand, A.H. (1998). Ectopic gene expression in Drosophila Using GAL4 system. *Methods, 14*(4), 367-379.

Philippens, I.H. (2018). Refinement of the MPTP model for Parkinson’s disease in the marmoset. *Drug Discovery Today: Disease Models, (25-26),* 53-61.

Poewe, W., Seppi, K., Tanner, C.M., Halliday, G.M., Brundin, P., Volkmann, J., Schrag, A.E., & Lang, A.E. (2017). Parkinson disease. *Nature Reviews Disease Primers, 3*, 17013.

Polymeropoulos, M.H., Lavedan, C., Leroy, E., Ide, S.E., Dehejia, A., Dutra, A., Pike, B., Root, H., Rubenstein, J., Boyer, R., Stenroos, E.S., Chandrasekharappa, S., Athanassiadou, A., Papapetropoulos, T., Johnson, W.G., Lazzarini, A.M., Duvoisin, R.C., Di Iorio, G., Golbe, L.I., & Nussbaum, R.L., (1997). Mutation in the α-synuclein gene identified in families with Parkinson's disease. *Science, 276*(5321), 2045-2047.

Rakovic, A., Grünewald, A., Kottwitz, J., Brüggemann, N., Pramstaller, P.P., Lohmann, K., & Klein, C. (2011). Mutations in PINK1 and parkin impair ubiquitination of mitofusins in human fibroblasts. *Public Library of Science, 6*(3), e16746.

Riparbelli, M.G., Persico, V., Gottardo, M., & Callaini, G. (2018). The developing Drosophila eye–a new model to study centriole reduction. *Journal of Cell Science, 131*(4), jcs211441.

Rorth, P., Szabo, K., Bailey, A., Laverty, T., Rehm, J., Rubin, G. M., & Cohen, S. M. (1998). Systematic gain-of-function genetics in Drosophila. *Development, 125*(6), 1049-1057.

Ryan, B.J., Hoek, S., Fon, E.A., & Wade-Martins, R. (2015). Mitochondrial dysfunction and mitophagy in Parkinson's: From familial to sporadic disease. *Trends in Biochemical Sciences, 40*(4), 200-210.

Şahin, H. B., & Çelik, A. (2001). Drosophila eye development and photoreceptor specification., *eLS.*

Savitt, J.M., Dawson, V.L., & Dawson, T.M. (2006). Diagnosis and treatment of Parkinson disease: Molecules to medicine. *The Journal of Clinical Investigation, 116*(7), 1744-1754.

Schapira, A.H.V. (2007). Mitochondrial dysfunction in Parkinson's disease, *Cell Death & Differentiation, 14*(7), 1261-1266.

Schapira, A.H. (1995). Nuclear and mitochondrial genetics in Parkinson's disease. *Journal of Medical Genetics, 32*(6), 411-414.

Scialò, F., Sriram, A., Fernández-Ayala, D., Gubina, N., Lõhmus, M., Nelson, G., Logan, A., Cooper, H.M., Navas, P., Enríquez, J.A., Murphy, M.P., & Sanz, A. (2016). Mitochondrial ROS produced via reverse electron transport extend animal lifespan. *Cell Metabolism, 23*(4), 725-734.

Seo, Y., Matozaki, T., Tsuda, M., Hayashi, Y., Itoh, H., & Kasuga, M. (1997). Overexpression of SAP-1, a transmembrane-type protein tyrosine phosphatase, in human colorectal cancers. *Biochemical and Biophysical Research Communications, 231*(3), 705-711.

Shahed, J., & Jankovic, J. (2007). Motor symptoms in Parkinson's Disease. *Handbook of Clinical Neurology, 83*, 329-342.

Skrzypczak, M., Goryca, K., Rubel, T., Paziewska, A., Mikula, M., Jarosz, D., Pachlewski, J., Oledzki, J., & Ostrowsk, J. (2010). Modeling oncogenic signaling in colon tumors by multidirectional analyses of microarray data directed for maximization of analytical reliability. *Public Library of Science, 5*(10), e13091.

Sosa, M.A.G., De Gasperi, R., & Elder, G.A. (2012). Modeling human neurodegenerative diseases in transgenic systems. *Human Genetics, 131*(4), 535-563.

St. Johnston, D. (2002). The art and design of genetic screens: *Drosophila melanogaster*. *Nature Reviews Genetics, 3*(3), 176-188.

Staveley, B. E. (2012). Successes of modelling Parkinson Disease in drosophila. *Mechanisms in Parkinson's disease-models and treatments- models and treatments*, Juliana Dushanova, IntechOpen. Available from: https://www.intechopen.com/books/mechanisms-in-parkinson-s-disease-models-and-treatments/successes-of-modelling-parkinson-disease-in-drosophila-

Sun, Y., Ye, L., Zheng, Y., & Yang, Z. (2018). Identification of crucial genes associated with Parkinson disease using microarray data. *Molecular Medicine Reports, 17*(3), 3775-3782.

Sun, Q., Bahri, S., Schmid, A., Chia, W., & Zinn, K. (2000). Receptor tyrosine phosphatases regulate axon guidance across the midline of the Drosophila embryo. *Development (Cambridge, England), 127*(4), 801-812.

Takada, T., Noguchi, T., Inagaki, K., Hosooka, T., Fukunaga, K., Yamao, T., Ogawa, W., Matozaki, T., & Kasuga, M. (2002). Induction of apoptosis by stomach cancer-associated protein-tyrosine phosphatase-1. *The Journal of Biological Chemistry, 277*(37), 34359-34366.

Tao, J., Bulgari, D., Berkhoudt, D.A., Calderon, M.J., Watkins, S.C., Fonseca Velez, H.J., Sabvena, N., Deitcher, D.L., & Levitan, E.S. (2019). Drosophila Ptp4E regulates vesicular packaging for monoamine-neuropeptide co-transmission. *Journal of Cell Science, 132*(7), jcs.224568.

Trinh, J., Amouri, R., Duda, J.E., Morley, J.F., Read, M., Donald, A., Vilariño-Güell, C., Thompson, C., Szu Tu, C., Gustavsson, E.K., Ben Sassi, S., Hentati, E., Zouari, M., Farhat, E., Nabli, F., Hentati, F., & Farrer, M. J. (2014). A comparative study of Parkinson's disease and leucine-rich repeat kinase 2 p. G2019S parkinsonism. *Neurobiology of Aging, 35*(5), 1125-1131.

Trushina, E., & McMurray, C. (2007). Oxidative stress and mitochondrial dysfunction in neurodegenerative diseases. *Neuroscience, 145*(4), 1233-1248.

Tsachaki, M., & Sprecher, S. G. (2012). Genetic and developmental mechanisms underlying the formation of the Drosophila compound eye. *Developmental Dynamics, 241*(1), 40-56.

Van Den Eeden, S.K., Tanner, C.M., Bernstein, A.L., Fross, R.D., Leimpeter, A., Bloch, D.A., & Nelson, L.M. (2003). Incidence of Parkinson’s disease: Variation by age, gender, and race/ethnicity. *American Journal of Epidemiology, 157*(11), 1015-1022.

Vincow, E.S., Merrihew, G., Thomas, R.E., Shulman, N. J., Beyer, R.P., MacCoss, M. J., & Pallanck, L.J. (2013). The PINK1-parkin pathway promotes both mitophagy and

selective respiratory chain turnover in vivo. *Proceedings of the National Academy of Sciences of the United States of America, 110*(16), 6400-6405.

Wang, B., Abraham, N., Gao, G., & Yang, Q. (2016). Dysregulation of autophagy and mitochondrial function in Parkinson's disease. *Translational Neurodegeneration, 5*(1), 19.

Wälchli, S., Espanel, X., & Van Huijsduijnen, R. H. (2005). Sap-1/PTPRH activity is regulated by reversible dimerization. *Biochemical and Biophysical Research Communications, 331*(2), 497-502.

Wooten, G., Currie, L., Bovbjerg, V., Lee, J., & Patrie, J. (2004). Are men at greater risk for Parkinson's disease than women? *Journal of Neurology, Neurosurgery & Psychiatry, 75*(4), 637-639.

Wu, T., & Hallett, M. (2013). The cerebellum in Parkinson's disease. *Brain, 136*(3), 696-709.

Yang, X., Seow, K.T., Bahri, S.M., Oon, S.H., & Chia, W. (1991). Two Drosophila receptor-like tyrosine phosphatase genes are expressed in a subset of developing axons and pioneer neurons in the embryonic CNS. *Cell, 67*(4), 661-673.

Yeh, E., Gustafson, K., & Boulianne, G. L. (1995). Green fluorescent protein as a vital marker and reporter of gene expression in Drosophila. *Proceedings of the National Academy of Sciences of the United States of America*, *92*(15), 7036-7040.

Zhang, P., Chen, Y., Zhang, C., Wang, Y., & Fernandez-Funez, P. (2018). Genetics of Parkinson's disease and related disorders. *Journal of Medical Genetics, 55*(2), 73-80.